UNIWERSYTET MEDYCZNY
IM. PIASTÓW ŚLĄSKICH WE WROCŁAWIU

Zakład Badań Ultrastrukturalnych

PRACA DOKTORSKA

Michał Jerzy Kulus

Metody biochemiczne, histologiczne i obrazowanie radiologiczne w ocenie stanu zdrowia populacji historycznych Dolnego Śląska

Promotor pracy: prof. dr hab. Marzenna Podhorska-Okołów
Promotor pomocniczy: dr Paweł Dąbrowski

Wrocław 2024

Badania do niniejszej pracy finansowane były ze środków grantu Narodowego Centrum Nauki, OPUS13, nr: DEC-2017/25/B/HS3/02006, pod kierownictwem dra Pawła Dąbrowskiego.

Pracę dedykuję wszystkim mężczyznom, kobietom i dzieciom, których szczątki badałem w niniejszej pracy. Mam nadzieję, że nie macie mi tego za złe.

Do zobaczenia, gdzieś tam, kiedyś tam.

~MJFK

Spis treści

Wykaz publikacji stanowiących rozprawę doktorską

1. Dąbrowski Paweł, **Kulus Michał Jerzy**, Cieślik Agata, Domagała Zygmunt, Wiglusz Rafał J., Kuropka Piotr, Kuryszko Jan, Thannhauser Agata, Szleszkowski Łukasz, Dzięgiel Piotr: A case of syphilis with high bone arsenic concentration from early modern cemetery (Wroclaw, Poland), Open Life Sciences, 2019, vol. 14, s. 427-439, DOI:10.1515/biol-2019-0048

   40 punktów, IF(0,69)

2. **Kulus Michał Jerzy**, Dąbrowski Paweł: How to calculate the age at formation of Harris lines? A step-by-step review of current methods and a proposal for modifications to Byers' formulas, Archaeological and Anthropological Sciences, 2019, vol. 11, nr 4, s. 1169-1185, DOI:10.1007/s12520-018-00773-5,

   100 punktów, IF(2,063)

3. **Kulus Michał J.,**Cebulski Kamil, Kmiecik Piotr, Sputa-Grzegrzółka Patrycja, Grzelak Joanna, Dąbrowski Paweł: New equations for the estimation of the age of the formation of the Harris lines, Life, 2024, vol. 14, nr 4, art.501 [13 s.], DOI:10.3390/life14040501

   70 punktów, IF(3,2)

Łączny IF: 5,952

Łączne punkty MEiN: 210

Streszczenie

Niniejsza rozprawa doktorska składa się z trzech publikacji, dwóch oryginalnych oraz jednej pracy przeglądowej. Ich wspólnym mianownikiem są badania bioarcheologiczne, gdzie pierwsza praca stanowi przykład ich wykorzystania w praktyce, pozostałe dwie stanowią próbę rozwinięcia i udoskonalenia obecnie istniejących metod. Publikacje oryginalne zostały przeprowadzone na materiale kostnym pochodzącym z dawnych wrocławskich cmentarzy – cmentarza Salwatora (obecnie okolice pl. Czystego) oraz cmentarza przy parafii św. Barbary (okolice dawnego szpitala Józefa Babińskiego).

Pierwsza praca ("***A case of syphilis with high bone arsenic concentration from early modern cemetery [Wroclaw, Poland]***") skupia się na analizie przypadku czaszki pochodzącej z dawnego cmentarza Salwatora we Wrocławiu. Czaszka odznaczała się nietypowymi uszkodzeniami, które w toku diagnostyki różnicowej zidentyfikowano jako późne stadium syfilisu. W trakcie dalszej analizy wykorzystano metody histologiczne, w celu znalezienia zmian charakterystycznych dla tej choroby oraz spektrometrię mas, w celu określenia składu pierwiastkowego kości badanego osobnika. Według wstępnych hipotez zakładano, że analiza pierwiastków kości może wykazać podwyższony poziom rtęci, gdyż jej sole w okresie wczesnonowożytnym były szeroko wykorzystywane w leczeniu tego schorzenia. W szczątkach kostnych osób cierpiących na syfilis wielokrotnie ujawniono znacznie zwiększone stężenie rtęci – zwłaszcza w szczątkach pochodzących z okresu wczesnonowożytnego.

Niespodziewanie, stężenie rtęci nie było w znaczący sposób podwyższone, ale analiza ujawniła znacznie podwyższony poziom arsenu – 16μg/g kości. Zazwyczaj szczątki kostne mają stukrotnie mniejsze stężenie. Ze względu na niewielkie stężenie tego pierwiastka w glebie, jego przybytek w kości w skutek diagenezy jest mało prawdopodobny. Wśród hipotez mogących tłumaczyć tak wysoki poziom arsenu najbardziej prawdopodobne wydają się dwie. Badany osobnik mógł pracować w kopalni złota bądź arsenu, które znajdowały się na Dolnym Śląsku w stosunkowo niewielkiej odległości od Wrocławia (m. in. w oddalonym o 80 km Złotym Stoku). Niemniej, artykuły opisujące poziom tego pierwiastka w szczątkach kostnych pochodzących z cmentarzy zlokalizowanych w pobliżu kopalni zawierających związki arsenu, wykazywały jego niższe stężenie, niż u badanego osobnika.

Kolejna hipoteza sugeruje, iż podwyższony poziom arsenu może stanowić ślady terapii podjętej w celu wyleczenia badanego osobnika. Niemniej, w toku przeprowadzonej kwerendy, nie udało się potwierdzić stosowania terapii opartej na związkach arsenu w leczeniu syfilisu dla badanego okresu – zawierający arsen płyn Fowlera stosowany był dopiero od 1786 roku, podczas gdy cmentarz Salwatora funkcjonował do 1771 roku. Niemniej, nie można wykluczyć, iż związki arsenu były wykorzystywane w stosowanej lokalnie terapii, o której informacje nie zachowały się w źródłach pisanych.

Kolejne dwie prace poświęcone są liniom Harrisa (LH). LH to poziome, nieprzejrzyste linie, widoczne na niektórych kościach długich w obrazowaniu

rentgenowskim. LH mogą powstać jedynie w trakcie okresu wzrastania kości na długość – tworzą się w miejscu, w którym w danym okresie rozwoju znajdowała się płytka wzrostowa. Etiologia LH jest dość różnorodna i pozostaje obiektem licznych kontrowersji i żywej naukowej dyskusji. Według dominującej hipotezy, powstawanie LH najczęściej towarzyszy epizodom szeroko pojętego stresu fizjologicznego – m.in. okresom niedożywienia lub przebiegowi ciężkiej choroby. Stąd też obecność LH jest używana w antropologii fizycznej jako niespecyficzny wskaźnik wstępowania epizodów stresu fizjologicznego w dzieciństwie bądź młodości.

Umiejscowienie LH na kości jest zależne od okresu życia, w którym doszło do zahamowania/wznowienia wzrostu. Im bliżej pierwotnego punktu kostnienia znajduje się LH, tym wcześniej ona powstała. To zjawisko umożliwia uzyskanie bardzo cennych z punktu widzenia bioarcheologii informacji – obecność LH pozwala nie tylko ustalić prawdopodobne występowanie epizodów stresu fizjologicznego, lecz także umożliwia określenie wieku, w którym ten epizod miał miejsce. Ponadto, LH mogą pozostać widoczne nawet pomimo zachodzącego stale procesu remodelacji kości, co pozwala na analizę okresu dzieciństwa i młodości na podstawie kości dorosłych osobników.

Ze względu na nieliniową dynamikę wzrostu kości opracowanie metody pozwalającej skutecznie oszacować wiek stanowiło pewne wyzwanie, którego w XX wieku podjęto się siedmiokrotnie. Każdą z uzyskanych wówczas metod dokładnie opisano w drugiej pracy wchodzącej w skład niniejszej rozprawy („***How to calculate the age at formation of Harris lines? A step-by-step review of current methods and a proposal for modifications to Byers' formulas***"). Począwszy od metody opracowanej przez Allison i wsp., na metodzie opracowanej przez Byersa kończąc.

Każda z metod oferowała pewne udoskonalenia, niemniej jednak ich dokładna analiza pozwoliła na zastosowanie dalszych optymalizacji. Metoda Byersa – choć została wskazana w niniejszej pracy jako najlepsza – nie umożliwiała przeprowadzenia obliczeń dla kości dzieci i młodzieży, a tylko na kościach dorosłych osobników. W pracy dokonane zostały modyfikacje, które poszerzyły możliwości metody Byersa także o kości dziecięce. Zastosowana modyfikacja była o tyle ważna, że przed jej opublikowaniem dokładne oszacowanie wieku powstania LH w kościach dzieci możliwe było tylko dla dystalnej części piszczeli.

Metody obliczania wieku powstania LH nadal można było udoskonalić, co było celem trzeciej pracy wchodzącej w skład niniejszej rozprawy („***New equations for the estimation of the age of the formation of the Harris lines***"). Poza jedną (obarczoną znacznymi błędami) metodą obliczania LH, każda z dotychczas opracowanych metod bazowała na tabelach, które pozwalały na obliczenie wieku LH z dokładnością do jednego roku. Sprowadzenie metod pozwalających obliczyć wiek LH do równań kwadratowych bądź równań wykładniczych umożliwiło uzyskanie dokładniejszego wyniku.

Znaczącym wyzwaniem w tej pracy był wybór najdokładniejszego modelu. Takiego, który wymaga najmniejszej liczby parametrów i generuje najmniej błędów. W tym

wyborze pomogło zastosowanie kryterium informacyjnego Akaike (AIC), które pozwoliło na selekcję optymalnego rozwiązania.

W efekcie uzyskano szereg równań dla proksymalnych i dystalnych części piszczeli i kości udowych, dla kobiet i mężczyzn, dzieci i dorosłych. Równania zostały zebrane w arkuszu kalkulacyjnym, który po wprowadzeniu dwóch zmiennych – odległości LH od końca kości oraz jej całkowitej długości – podaje przybliżony czas powstania linii. To proste narzędzie pozwala oszacować czas powstania LH szybciej i dokładniej niż którakolwiek z zaproponowanych dotąd metod.

Nowo opracowaną metodę przetestowano na kościach pochodzących z cmentarza przy dawnej parafii św. Barbary. Uzyskano pozytywne rezultaty, wskazujące na spójność dokonanych obliczeń.

Mimo dokonanego postępu, dalsza optymalizacja nadal jest możliwa – największym ograniczeniem dokładności opracowanej metody jest różnorodna dynamika wzrostu kości w różnych populacjach i okresach historycznych, co uniemożliwia wyprowadzenie jednego, uniwersalnego wzoru. Dalsza optymalizacja mogłaby uwzględniać dostosowywanie wzorów dla poszczególnych populacji historycznych.

Niezależnie od wymienionych ograniczeń, dwie ostatnie prace wchodzące w skład cyklu powinny znacznie poprawić jakość prowadzonych w przyszłości badań uwzględniających analizę LH.

Summary

The current doctoral dissertation comprises three publications: two original articles and one review paper. The doctoral dissertation's principal focus is on bioarchaeology, with the initial publication exemplifying its practical applications. The remaining two papers endeavour to refine and enhance existing methodologies.

The first paper ('A case of syphilis with high bone arsenic concentration from early modern cemetery [Wroclaw, Poland]') focuses on a case study of a skull from the old Salwator cemetery in Wroclaw. The skull was characterised by atypical lesions, which in the differential diagnosis were identified as late-stage syphilis. Further analysis used histological methods to find lesions characteristic of the disease and mass spectrometry to determine the elemental composition of the bones in the sample. Initial hypotheses were that elemental analysis of the bones might reveal elevated levels of mercury, as its salts were widely used to treat the disease in the early modern period. Bone remains from syphilis sufferers repeatedly showed significantly elevated levels of mercury, particularly in remains from the early modern period.

Surprisingly, mercury concentrations were not significantly elevated, but the analysis revealed significantly elevated levels of arsenic – 16µg/g. Most bone remains tend to have concentrations 100 times lower. Given the low concentration of this element in the soil, an increase through diagenesis is unlikely. Among the hypotheses that could explain such high arsenic levels, two seem most likely. The studied individual could have worked in a gold or arsenic mine, which were located in Lower Silesia at a relatively short distance from Wrocław (e.g. in Złoty Stok, 80 km away). However, articles describing the levels of these elements in bone remains from cemeteries located near mines containing arsenic compounds were much lower.

A further hypothesis suggests that the elevated arsenic levels may represent traces of a therapy undertaken to cure the individual under study. However, in the course of the search carried out, it was not possible to confirm the use of arsenic compound therapy in the treatment of syphilis for the period under study - the arsenic-containing Fowler's solution was only used from 1786, where the Salvator cemetery was in operation until 1771. Nevertheless, it cannot be ruled out that arsenic compounds were used in a locally applied therapy only, information about which has not survived in written sources.

The next two papers are devoted to Harris lines (HLs). HLs are horizontal, opaque lines visible on some long bones on X-ray imaging. HLs can only form during the period of bone growth in length - they form where the growth plate was located during the given period of development. The aetiology of HL is quite diverse and remains the subject of much controversy and lively scientific debate. According to the prevailing hypothesis, HL formation most often accompanies episodes of broad physiological stress - including periods of malnutrition or as a result of the course of severe disease. Hence, the presence of HL is used in physical anthropology as a non-specific indicator of the onset of episodes of physiological stress in childhood or adolescence.

The location of the HL on the bone is dependent on the period of life in which growth inhibition or recovery occurred. The closer the HL is to the primary ossification center, the earlier it was formed. This phenomenon makes it possible to obtain very valuable information from a bioarchaeological point of view - the presence of HLs not only makes it possible to establish the likely occurrence of episodes of physiological stress, but also to determine the age at which the episode took place. In addition, HLs can remain visible even despite the ongoing process of bone remodelling, making it possible to analyse childhood and youth from the bones of adult individuals.

Due to the non-linear dynamics of bone growth, the development of a method to effectively estimate age was somewhat of a challenge, which was tackled seven times in the 20th century. Each of the methods obtained at that time is described in detail in the second paper of this thesis ("How to calculate the age at formation of Harris lines? A step-by-step review of current methods and a proposal for modifications to Byers‘ formulas’). Starting from the method developed by Allison et al. up to the method developed by Byers.

Each method offered some improvements, but careful analysis nevertheless allowed further optimisations to be applied. The Byers method – although identified as the best method in the present study - did not allow calculations to be carried out for the bones of children and adolescents, but only on the bones of adult individuals. In the present study, modifications were made that extended the Byers method's capabilities to also include the bones of non-adult individuals. The modification used was important because, prior to its publication, an estimation of age at HL formation on the proximal parts of children's tibias was essentially impossible.

However, the methods for calculating the age of HLs formation could still be improved, which was the aim of the third paper included in this thesis (‘New equations for the estimation of the age of the formation of the Harris lines’). Apart from one (with significant errors) method for calculating the LH, each method relied on tables that allowed the age of the LH to be calculated to the nearest year. Reducing the methods to calculate the age of the LH to quadratic or exponential equations allowed a more accurate result.

A significant challenge in this work was the selection of the most accurate model – which requires the least number of parameters and generates the fewest errors. This choice was aided by the use of the Akaike Information Criterion (AIC), which allowed selection of the optimal solution.

This resulted in a series of equations for the proximal and distal parts of the tibia and femur, for men and women, children and adults. The equations were compiled into a spreadsheet that, when two variables - the distance of the LH from the end of the bone and its total length – are entered, gives an approximate time of line formation. Faster and more accurate than any of the proposed methods.

The newly developed method was tested on bones from the cemetery at the former St Barbara's parish, with positive results indicating the internal consistency of the calculations made.

Although further optimisation is still possible - the most significant limitation of the accuracy of the developed method is the diverse dynamics of bone growth in different populations and historical periods, making it impossible to derive a single, universal formula. Further optimisation could include adapting the formulae to average growth data for different historical populations.

Notwithstanding these limitations, the last two papers in the series should significantly improve the quality of future research involving LH analysis.

Wstęp

Wrocław jako miasto z długowieczną, wielokulturową tradycją stanowi szczególnie interesujący obiekt badań bioarcheologicznych. Do połowy XVIII wieku zmarłych z Wrocławia grzebano głównie na przykościelnych cmentarzach. Badania porównawcze szczątków z różnych cmentarzysk umożliwiają w praktyce określenie różnic pomiędzy populacjami wyznającymi różne religie oraz pochodzących z różnych warstw społecznych (1). Ważnym aspektem jest też znany precyzyjny czas funkcjonowania wrocławskich cmentarzy. W drugiej połowie XVIII wieku, król Prus Fryderyk II zakazał grzebać zmarłych wewnątrz miast i nakazał przeniesienie nekropolii poza mury pruskich miast. Nowe zasady został wprowadzone we Wrocławiu w 1775 roku (2), wygaszając działalność wszystkich cmentarzy zlokalizowanych w obrębie murów miejskich i przenosząc je w okolice przedmurza. Z tego względu badania cmentarzy wrocławskich mogą dostarczyć ważnych informacji związanych z wczesnonowożytnymi populacjami Dolnego Śląska.

Badania z zakresu bioarchoelogii oraz antropologii fizycznej/biologicznej stanowią cenne uzupełnienie badań archeologicznych oraz kwerend źródeł historycznych (3). Źródła pisane przekazują jedynie informacje, które autorzy mogli i chcieli w nich zamieścić, niekiedy w jedynie umiarkowanym stopniu oddając rzeczywistość – czy to ze względu na ich niewiedzę czy też celowe działanie. Badania archeologiczne umożliwiają poznanie historii w bardziej obiektywny sposób, poprzez analizę materialnych śladów zostawianych przez dawne populacje dostarczając informacji na temat historii oraz zmian kulturowych, technologicznych oraz społecznych. Przywoływane powyżej dziedziny nauki nie pozwalają jednak na bezpośrednie określenie stanu zdrowia przedstawicieli dawnych populacji. W tym celu należy zastosować techniki oferowane przez antropologię fizyczną oraz bioarcheologię.

Obie dziedziny mają na celu ustalenie stanu zdrowia dawnych populacji, gdzie antropologia fizyczna korzysta głównie z makroskopowych oględzin, bioarcheologia – z badań mikroskopowych i laboratoryjnych. Te metody często pozwalają zweryfikować odkrycia historyczne oraz archeologiczne, umożliwiając doskonalszą kompilację pełnego obrazu dawnych populacji (4).

Z założenia bioarcheologia wymaga interdyscyplinarnego podejścia i wielopłaszczyznowej analizy. Materiał dostępny do badań jest często niekompletny, a wraz z upływem lat ulega zmianom tafonomicznym, które przy brak odpowiedniej badawczej ostrożności mogą prowadzić do błędnych wniosków. Prace badawcze z tej dziedziny powinny opierać się na uzupełniających się metodach, a sama metodologia badań musi być stale udoskonalana.

Wśród metod, które stanowią klasyczny marker do szacowania poziomu stresu fizjologicznego w populacjach historycznych, należy analiza linii Harrisa (LH) – poziomych linii widocznych czasem na kościach długich w obrazowaniu rentgenowskim (5). Mikroskopowo, LH są obszarem, w którym beleczki kostne tworzą grubą warstwę ułożoną poprzecznie do osi długiej kości. Etiologia LH może być dość różnorodna.

Większość czynników, które je wywołuje, jest niekorzystna dla organizmu – wymienia się m.in. niedożywienie, ciężkie choroby, alkoholizm czy zatrucie metalami ciężkimi (5,6).

LH powstają jedynie w okresie wzrostu kości na długość, w obszarze płytki wzrostowej. Dokładny mechanizm powstawania nie został ustalony. Najczęściej wymienia się dwie hipotezy – „zatrzymanego wzrostu" i „wznowionego wzrostu". Według pierwszej, LH zaczynają tworzyć się w momencie, w którym wzrost kości na długość zostaje zatrzymany, druga zakłada tworzenie się LH jako efekt wznowienia wzrostu kości po okresie zahamowanego wzrastania. Niezależnie jednak od uznanego modelu, można założyć, że występowanie LH będzie zbieżne w czasie z występowaniem niekorzystnych dla organizmu zdarzeń (6).

Umiejscowienie LH na kości jest zależne od okresu życia, w którym doszło do zahamowania/wznowienia wzrostu. Im dalej od nasady kości znajduje się linia, tym wcześniej ona powstała (7). Z tego względu badanie LH pozwala nie tylko określić samo występowanie epizodów mocnego stresu fizjologicznego, lecz również oszacować wiek, w którym one wystąpiły. LH mogą przetrwać nawet dekady remodelacji kości, w związku z czym pozwalają one na retrospektywną ocenę stanu zdrowia w dzieciństwie i młodości nawet u dorosłych osobników (8).

Z tego względu LH są dość często wykorzystywane w populacyjnych badaniach bioarcheologicznych – nawet jeśli dostarczają dość niespecyficznych informacji, mogą pomóc w oszacowaniu różnic związanych z jakością życia wśród różnych populacji historycznych, dobrze uzupełniając bardziej szczegółowe metody.

Dość często jednak w badaniach porównuje się samą liczbę LH, ignorując chronologię ich powstawania (9). Metody obliczania chronologii powstawania LH są dość skomplikowane, brakowało też pracy podsumowującej i uporządkowującej techniki obliczania czasu powstania tych linii. Na wielu poziomach możliwa była też ich znacząca optymalizacja, której dokonałem w dwóch pracach wchodzących w skład niniejszej rozprawy. W jednej z nich do oceny jakości udoskonalonej metody wykorzystane zostały szczątki pochodzące z cmentarza przy parafii św. Barbary, zlokalizowanego w okolicy dawnego szpitala Babińskiego.

W bioarcheologii zaskakująco dużą rolę odgrywają nie tylko prace populacyjne, lecz również kazuistyczne, gdzie odkrycia nawet na poziomie pojedynczego osobnika mogą mocno zmienić postrzeganie badanego okresu historycznego (10). Prace kazuistyczne mogą odgrywać szczególne znaczenie w poszerzaniu naszej wiedzy na temat epidemiologii dawnych chorób oraz na temat metod ich leczenia.

W niniejszej pracy zastosowano narzędzia z zakresu antropologii fizycznej oraz bioarcheologii do opisania czaszki znalezionej na dawnym protestanckim cmentarzu Salwatora (1). Dzięki nim udało się znaleźć możliwe ślady leczenia syfilisu nieopisywane do tej pory dla badanego obszaru oraz okresu historycznego.

Przypisy:

1. Burak M, Okólska H. Cmentarze Dawnego Wrocławia; Wydawnictwo Muzeum Architektury: Wroclaw, Poland, 2007. Wrocław; 2007.

2. II F. Circulare an sämtliche Breslauer Kammer- Departaments wegen Beerdigung der Leichen aller Religions- Verwandten außerhalb den Städten, [w:] Sammlung aller in den souvereinen Herzogtum Schlesien und demselben incorporierten Grafschatz Glatz in Financen, Ordnungen, Edicte, Breslau. 1785.

3. Buikstra JE, Ubelaker DH. Standards for data collection from human skeletal remains. Réimpression. Fayetteville (Ark.): Arkansas archeological survey; 1994. (Arkansas archeological survey research series).

4. Buikstra JE, Beck LA. Bioarchaeology: The Contextual Analysis of Human Remains. Taylor & Francis; 2017. 629 s.

5. Kulus MJ, Dąbrowski P. How to calculate the age at formation of Harris lines? A step-by-step review of current methods and a proposal for modifications to Byers' formulas. Archaeol Anthropol Sci. kwiecień 2019;11(4):1169–85.

6. Georgiadis AG, Gannon NP. Park-Harris Lines. J Am Acad Orthop Surg [Internet]. 6 luty 2023 [cytowane 16 wrzesień 2024]; Dostępne na: https://journals.lww.com/10.5435/JAAOS-D-22-00515

7. Byers S. Calculation of age at formation of radiopaque transverse lines. Am J Phys Anthropol. lipiec 1991;85(3):339–43.

8. Papageorgopoulou C, Suter SK, Rühli FJ, Siegmund F. Harris lines revisited: Prevalence, comorbidities, and possible etiologies. Am J Hum Biol. maj 2011;23(3):381–91.

9. Kulus MJ, Cebulski K, Kmiecik P, Sputa-Grzegrzółka P, Grzelak J, Dąbrowski P. New Equations for the Estimation of the Age of the Formation of the Harris Lines. Life. 13 kwiecień 2024;14(4):501.

10. Simpson R, Cooper DML, Swanston T, Coulthard I, Varney TL. Historical overview and new directions in bioarchaeological trace element analysis: a review. Archaeol Anthropol Sci. styczeń 2021;13(1):24.

Cel i założenia pracy

Głównym celem niniejszej pracy jest rozwój obecnych metod stosowanych w bioarcheologii oraz zastosowanie ich na szczątkach kostnych pochodzących z wrocławskich cmentarzy, ze szczególnym uwzględnieniem cmentarza Salwatora (obecnie – okolice pl. Czystego we Wrocławiu) oraz cmentarza przy parafii św. Barbary (obecnie - okolice byłego szpitala Józefa Babińskiego we Wrocławiu). Do realizacji tego zamierzenia wyznaczyłem 2 cele szczegółowe:

1. W pierwszej z prac wchodzącej w skład niniejszego cyklu, celem było dokładne zbadanie czaszki pochodzącej z wrocławskiego cmentarza Salwatora. Uszkodzenia obecne na niej sugerowały chorobę o przewlekłym przebiegu, czaszkę zbadano więc pod kątem zarówno określenia śladów choroby, jak i ewentualnego leczenia. Według pierwotnych założeń, badany osobnik cierpiał na zaawansowane stadium syfilisu i w związku z tym można było założyć stosowanie terapii z użyciem soli rtęci, co mogło być odzwierciedlone w składzie pierwiastkowym kości.

2. Dwie kolejne prace poświęcone są udoskonaleniu metod oszacowania wieku powstania linii Harrisa (LH). W pierwszej celem było usystematyzowanie dotychczasowych metod oraz opracowanie nowej, umożliwiającej szacowanie wieku powstania LH na kościach dzieci i młodzieży. W drugiej celem było dalsze udoskonalenie i uproszczenie zmodyfikowanych metod oraz ich wdrożenie na populacji pochodzącej w wrocławskiego cmentarza przy parafii św. Barbary.

Publikacje wchodzące w skład rozprawy doktorskiej

1. Dąbrowski Paweł, **Kulus Michał Jerz**y, Cieślik Agata, Domagała Zygmunt, Wiglusz Rafał J., Kuropka Piotr, Kuryszko Jan, Thannhauser Agata, Szleszkowski Łukasz, Dzięgiel Piotr: *A case of syphilis with high bone arsenic concentration from early modern cemetery (Wroclaw, Poland)*, Open Life Sciences, 2019, vol. 14, s. 427-439, DOI:10.1515/biol-2019-0048, łączna liczba autorów: *12*, 40 punktów, IF(0,69)

2. **Kulus Michał Jerzy**, Dąbrowski Paweł: *How to calculate the age at formation of Harris lines? A step-by-step review of current methods and a proposal for modifications to Byers' formulas*, Archaeological and Anthropological Sciences, 2019, vol. 11, nr 4, s. 1169-1185, DOI:10.1007/s12520-018-00773-5, 100 punktów, IF(2,063)

3. **Kulus Michał J**., Cebulski Kamil, Kmiecik Piotr, Sputa-Grzegrzółka Patrycja, Grzelak Joanna, Dąbrowski Paweł: *New equations for the estimation of the age of the formation of the Harris lines*, Life, 2024, vol. 14, nr 4, art.501 [13 s.], DOI:10.3390/life14040501, 70 punktów, IF(3,2)

Łączny IF: 5.953

Łączna punktacja MEiN: 210

DE GRUYTER Open Life Sci. 2019; 14: 427–439

Research Article

Pawel Dabrowski*, Michal Jerzy Kulus, Agata Cieslik, Zygmunt Domagala, Rafał J. Wiglusz, Piotr Kuropka, Jan Kuryszko, Agata Thannhauser, Lukasz Szleszkowski, Piotr Marian Wojtulek, Daniel Solinski, Piotr Dziegiel

A case of syphilis with high bone arsenic concentration from early modern cemetery (Wroclaw, Poland)

https://doi.org/10.1515/biol-2019-0048
Received October 31, 2018; accepted August 2, 2019

Abstract: Venereal syphilis is a sexually transmitted disease caused by Treponema pallidum – Gram-negative, slowly growing bacteria. The spread of the disease in the Old World was due to increased birth rate, urban population growth, migration and lack of knowledge concerning the epidemiology. In the past, the treatment was mainly symptomatic and included application of mercury compounds. The goal of the study was to present the case of advanced venereal syphilis found in early modern (16th–18thc) graveyard localized in Wroclaw, Poland. The object of the study is a cranium of a male whose age at death has been estimated to be over 55. In order to observe the morphological and paleopathological characteristics of the examined material, anthropometrics, computed tomography, spectrometry and microscopic methods were incorporated. Microscopic analysis revealed the presence of the extensive inflammatory lesions. Analyses indicate tertiary stage of venereal syphilis as the most probable cause of the observed lesions. Concentration of arsenic (16.17±0.58 μg/g) in examined bone samples was about hundred times bigger than average arsenic concentration in bones reported in other studies. Advanced stage of observed lesions along with high arsenic level may suggest long-lasting palliative care and usage of arsenic compound in therapeutic treatment of this chronic disease.

Keywords: syphilis, mercury, treponematoses, bioarchaeology, paleopathology

Abbreviations: CT – computed tomography; LCH - Langerhans cell histiocytosis; H&E – hematoxylin and eosin stain; MM – multiple myeloma

***Corresponding author: Pawel Dabrowski,** Department of Human Morphology and Embryology, Division of Normal Anatomy, Wroclaw Medical University, ul. Chalubinskiego 6a, 50-368 Wroclaw, Poland
E-mail: pawel.dabrowski@umed.wroc.pl
Zygmunt Domagala, Department of Human Morphology and Embryology, Division of Normal Anatomy, Wroclaw Medical University, ul. Chalubinskiego 6a, 50-368 Wroclaw, Poland
Michal Jerzy Kulus, Department of Human Morphology and Embryology, Division of Ultrastructure Research, Wroclaw Medical University, ul. Chalubinskiego 6a, 50-368 Wroclaw, Poland
Piotr Dziegiel, Department of Human Morphology and Embryology, Division of Histology and Embryology, Wroclaw Medical University, ul. Chalubinskiego 6a, 50-368 Wroclaw, Poland
Agata Cieslik, Department of Anthropology, Institute of Immunology and Experimental Therapy, Polish Academy of Sciences in Wroclaw, ul. Weigla 12, 53-114 Wroclaw, Poland
Rafał J. Wiglusz, Institute of Low Temperature and Structure Research, Polish Academy of Sciences, ul. Okolna 2, 50-422 Wroclaw, Poland
Rafał J. Wiglusz, Centre for Advanced Materials and Smart Structures, Polish Academy of Sciences, ul. Okolna 2, 50-422 Wroclaw, Poland
Piotr Kuropka, Jan Kuryszko, Department of Histology, Wroclaw University of Environmental and Life Sciences, ul. Norwida 25, 50-375 Wroclaw, Poland
Agata Thannhauser, Lukasz Szleszkowski, Department of Forensic Medicine, Wroclaw Medical University, ul. Mikulicza-Radeckiego 4, 50-345 Wroclaw, Poland
Piotr Marian Wojtulek, Institute of Geological Sciences, University of Wroclaw, Pl. Borna 9, 50-205 Wroclaw, Poland

1 Introduction

Venereal syphilis has been given many names over five centuries and they have been usually connected with the history of its spread (e.g., lues, French disease, Hungarian disease, or Neapolitan disease) [1]. The disease has been recognized for hundreds of years from South America to the Far East [2–6]. Among researchers, there are different opinions as for geographical regions of the primary outbreaks as well as paths of the disease spread. There

is also no unanimity as whether syphilis originated from Europe or North or South of America. Some authors claim to have found evidence for syphilis in Europe even before Columbus discoveries [7–9], although other authors present just opposite arguments [10,11]. Genetic analyses of the sequenced genomes of modern *Treponema pallidum* strains indicate a common ancestor after the fifteenth century, within the early modern era [12]. Nevertheless, it had become a pandemic disease by the end of the 15th century [13,14].

In Poland, the first well documented syphilis case was recorded in historical sources two years after Columbus' return from his first expedition [15]. However, there is a study indicating a probable case of syphilis dating from the 14th century from Wroclaw, Poland [16–18].

Venereal syphilis is a disease caused by *Treponema pallidum subsp. pallidum* – Gram-negative bacteria which is slowly growing, usually 6–15 μm long and 0.1–0.2 μm in diameter. It reveals small tolerance for extracorporeal conditions. There are no methods to grow the *T. pallidum* bacterial culture for clinical purposes [19]. One can get infected with venereal syphilis only by direct contact with infected tissue (usually as a result of sexual intercourse or contact with exudative lesions). Due to bacteria slow growth, it takes 2-3 weeks pass for the infection to develop the first symptoms. The disease is manifested with painless, generally solitary and indurated ulcerative lesions [19]. Besides venereal syphilis, *Treponema* bacteria are also responsible for other diseases, such us non-venereal/endemic syphilis (caused by *T. p. endemicum*), yaws (*T. p. pertenue)* and pinta (*T. caretum*). All these four diseases are defined as treponematoses. However, only venereal syphilis has been widely spread in Europe; whereas pinta remains restricted to Central and South America, yaws – to tropical regions and endemic syphilis – to Middle East mainly [20]. We can distinguish three stages of treponematoses. In venereal syphilis, primary symptoms (painless lesion called "chancre" located in the inoculation site, mostly on sex organs) disappear without medical treatment after 3 to 6 weeks with no visible scars [19,20]. Secondary stage occurs shortly after the onset of primary symptoms. It is manifested with diverse, painless rash (1-2 cm diameter), lesions on palms and soles, sore throat, fever, loss of appetite, headache and meningitis which take from a couple of weeks to several months. As the symptoms tend to take variant course, other diseases can be misdiagnosed instead of syphilis [19]. The third stage of the disease can develop in the period from a few years up to decades after infection and its most characteristic lesions include gummata (effect of chronic granulomatous processes) and non granulomatous inflammations [18,21,22]. Both types of lesions can affect bones as inflammation usually begins in periosteum or in the bone cortex and finally involves both structures as well as medullary cavity. They are characteristic for excessive osteosclerosis and soft tissue (skin, mucous membranes, nostrils) get ulcerated. Lesions resulting from tertiary syphilis are most often found in long bones, however, other bones, including skull, may be affected as well [22–25].

In the past, venereal syphilis was called "the Great Imitator" for its diagnostic difficulties [25–28]. Syphilis results in diverse inflammatory changes which are similar to the effects of other diseases like: myeloma, Langerhans cell histiocytosis, leprosy and other treponematoses [29].

Even at present, syphilis may evoke clinical problems being mistaken for other diseases (especially when a clinician is not acquainted with patient's sexual history). Although the treatment may prove problematic in the case of antibiotic resistant strains or patient's allergy to antibiotics [19], yet still it is curable. However, in the past ,there was no effective drug for this disease. Trials of syphilis treatment in medieval and early modern period concentrated mainly on "cleansing" the organism with the use of diaphoresis or diuresis [9]. However, despite applied methods, they could not bring expected healing effects [30]. Mercury and its derivatives were the most common agents applied in these procedures and they were widely promoted by Paracelsus (1493-1541) [9]. Signs of chronic mercury treatment can be observed in elevated concentrations of this element in bone material harvested from archaeological sites [31,32].

Undoubtedly, the spread of venereal syphilis within the Old World was due to increased birthrate, urban population growth, migration and lack of knowledge about its epidemiology [3,33]. Gilewska-Dubis (2000), in her study of medieval Wroclaw, observed that syphilis was one of the most frequent causes of death among city inhabitants in the late 15th century. In Poland, the oldest case attributed to venereal syphilis is a skull and fragments of limb bones harvested from the church of St. Giles (14th century)[16]. However, some authors still remain skeptical about this report [34]. The first case of venereal syphilis in Poland was officially recorded in 1495, [18] whereas the treatment of veneral syphilis on a large scale began in 1528, in St. Roch Hospital in Krakow. Half of the facilities in that place were dedicated solely to syphilis treatment. During last five centuries, this disease has been mentioned in many Polish written sources and described sign and symptoms imply venereal syphilis

rather than other treponematoses [35]. This report, presents pathological evaluation of a of skull of an adult, which was subsequently classified as a possible case of venereal syphilis.

2 Material

The research was conducted on a skull obtained during excavations carried on in 2006-2007 on Pl. Czysty (Czysty Square) in Wroclaw (Poland), former Cemetery of Our Saviour (Fig. 1). Excavations were thoroughly described elsewhere [36,37].

In total, 1426 burials including 103 secondary interments were explored. The burials were often multiple, with visible displacements, disturbances and loose bones [36,37]. However, no sign of intentional looting or desecration were observed. The cemetery was used to bury inhabitants of surrounding villages and socially excluded people (such as suicides and convicts).

The analyzed skull (marked after the exploration of the grave as object No. 2000) was a isolated element without a sepulchral context or postcranial skeleton within grave No. 942, bearing the traces of grave reutilization [36].

All remains harvested from the cemetery were dated on the basis of information contained in parish chronicles and artifacts, i.e. coins or belt components. However, it is obvious that precise dating with coins in this case is rather inconclusive as in the graves, coins 100 years older than the cemetery were found. There were no Prussian coins found in findings which implies that the cemetery functioned at the latest to the first half of the 18th century and it remains consistent with written historical sources [37,38]. The examined skull is be assessed as originating from the late 16th to the mid 18th century [36], which overlaps the whole period of the cemetery existence. The material consisted of skull without mandible, with ovoid shape in *norma verticalis*. Preliminary macroscopic examination revealed *antemortem* teeth loss and the presence of extensive osteolytic lesions involving the parietal bone cortex and about 60% of the frontal bone. It was the most damaged *antemortem* skull in the whole Cemetery of Our Saviour material.

3 Methods

3.1 Sex and age at death evaluation

The following macroscopic characteristics of skull were observed to define the sex of the individual: nuchal crest, mastoid process, supraorbital margin and prominence of glabella, [39,40]. The evaluation of sex was supported by analysis of skull morphometrics. The measurements used were g-op (glabella-ophistocranion), eu-eu (eurion-eurion), ba-b (basion-bregma), zy-zy (zygion-zygion), mf-ek (maxillofromtale-ektokonchion), sbk-spa (subconchion-supraconchion), apt-apt (aperthion-aperthion). Measurement listed were compared with mean values obtained for males and females from the cemetery.

Skull morphological features were examined with the

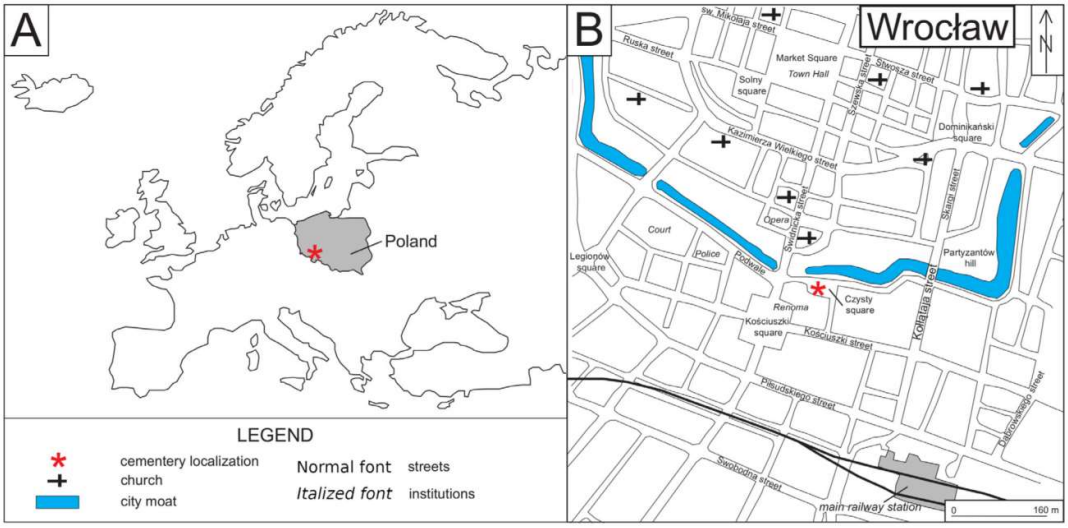

Fig. 1. A: Wroclaw City/Poland B: Former Cemetery of our Saviour (Czysty Square/present)

use of measurement techniques established by Martin and Saller [41,42] with spreading caliper and sliding caliper and then compared with other skulls from Cemetery of Our Saviour [37]. Due to lack of postcranial skeleton, the age at death of the individual was assessed basing on cranial sutures obliteration[40], examination of histological slides as well as according to Kerley's observations (1965) and finally, interstitial lamellae (remnants of former osteons, abundant in bones of old individuals) and the amount of unremodelled bone and the number of nonosteonal vascular canals (which are typical for bones of younger individuals) were evaluated.

3.2 Macroscopic evaluation of bone lesions

Assessment was performed with descriptive techniques including comparative data on the extent and shape of bone tissue defects [44,45].

Differential macroscopic analysis of bone lesions and osteolytic lesions were also performed in accordance with the differentiation criteria described by Ortner [22] and Putschar [46].

3.3 Computed tomography

Analysis of neurocranium and facial skeleton was made with the use of dual source computed tomography (DSCT) SIEMENS Somatom AS+; 80kv i 120kV/20 mAs; scanned with 1 mm layers.

3.4 Histological slides

Samples for histological analysis were harvested from the frontal bone in the Institute of Geological Sciences, University of Wroclaw with the use of a diamond saw.

Two methods were incorporated to elicit histological slides. The first sample was used to create a histological thick section with polisher-grinder and finally affixed to the glass. The second sample was fixed overnight in 4% formaldehyde which was followed by decalcification in EDTA for two weeks, and then for a month in sodium citrate and formic acid solutions. Decalcified sample was then used to prepare thin histological sections, which were stained with hematoxylin and eosin (H&E) with standard protocol [44].

The images were processed using Nikon 80i Eclipse with a UV-2A filter with a CCD Nikon camera (Nikon, Tokyo, Japan).

3.5 Electron Microscopy

Two 150 µm thick sections were prepared in the Institute of Geological Sciences at the University of Wroclaw for electron microprobe investigations. The major element composition of minerals was analyzed by electron microprobe (Cameca SX-100 at the Faculty of Geology, University of Warsaw, Poland) with energy dispersive X-ray spectroscopy (EDS). This method provides information on elemental and mineral composition of the histological section.

3.6 Analysis of elemental composition

Analysis was carried on 3 samples harvested from the left side of the frontal bone, 0,45 g each (powdered in agate mill) as well as from samples of dirt adjacent to the skull. The weighed amount of samples was etched in 2 ml of concentrated nitric acid, evaporated and dissolved in 10 ml.

The analysis was measured with inductively coupled plasma optical emission spectrometry (ICP-OES; Agilent 720,Wroclaw, Poland). Analytical lines: As: 194 nm, Hg: 273 nm and Pb: 220 nm.

4 Results

4.1 Sex and age at death evaluation

Diagnostic characteristics of the skull such as strongly defined glabella, massive superciliary arch, thickened supra-orbital margin and pronounced inferior nuchal line as well as external occipital protuberance indicate male sex of the individual.

The skull was assessed as short and low in its neurocranial part (*brachycranius* and *tapeinocranius*), with a medium-height orbit (*mesoconch*). Detailed anthropometric parameters are presented in Figure 2. The profile presents normalized values of differences between certain measurements of the skull and mean values of the assessment for male skulls from Czysty Square in Wroclaw. There are no statistically significant disparities as they do not exceed 1.96 SD.

Morphological and histological characteristics of the skull were used to estimate the biological age as over 55 years. Assessment was based on the course and obliteration of sutures, i.e. sagittal and lambdoid ones. Histological assessment (suggesting similar age) was based on relatively high amount of fragments of remodeled

osteons and low amount of non-osteal vascularization Numerous interstitial lamellae, as the remains of earlier generations of lamellae postponed from the periosteal and endosteal side and osteons in the middle part of the frontal bone were detected. They confirmed the observation that the skull belonged to an older adult [47]. More accurate assessment of age was impossible, as the postcranial skeleton was missing.

4.2 Macroscopic evaluation of bone lesions

Irregular malformation of 9 × 6.7 cm (Fig. 3A, B) was found within frontal bone left side squama. The lesions were configured as wide irregular bone defects extending to the anterior part of the frontal sinus on the left side of the frontal bone. The frontal bone in this region was markedly thinner as a result of extensive bone loss. The edges of this opening were thick, convex, and rounded, which was attributed to bone remodelling indicative of the sclerotic healing process. On the right side of the basal part of the frontal bone, there was a regular round lesion (1.0 cm in diameter) penetrating towards the interior of the frontal sinus. Below the left frontal tuber, there was an irregular defect, 3.5 × 1.3 cm, exposing the spongy tissue of the frontal bone and leading to the anterior cranial fossa.

Within the anterior nasal aperture, significant loss of nasal bone caused by the osteolytic process and a convex deformation near the frontonasal suture could be observed. On the left side of the nasal cavity, traces of osteolysis in the nasal conchae were visible, along with signs of osteolysis around the maxillary hiatus. The bony nasal septum showed traces of the healed fracture with vomer displacement towards the left side.

In the orbital plate of the ethmoid bone, an extensive oval bone defect was detected. The left frontal process of the maxilla was reduced and the right proved thinner. Deformation in the form of thickening of the lower edge of the right orbit could be also found, probably resulting from a healed Le Fort II fracture within the zygomaticomaxillary suture [48] (Fig. 3C).

The lesions penetrating the frontal bone and traces of osteolysis were confirmed by CT imaging. On the CT scans, the lesions are visible as lucencies and rarefactions in the cortical bone and diploë. Moreover, CT scans revealed the presence of an ongoing inflammatory process within the anterior cranial fossa and the left side of the middle cranial fossa (Fig. 3D, E).

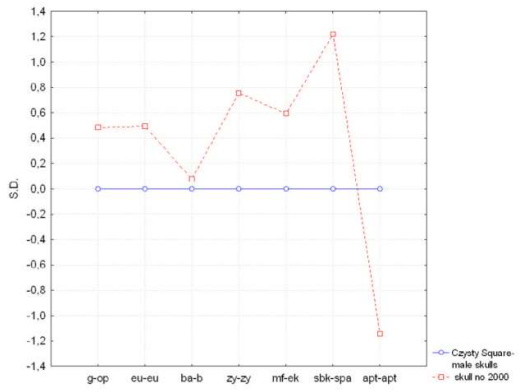

Fig. 2. Profile presenting normalized values of differences between some measurements of the skull from grave no. 2000 and mean values of the assessment of male skulls from Czysty Square in Wroclaw. The anthropometric parameters do not differ significantly (differences do not exceed 1.96 S.D.) as compared to average values of measurements of male skulls from Czysty Square in Wroclaw, which suggest that the skull belonged to the male individual.

4.3 Paleopathological differential diagnosis

In the macroscopic picture of the disease, the predominating signs are extensive osteolytic lesions, manifested as bone loss foci with sclerotic margins observed mainly on the frontal bone and within the nasal cavity structures. Such signs may result from granulomatous inflammation, thus other pathologies that share the mechanism of the infection should be taken into consideration in the differential diagnosis. One of granulomatous chronic infections is tuberculosis (caused by *Mycobacterium tuberculosis*). It can produce destructive lesions within different elements of the skeletal system [49]. However, even in the pre-antibiotic era, calvarial tuberculosis was extremely rare with the prevalence estimated at the level below 1% of all skeletal tuberculosis cases [22]. Leprosy was another mycobacterial disease considered as a possible cause of the pathological changes observed in the facial skeleton of the cranium No. 2000 for the fact that at the advanced stage of this disease, extensive damages within the nasal cavity (in the form of rhinomaxillary syndrome) could be observed. Leprosy is characteristic for resorption of the anterior nasal spine and the alveolar bone crest below as well as for the osteolysis within the upper alveolar arch. Bilateral changes in the shape of the piriform aperture, with remodeling of its edge [50,51] are another specific quality of this abnormality. In the examined case, we observed osteolysis only within the nasal cavity walls and nasal conchae with pronounced loss of the nasal bones. In the lower part of the piriform aperture, the anterior nasal

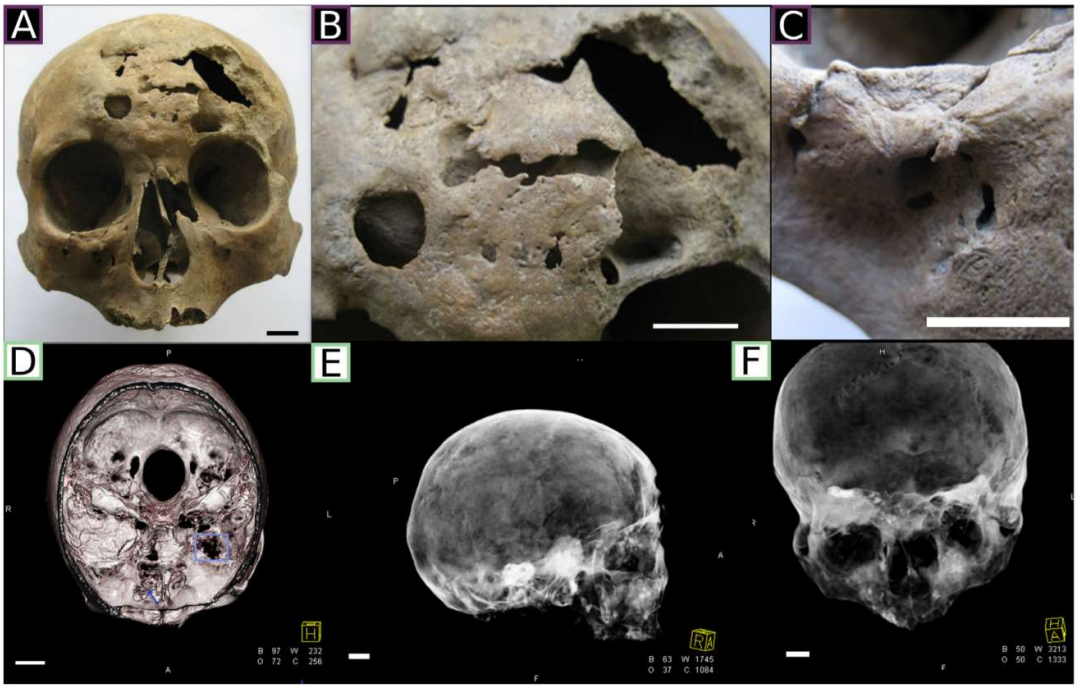

Fig. 3. The skull 2000. A: Frontal view. B: Highly damaged frontal bone. C: Fracture in the right zygomaticomaxillary suture. D: Cross-horizontal-section of the skull in CT. Arrow and square indicate the inflammation on the base of theskull (anterior and middle cranial fossa) E: CT image of the right side of the skull. In the base of the vault lucencies are visible. F: CT image of the front of the skull. All damages and lesions of the skull have been thoroughly described in the results section. Scale bar=1cm.

spine was preserved, which suggested excluding leprosy as possible diagnosis.

The observation of multiple osteolytic lesions within the cranium No. 2000 from Czysty Square in Wroclaw was also the cause for concern for the possibility of the neoplastic etiology of the pathological changes. Among proliferative diseases which could have produced lesions similar to those observed in the case presented in our study, multiple myeloma (MM) and other tumors as well as Langerhans cell histiocytosis (LCH) were considered in differential diagnosis.

In the course of MM, numerous osteolytic foci, scallope-edged, round or oval in shape could be usually observed in the CT imaging. The most characteristic feature of those lesions was the extensive cortex loss without osteoblastic response. The most frequently observed clinical manifestation of MM in the cranium were numerous, well-delineated, lytic bone lesions and punched out lucencies which could be observed in CT imaging. [52,53]. Such changes were absent in the CT scans of the examined skull. Also, other tumors – metastatic or primary – were not likely to be included in this group. The margins of lesions caused by lytic metastases tend to be similar as for MM, however they may present osteoblastic reaction [54]. Blastic metastasis or benign tumor would result in osteoblastic lesions, absent on the skull.

Another option considered in differential diagnosis was LCH. The most frequent sign in the course of the disease is extensive loss within the flat bones (including skull bones). A description of the *clinical picture of LCH included numerous, round superficial defects and perforations of the skull vault without any visible signs of regenerative process* [55]. Lesions could be observed also in the basal part of sella turcica. This abnormality affects mainly juveniles and young adults (15-18 years old) [56]. In the examined cranium no analogy to this description was found.

Both localization and morphology of lesions can be considered as typical for late stage (tertiary) of treponematoses, i.e. venereal syphilis. In the course of venereal syphilis, the disease affects mainly these elements of the skeleton in which periosteum strictly adheres to the bone surface. They are mainly frontal and parietal bones of the neurocranium and proximal parts of the long bones shafts. The lesions within

neurocranium characteristic for the tertiary syphilis are usually caused by gummata production, which subsequently stimulates the periosteum to inflammatory response. Gummata can derive from the subcutaneous tissue, bone, periosteum or muscles [57]. In the case of the cranial bones, gummata are usually situated on the frontal and parietal bones and they cause pathological changes called caries sicca. Caries sicca is a scar remaining after healing of superficial gummatous osteitis of calvaria [58]. This sequence of caries sicca formation begins from appearance of clustered pits followed by absorption of the cortical and cancellous bone leading to exposing wide regions of the cranial dura mater and ends with bone remodelling and scarring [24,59]. In the facial skeleton, the loss of nasal bones with destructive remodeling of piriform aperture and frontal processes of the maxilla can be observed [22]. Moreover, perforations in the thin-walled structures of the maxillary corpus and within the walls of the orbits are possible. The thinning of the lateral walls of the nasal cavity, palatine process and nasal septum may also occur. The shape of the nasal spine usually remains unchanged [24]. Pathological changes observed macroscopically as a complex of extensive osteolytic and hyperplastic lesions within the supraorbital region, as well as in the infraorbital and nasal part of the viscerocranium corresponded with the description of features characteristic for skeletal signs of tertiary stage of treponematose as the primary cause of the lesions observed in the cranium No 2000.

In conclusion, in respect of this paper, the signs of disease like perforating lesions with serpiginous cavitations and osteolysis, can be considered as the effects of a chronic inflammatory process associated with bone remodeling resulting in osteolytic complications. It was evidenced by the CT imaging as lucencies and rarefactions revealed in the cortical bone. It has already been mentioned that both macroscopic and CT images of the disease correspond with the traits characteristic for venereal syphilis as the most common treponematose [4,46,60]. Treponematoses have diverse course and many cases do not have characteristic pattern of skeletal lesions, which makes diagnosis quite challenging [60]. Also, the course may be modified by other infections accompanying treponemal syndromes, such as fungal or bacterial infections, which also may be destructive for nasal or palate tissue and cannot be excluded from diagnosis [54]. Although other treponematoses such as yaws or endemic syphilis cannot be clearly distinguished from venereal syphilis in the macroscopic evaluation, venereal syphilis is the most probable diagnosis. Yaws is usually acquired in childhood and is a tropical disease, uncommon in Central Europe, and endemic syphilis is usually most common in Middle East and Africa [22].

4.4 Histological examination

Histological examination revealed irregular bone matrix saturation with hydroxyapatite (Fig. 4). The inclusions of unspecified foreign compounds were found, visible as areas of different emission of excited light (Fig. 4F, yellow color). Different excisions of various intensity were observed in some lacunae and canaliculi. Because of the presence of minor impurities, there were lacunae emitting white-blue or yellow light or showing no excision. In some areas of the frontal bone, inclusions could be found extracellularly in the bone matrix. Bone tissue was mostly normal, yet there were areas with pronounced osteolysis with visible traces of regeneration (Fig 4A-E, orange arrows).

Analysis of slides stained with H&E confirmed observations made with fluorescent microscopy.

4.5 Electron microscopy

Electron EDS microscopy investigations of the samples showed that the bone consists mostly of apatite ($Ca_5(PO_4)_3$). Locally numerous, minute (1-3 μm) sulphide inclusions (galena - PbS, sphalerite - ZnS and covellite - CuS) occured along boundaries between various generations of apatite (Fig. 5 and 6). As or Hg containing minerals were not detected.

4.6 Elemental composition evaluation

Results of analysis are presented in Table 1. Content of As, Hg and Pb is significantly higher in bone than in dirt samples. Cemetery of Our Saviour soil is mostly composed of sand, clay and loess formations. Its formation fits the lowland category, Fluvisols and Cambisol group. Brown and acid brown soils occur predominantly [61,62]. Obtained results are typical for soil in Wroclaw [62,63].

Table 1. Concentration of arsenic, mercury and lead in skull and adjacent dirt.

Element	Skull (μg/g)	Dirt (μg/g)
Arsenic (As)	16.17±0.58 μg/g	0.0954±0.006 μg/g
Mercury (Hg)	0.311±0.019 μg/g	0.0310±0.0010 μg/g
Lead (Pb)	44.02±0.71 μg/g	0.367±0.014 μg/g

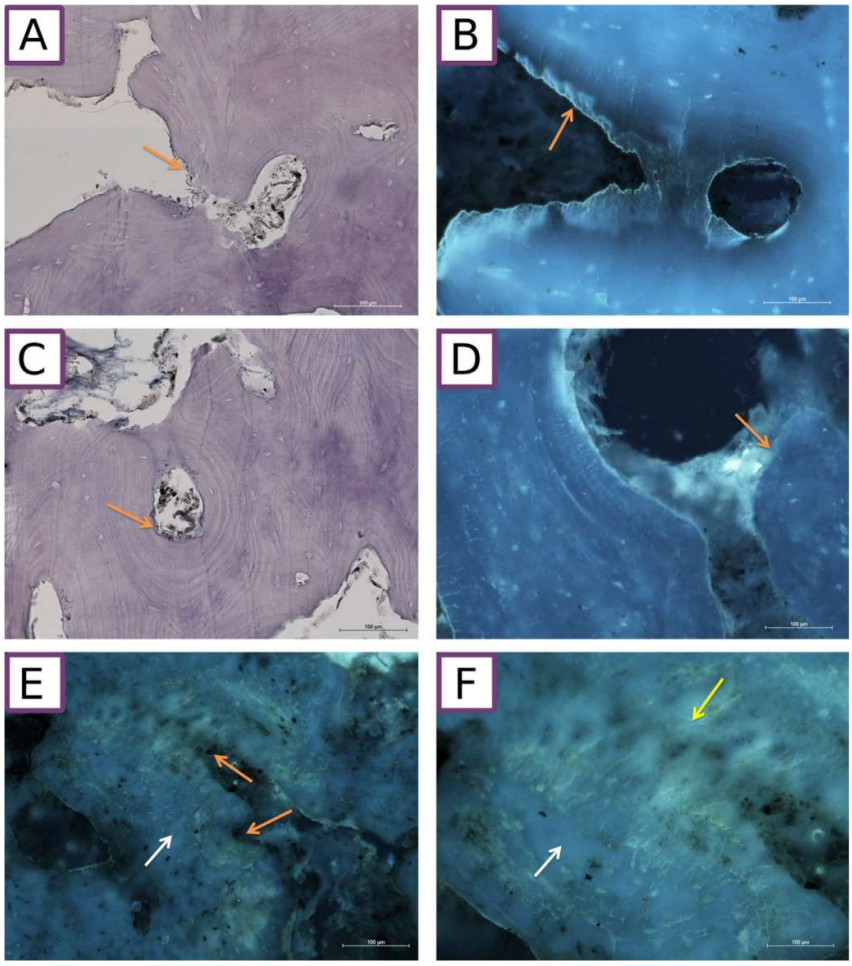

Fig. 4. Histological microsections. A, C: Stained with H&E, light microscopy. B, D, E, F: Unstained, autofluorescence. There are areas of bone covered by several layers of bone lamellae and rough areas presenting osteolysis (orange arrows). Moreover, there is no trace of osteogenesis which should follow resorption. E,F: Diverse autofluorescence of different areas of bone matrix. Proper, blue (white arrow) and untypical, light-yellow (yellow arrow).

5 Discussion

Skull No. 2000 belonged to a older adult male. It didn't differ with its shape or anthropological parameters from average values calculated from all male skulls found in Cemetery of Our Saviour. The proportions corresponded with features of other male skulls from several Early Modern cemeteries in Wroclaw [64,65]

Macroscopic examinations indicated tertiary venereal syphilis. According to many researches, this disease is manifested (among others) with extensive osteolytic bone loss with an ongoing regeneration process [22,54,59]. In the case of the studied skull, the expanse of bone lesions of the frontal bone suggested bacterial spreading to dura mater and subdural structures up to nervous tissue [66]. Observed osteolytic loss and fistulas in the facial skeleton, especially in the center of frontal bone and within the nasal cavity along with remodeling of the surroundings of the frontonasal suture, indicated chronic disease [67], which might have had destructive influence on the nasociliary and facial nerve [68].

Rarefaction of the compact bone structure combined with endocranial perforating lesions visible in the CT

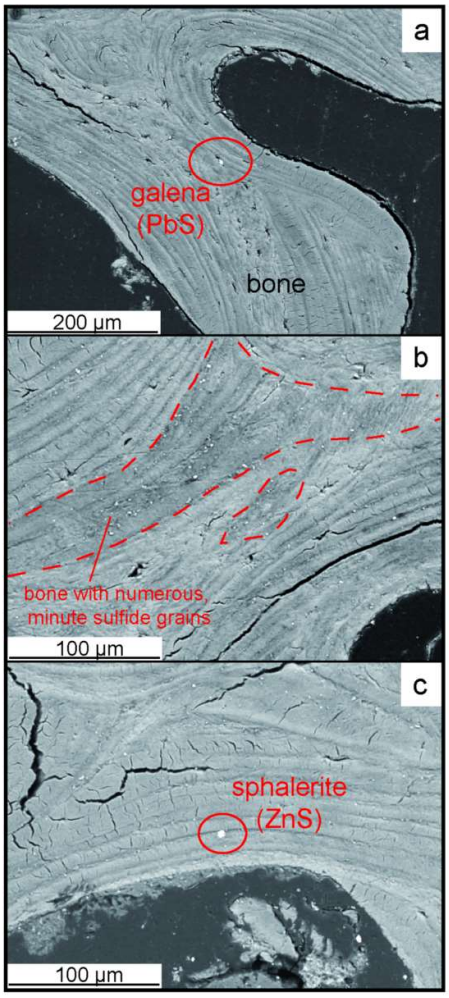

Fig. 5. Back-scattered electron images of the bone from the Czysty Square: a - general view of the bone structure showing various generations of apatite, b - minute sulphide mineralization in the bone structure (surrounded by red line), c - a grain of sphalerite - ZnS (white) occurring between various kinds of apatite.

image confirmed the destructive course of acquired syphilis. The osteolytic process penetration of the sinuses, anterior cranial fossa and areas to the left side of the middle cranial fossa was particularly visible.

Microscopic analysis (unstained thick sections and H&E stained sections) indicated extensive osteolysis, which was followed by bone regeneration. The region that was especially vulnerable were periosteal cell directly adjacent to skin. However, suppressed osteosynthesis was observed on the endosteal side. It could have been caused by arsenic, as it blocks proteins sulfhydryl groups, which leads to, among other things, cell cycle arrest in S phase and therefore to inhibition of bone regeneration [69,70].

Syphilis was treated in medieval and early modern times with mercury compounds, although the treatment was ineffective [9]. Such a therapy can result in the deposition of a considerable amount of this metal in the bones [32]. The concentration of mercury (Hg) in bone tissue differs according to the location of the sample. Increased Hg levels are observed in the most spongy structures, whereas in compact bone, levels are significantly lower [32]. There are no established standards for mercury concentration in bone structures. In some publications[31,71,72], the average concentration of Hg in bone tissue is approximately several dozen ng/g of dry mass. However, Rasmussen et al. (2008) found remains with no visible lesions (including syphilitic lesions) with a concentration of up to 300 ng/g of dry mass.

The results of chemical analysis revealed a moderately high Hg concentration (0.31 µg/g) in the examined bone fragments. It is unclear whether the subject was treated with mercury compounds. The concentration of this element in syphilitic patients treated with its compounds is usually significantly higher, even above 3 µg/g [31,73]. The presence of mercury in the skull may have been unrelated to the treatment of syphilis. In the Middle Ages and Early Modern period mercury was used as laxative as well as a drug for conjunctivitis, corneal irritation, psoriasis, eczema, tinea, skin lesions and others [74]. In addition, mercury was used as an ink and painting pigment, a gold treatment agent and a cosmetic ingredient [32].

The second heavy metal examined was arsenic, the concentration of which in frontal bone samples was 16.17±0.58 µg/g. However, the concentration of this element did not lead to formation of minerals detectable by EDS scanning microscopy, yet it exceeded significantly the values obtained by other researchers from bone material without long-lasting contact with arsenic compounds [72,75,76]. Diagenetic uptake of arsenic is unlikely, due to lack of this element is dirt samples. Its presence in bones can be explained in several ways.

Arsenic-containing medicines were already used in Antiquity. Hippocrates used aurapigment and realgar (As_2S_3 and As_2S_2, respectively) as ingredients in salves, whereas in ancient Rome, Galen used mentioned salts to treat ulcers [77]. In the Renaissance period, arsenic compounds were recommended by Paracelsus and William Whithering [77].

These early physicians used the antiseptic, antipyretic, cholagogic, diastolic, calming and tonic properties of arsenic compounds [78]. Although arsenic (As) was used in Chinese medicine [78], there is no information

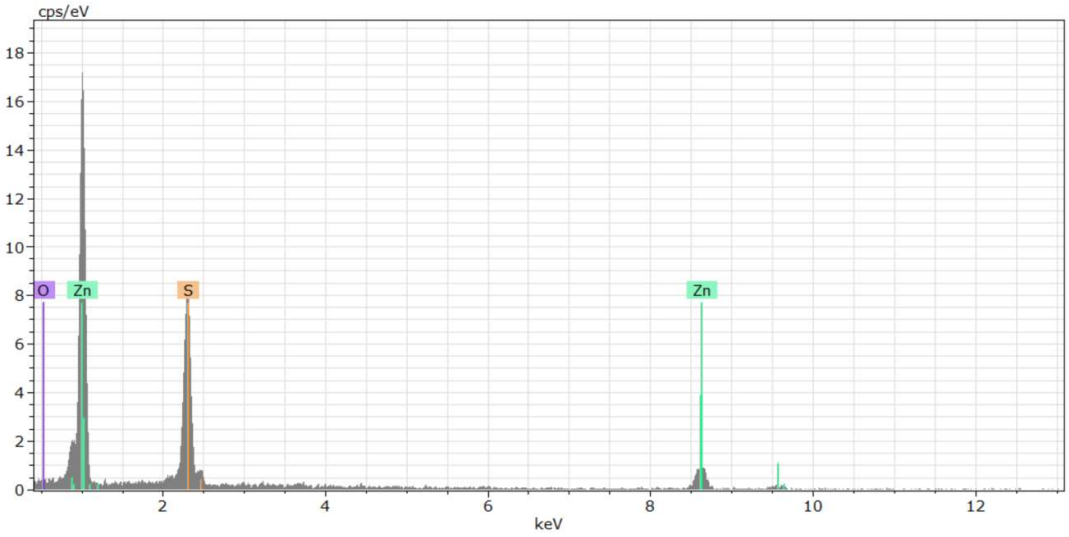

Fig. 6. Representative EDS analysis of sulphide (sphalerite - ZnS) grains occurring within the bone showing the peaks of the Zn and S. Cps/eV – count per second electron-volt, keV: kilo-electron-volt.

about common usage of As in medieval or Early Modern Europe. The first broadly used treatment of syphilis with arsenic compound was Fowler's solution however, it was introduced in the second half of XVIII century, whereas the studied skull was older [79]. However, syphilis, called in the past "the Great Imitator" [29], was often misdiagnosed as a tumor, tuberculosis, bone inflammations or leprosy [26], which could be treated with arsenic compounds. In addition, arsenic was quite accessible in Lower Silesia, as arsenic mines were present nearby and could be widely used in medicine by the local community [80].

It is possible that As presence was not strictly connected with treatment, but rather with occupational activity. Arsenic was used as a component of paints or stained glass as well as for leather and wood preservation [78]. The processes associated with these products could have resulted in increased arsenic concentration in bones.

In Zloty Stok (about 80 km from Wroclaw), gold and arsenic mines have been located since 13th century [80]. Work in mining with arsenic salts could significantly increase the level of As in bone tissue [81]. However, this theory has a weak point, because the examined skull belonged to an elderly, sick man. Most likely, he would not have been in the condition for hard and physical work.

Acute and lethal arsenic poisoning significantly increases the concentration of arsenic in hair and soft tissues; it does not, however, leave significant traces in bone tissue [82]. Therefore, acute poisoning should be excluded in this case. The diagenetic intake of this element is also improbable, as the soil samples from the grave did not contain high amounts of As [83].

Lead concentration did not differ significantly from the mean values obtained in previous studies [72,84]. Minerals found by EDS microscopy (galena - PbS, sphalerite - ZnS and covellite – CuS) proved typical for bone tissue and did not indicate any pathological conditions [85] as did not forms of distinct biominerals in the bone structure, detectable by electron EDS microscopy.

6 Conclusions

The above results most likely indicate acquired syphilis treated with arsenic compounds or arsenic damage effects occupational activity. The issue of arsenic level in bones in Lower Silesia may be interesting for future research.

Acknowledgements: We would like to thank prof. Slawomir Koziel from the Department of Anthropology, Institute of Immunology and Experimental Therapy in Wroclaw, for sharing osteological material from Czysty Sq. for our studies. We would like to thank also prof. Urszula Zaleska-Dorobisz and PhD Roman Badowski from the Wroclaw Medical University, Department of Radiolgy, for valuable consultations in interpretation of CT images. We would like also to honour Stanislaw Gronkiewicz, who has passed away recently, for cooperation in preliminary study on the specimen.

Conflict of interests: Authors state no conflict of interest .

References

[1] Tagarelli A, Tagarelli G, Lagonia P, Piro A. A brief history of syphilis by its synonyms. Acta Dermatovenerologica Croat. 2011;19(4):228–236.

[2] Suzuki T. Palaeopathological and palaeoepidemiological study of osseous syphilis in skulls of the Edo period. 1984. University of Tokyo Press https://catalog.hathitrust.org/Record/000566303. Accessed 16 March 2017.

[3] Grmek MD. Historia chorób u zarania cywilizacji zachodniej. 2002. Warszawa. W.A.B.

[4] Marden K, Ortner DJ. A case of treponematosis from pre-Columbian Chaco Canyon, New Mexico. Int J Osteoarchaeol. 2011;21(1):19–31.

[5] Gawlikowska-Sroka A, Dzięciołowska-Baran E. Syphilis in the past and present. Ann Acad Med Stetin. 2013;59(2):162–165.

[6] Castro MM, Benavente MA, Ortega J, Acuña R, Montero C, Thomas C, et al. Thoracic aortic aneurysm in a pre-Columbian (210 BC) inhabitant of Northern Chile: Implications for the origins of syphilis. Int J Paleopathol. 2016;13:20–26.

[7] Mays S, Crane-Kramer G, Bayliss A. Two probable cases of treponemal disease of Medieval date from England. Am J Phys Anthropol. 2003;120(2):133–143.

[8] Erdal YS. A pre-Columbian case of congenital syphilis from Anatolia (Nicaea, 13th century AD). Int J Osteoarchaeol. 2006;16(1):16–33.

[9] Tampa M, Sarbu I, Matei C, Benea V, Georgescu SR. Brief history of syphilis. J Med Life. 2014;7(1):4–10.

[10] Harper KN, Ocampo PS, Steiner BM, George RW, Silverman MS, Bolotin S, et al. On the origin of the treponematoses: A phylogenetic approach. PLoS Negl Trop Dis. 2008;2(1). doi:10.1371/journal.pntd.0000148.

[11] Šmajs D, Norris SJ, Weinstock GM. Genetic diversity in Treponema pallidum: Implications for pathogenesis, evolution and molecular diagnostics of syphilis and yaws. Infect Genet Evol. 2012;12(2):191–202.

[12] Arora N, Schuenemann VJ, Jäger G, Peltzer A, Seitz A, Herbig A, et al. Origin of modern syphilis and emergence of a pandemic Treponema pallidum cluster. Nat Microbiol. 2016;2(December):1–6.

[13] Quétel C, Podgórska-Klawe Z. Niemoc z Neapolu czyli historia syfilisu. 1991. Zakład Narodowy im. Ossolińskich Wrocław.

[14] Gładykowska-Rzeczycka JJ. Syphilis in ancient and medieval Poland. Orig Syph Eur Before or After. 1994;1493:116–118.

[15] Steciwko A, Siejka D. Choroby, które zmieniły bieg historii. Przew Lek GPs. 2010;13(2):11–15.

[16] Kwiatkowska B, Nowakowski D, Drukier P, Trnka J, Busko C. Zmiany chorobowe średniowiecznego szkieletu z kościoła św. Idziego we Wrocławiu. Acta Univ Wratislav. 2002;(2423):27–37.

[17] Gładykowska-Rzeczycka J, Pudło A. Próba odtworzenia struktury morfologiczno-demograficznej ludności pochowanej na cmentarzysku z okresu rzymskiego w Pruszczu Gdańskim, stanowisko 7. In: *XIII Sesja Pomorzoznawcza. Od wczesnego średniowiecza do czasów nowożytnych*. 2003: 319–333.

[18] Dzięciołowska-Baran E, Gawlikowska-Sroka A. Kiła dawniej i dziś. Ann Acad Med Stetin. 2013;59(2):162–165.

[19] Hook EW. Syphilis. Lancet. 2016;6736(16). doi:10.1016/S0140-6736(16)32411-4.

[20] Powell ML, Cook DC. The Myth of Syphilis: The Natural History of Treponematosis in North America. 2005 doi:10.1002/evan.20077.

[21] Greenfield GB. Radiology of bone disease. 1986.

[22] Ortner DJ. Identification of Pathological Conditions in Human Skeletal Remains. 2003. San Diego. Elsevier.

[23] Steinbock RT. Paleopathological diagnosis and interpretation: bone diseases in ancient human populations. 1976. Charles C Thomas Pub Limited.

[24] Schultz M. Comparative histopathology of syphilitic lesions in prehistoric and historic human bones. Orig Syph Eur before or after. 1994;1493:63–67.

[25] Aufderheide AC, Rodriguez-Martin C, Langsjoen O. The Cambridge encyclopedia of human paleopathology. 1998. Cambridge University Press.

[26] King A, Catterall R. Syphilis of bones. Br J Vener Dis. 1959;35:116–28.

[27] Gładykowska-Rzeczycka J. Schorzenia swoiste ludności z dawnych cmentarzysk Polski. Przegląd Antropol. 1982;48(1–2):39–54.

[28] Mann RW, Hunt DR. Photographic regional atlas of bone disease: a guide to pathologic and normal variation in the human skeleton. 2013. Charles C Thomas Publisher.

[29] Fitzgerald F. The Great Imitator, Syphilis-Medical Staff Conference, University of California, San Francisco. J West Med. 1981;(May):424–432.

[30] Zuckerman MK. More Harm than Healing? Investigating the Iatrogenic Effects of Mercury Treatment on Acquired Syphilis in Post-medieval London. Open Archaeol. 2016;2(1):42–55.

[31] Rasmussen KL, Boldsen JL, Kristensen HK, Skytte L, Hansen KL, Malholm L, et al. Mercury levels in Danish Medieval human bones. J Archaeol Sci. 2008;35(8):2295–2306.

[32] Rasmussen KL, Skytte L, Pilekær C, Lauritsen A, Boldsen JL, Leth PM, et al. The distribution of mercury and other trace elements in the bones of two human individuals from medieval Denmark - the chemical life history hypothesis. Herit Sci. 2013;1(1):10.

[33] Gilewska-Dubis J. Życie codzienne mieszczan wrocławskich w dobie średniowiecza. 2000. Wydawn. Dolnośląskie.

[34] Harper KN, Zuckerman MK, Harper ML, Kingston JD, Armelagos GJ. The origin and antiquity of syphilis revisited: An Appraisal of Old World pre-Columbian evidence for treponemal infection. Am J Phys Anthropol. 2011;146:99–133.

[35] Koleta-Koronowska S. 430 lat wenerologii polskiej [430 years of Polish veneralogy]. Now Lek. 2010;6(79):487–494.

[36] Guszpit P, Mruczek R, Wojcieszak J, Wojcieszak M, Wójcik M. Pierwszy wrocławski cmentarz protestancki przy kościele imienia Salwatora – wstępne wyniki badań. In: Śródmiejska Katedra. Kościół św. Marii Magdaleny w dziejach i kulturze Wrocławia. 2010.

[37] Wachowski K, Klápště J, Krabath S, Młynarska-Kaletynowa M, Piekalski JI. Wratislavia Antiqua, t. 21. Cmentarz Salwatora. Pierwsza nekropolia wrocławskich protestantów. 2015. Uniwersytet Wrocławski, Instytut Archeologii.

[38] Książek K. Monety z dawnego cmentarza przy kościele Salwatora we Wrocławiu: opóźniona depozycja monet w darach grobowych. Wiadomości Numiz. 2010;54(1 (189)):7–71.
[39] Ascádi G, Nemeskéri I. History of human life span and mortality. 1970 http://www.jstor.org/stable/pdf/2740808.pdf. Accessed 15 December 2016.
[40] Buikstra JE, Ubelaker DH. Standards for Data Collection From Human Skeletal Remains. Arkansas Archaeol Surv Res Ser. 1994;44(5):272.
[41] Martin R, Saller K. Lehrbuch der Anthropologie. 1957. Stuttgart.
[42] Slice D. Modern morphometrics in physical anthropology. 2006, Springer US.
[43] Kerley ER. The microscopic determination of age in human bone. Am J Phys Anthropol. 1965;23(2):149–163.
[44] DiMaio V, DiMaio D. Forensic Pathology, Second Edition. 2001. CRC Press doi:10.1201/9781420042412.
[45] Kimmerle EH, Baraybar JP, Love JC. Skeletal Trauma: Identification of Injuries Resulting from Human Rights Abuse and Armed Conflict. 2008 doi:10.1007/s12024-008-9048-6.
[46] Putschar W, Ortner DJ, Walter GJ. Identification of Pathological Conditions in Human Skeletal Remains. Smithson Contrib to Anthropol. 1981;(28).
[47] Mnich B, Skrzat J, Szostek K. Estimating age at death from an archaeological bone sample - A preliminary study based on comparison of histomorphometric methods. Anthropol Rev. 2017;80(1):37–55.
[48] Fraioli RE, Branstetter BF, Deleyiannis FW-B. Facial Fractures: Beyond Le Fort. Otolaryngol Clin North Am. 2008;41(1):51–76.
[49] Tsangaras K, Greenwood AD. Museums and disease: Using tissue archive and museum samples to study pathogens. Ann Anat. 2012;194(1):58–73.
[50] Manchester K. Bone changes in leprosy: pathogenesis, palaeopathological diagnostic criteria, and clinical interpretation. 2012.
[51] Sharma VK, Bapuraj JR, Mann SB, Kaur I, Kumar B. Computed tomographic study of paranasal sinuses in lepromatous leprosy. IntJLeprOther MycobactDis. 1998;66(0148–916X):201–207.
[52] Rajkumar SV, Dimopoulos MA, Palumbo A, Blade J, Merlini G, Mateos MV, et al. International Myeloma Working Group updated criteria for the diagnosis of multiple myeloma. Lancet Oncol. 2014;15(12):e538–e548.
[53] Röllig C, Knop S, Bornhäuser M. Multiple myeloma. Lancet2014;385:2197–208.
[54] Grauer AL. A Companion to Paleopathology. 2012 doi:10.1002/9781444345940.
[55] David R, Oria RA, Kumar R, Singleton EB, Lindell MM, Shirkhoda A, et al. Radiologic features of eosinophilic granuloma of bone. AJR Am J Roentgenol. 1989;153(5):1021–6.
[56] Ardekian L, Peled M, Rosen D, Rachmiel A, Abu el-Naaj I, Laufer D, et al. Clinical and radiographic features of eosinophilic granuloma in the jaws: review of 41 lesions treated by surgery and low-dose radiotherapy. Oral Surg Oral Med Oral Pathol Oral Radiol Endod. 1999;87(2):238–242.
[57] Jabłońska S, Majewski S. Choroby skóry i choroby przenoszone drogą płciową. 2010. Warszawa. Wydawnictwo Lekarskie PZWL.
[58] Hackett CJ. An introduction to diagnostic criteria of syphilis, treponarid and Yaws (treponematoses) in dry bones, and some implications. Virchows Arch A Pathol Anat Histol. 1975;368(3):229–241.
[59] Hackett CJ. Diagnostic Criteria of Syphilis, Yaws and Treponarid (Treponematoses) and of Some Other Diseases in Dry Bones. 1976. Berlin. Springer-Verlag.
[60] Ortner DJ. Methods used in the analysis of skeletal lesions. In: Identification of Pathological Conditions in Human Skeletal Remains. San Diego, 2003;45–55.
[61] Szewrański S, Kazak J, Żmuda R, Wawer R. Indicator-based assessment for soil resource management in the Wrocław larger urban zone of Poland. Polish J Environ Stud. 2017;26(5):2239–2248.
[62] Kabala C, Chodak T, Szerszen L, Karczewska A, Szopka K, Fratczak U. Factors influencing the concentration of heavy metals in soils of allotment gardens in the city of Wroclaw, Poland. Fresenius Environ Bull. 2009;18(7):1118–1124.
[63] Dradrach A, Karczewska A. Mercury in soils of municipal lawns in Wrocław, Poland. Fresenius Environ Bull. 2013;22(Januart):968–972.
[64] Kwiatkowska B. Mieszkańcy średniowiecznego Wrocławia. Ocena warunków życia i stanu zdrowia w ujęciu antropologicznym. 2005. Wydawn. Uniwersytetu Wrocławskiego
[65] Kwiatkowska B, Nowakowski D. Charakterystyka antropologiczna szczątków kostnych z cmentarza przy kościele św. Marii Magdaleny we Wrocławiu (XVI-XVIII w.). 2011;(583):25–43.
[66] Minonzio G, Paolucci Colico M, Ghezzi A, Zarcone D. Imaging of cranio-meningeal infectious and inflammatory involvement. Neurol Sci. 2008;29(SUPPL. 2):279–282.
[67] Little JW. Syphilis: An update. Oral Surgery, Oral Med Oral Pathol Oral Radiol Endodontology. 2005;100(1):3–9.
[68] Leão JC, Gueiros LA, Porter SR. Oral manifestations of syphilis. Clinics (Sao Paulo). 2006;61(2):161–6.
[69] Izdebska M, Grzanka A, Szczepański MA, Litwiniec A. Selected mechanisms of the therapeutic effect of arsenic trioxide in cancer treatment. Postepy Hig Med Dosw (Online). 2008;62:463–467.
[70] Petres J, Baron D, Hagedorn M. Effects of arsenic cell metabolism and cell proliferation: cytogenetic and biochemical studies. Environ Health Perspect. 1977;19:223–7.
[71] Lanocha N, Kalisinska E, Kosik-Bogacka DI, Budis H, Sokolowski S, Bohatyrewicz A. Comparison of metal concentrations in bones of long-living mammals. Biol Trace Elem Res. 2013;152(2):195–203.
[72] Lindh U, Brune D, Nordberg G, Wester PO. Levels of antimony, arsenic, cadmium, copper, lead, mercury, selenium, silver, tin and zinc in bone tissue of industrially exposed workers. Sci Total Environ. 1980;16(2):109–116.
[73] Kępa M, Kozłowski T, Szostek K, Drozd A, Walas S, Mrowiec H, et al. Analysis of mercury levels in historical bone material from syphilitic subjects – pilot studies (short report). Anthropol Anzeiger. 2012;69(3):367–377.
[74] Kłys M. Z rtęcią (i ...) przez stulecia. Arch Med Sąd Kryminol. 2010;298–307.
[75] Brodziak-Dopierała B, Kwapuliński J, Kowol J. Occurrence of arsenic in selected parts of the human femur head. Polish J Environ Stud. 2011;20(6):1633–1636.
[76] Wiechula D, Jurkiewicz A, Loska K. Arsenic content in the femur head of the residents of southern and central Poland. Biol Trace Elem Res. 2003;92(1):17–26.
[77] Litwin I, Lis P, Maciaszczyk-Dziubińska E. Dwie twarze arsenu. Kosmos. 2009;58(1):187–198.

[78] Kulik-Kupka K, Brończyk-Puzoń A, Gwizdek K, Zubelewicz-Szkodzińska B. Arsen – trucizna czy lek? 2016;67(1):89–96.
[79] Sarquis M. Arsenic and old myths. R I Med. 1994;77(7):233–4.
[80] Lorenc MW. Podziemna Trasa Turystyczna „Kopalnia Złota" w Złotym Stoku (Dolny Śląsk). Geoturystyka. 2004;1(1):25–34.
[81] Oakberg K, Levy T, Smith P. A Method for Skeletal Arsenic Analysis, Applied to the Chalcolithic Copper Smelting Site of Shiqmim, Israel. J Archaeol Sci. 2000;27(10):895–901.
[82] Mari F, Polettini A, Lippi D, Bertol E. The mysterious death of Francesco I de' Medici and Bianca Cappello: an arsenic murder? BMJ Br Med J. 2006;333(7582):1299–1301.
[83] Pike AWG, Richards MP. Diagenetic Arsenic Uptake in Archaeological Bone. Can we Really Identify Copper Smelters? J Archaeol Sci. 2002;29(6):607–611.
[84] Noceń I. Analiza porównawcza składu mineralnego kości u ludzi w materiale archeologicznym z różnych rejonów Polski. Ann Acad Med Stetin. 1999;45:25.
[85] Frank Van de Vyver. Trace Metals and Fluoride in Bones and Teeth. 1990. Boston, MA.

Archaeological and Anthropological Sciences (2019) 11:1169–1185
https://doi.org/10.1007/s12520-018-00773-5

REVIEW

How to calculate the age at formation of Harris lines? A step-by-step review of current methods and a proposal for modifications to Byers' formulas

Michał Jerzy Kulus[1] · Paweł Dąbrowski[2]

Received: 6 August 2018 / Accepted: 21 December 2018 / Published online: 11 January 2019

Abstract
Harris lines (HL; also known as "growth arrest lines" or "transverse radiopaque lines") are horizontal sclerotic lines formed in the metaphyseal or diaphyseal part of long bones, usually visualized using X-ray images. Among the factors that may lead to a temporary arrest of bone growth (and thus—to HL deposition), the most commonly mentioned are nutritional disorders (malnutrition, protein, vitamin, and mineral deficiencies), a history of smallpox, pneumonia or other diseases, food poisoning, or alcohol abuse. The position of the HL is related to the period of incidence of physiological stress inhibiting bone growth, which enables the estimation of the age at which the subject was exposed to it. Such information can be valuable in the study on archeological populations; therefore, various methods have been developed to determine the age of HL deposition. In this review, six known methods for calculating the age of HL origin are presented and compared: Allison/McHenry, Hunt and Hatch, Clarke, Hummert and van Gerven, and Maat and Byers' methods. In addition, the authors propose here a modification to the last method in order to enable calculations on non-adult bones.

Keywords Harris lines · Transverse radiopaque lines · Age-at-line formation · Bone growth · Physiological stress

Introduction

Harris lines (HL; also known as "growth arrest lines" or "transverse radiopaque lines") are horizontal sclerotic lines formed in the metaphyseal or diaphyseal part of long bones, usually visualized using X-ray images (Nowak and Piontek 2002a), although also visible in computed tomography (Chauveau et al. 2016; Primeau et al. 2016), magnetic resonance imaging (Laor and Jaramillo 2009), or in histological slides (Miszkiewicz 2015). Most often they form on the tibia and therefore, it is the most frequently used bone for the study of HLs (Papageorgopoulou et al. 2011); nevertheless, they can form on any endochondral bone (Scott and Hoppa 2015).

HLs are a trace of a temporary bone growth arrest. Undisturbed secondary endochondral ossification has been presented and described in Fig. 1. Disruption of the process of chondrocyte proliferation or calcification means that the growth plate remains impenetrable for osteoblasts, which in turn cause mineralization along the horizontal chondrocyte layer at the end of the growth plate, forming the "primary stratum" perpendicularly to the long axis of the medullar cavity. Prolonged periods of growth arrest result in the thickening of the primary stratum, which leads to the deposition of the Harris line (Scott and Hoppa 2015). However, according to a different model, a HL forms when growth is re-established; increased cartilaginous proliferation and osteoblasts activity contribute to the thickening and forming of the transverse line, suggesting HLs are growth restart rather than growth arrest lines (Sajko et al. 2011).

Among the factors that may lead to a temporary arrest of bone growth (and thus—to HL deposition), the most

Electronic supplementary material The online version of this article (https://doi.org/10.1007/s12520-018-00773-5) contains supplementary material, which is available to authorized users.

✉ Michał Jerzy Kulus
mkulus@gmail.com

[1] Division of Histology and Embryology, Department of Human Morphology and Embryology, Wroclaw Medical University, ul. Chałubińskiego 6a, 50-368 Wrocław, Poland

[2] Division of Normal Anatomy, Department of Human Morphology and Embryology, Wroclaw Medical University, Wrocław, Poland

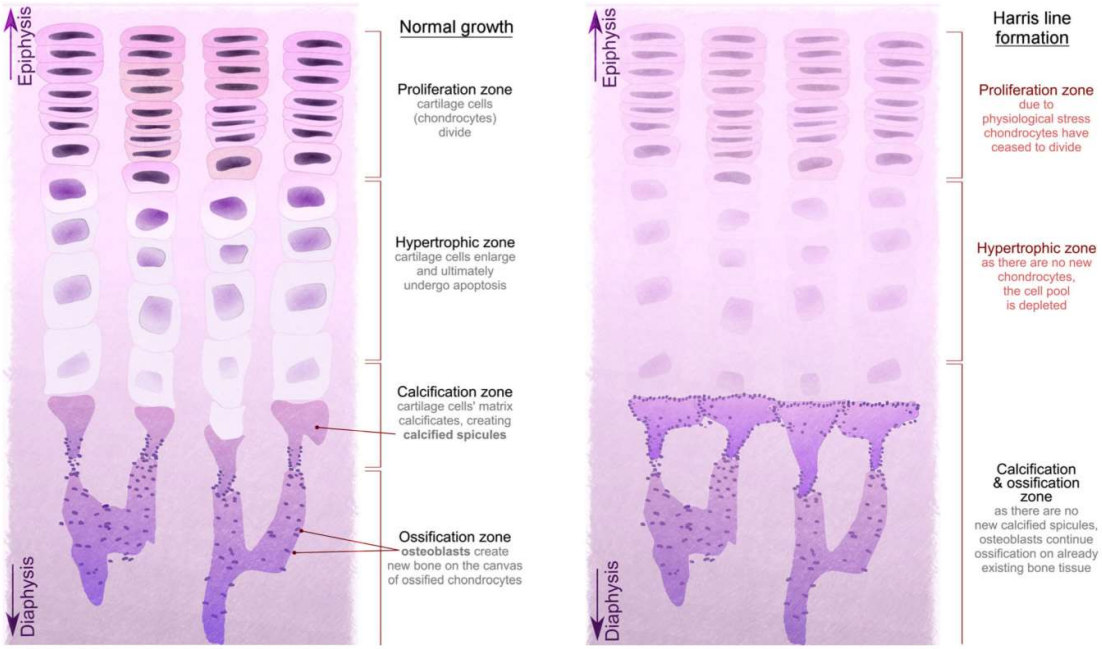

Fig. 1 Endochondral bone growth and the Harris lines deposition theory. Drawing on the left side presents undisturbed bone growth. (1) Chondrocytes (cartilage cells) from the resting cartilage zone move towards the bone diaphysis. (2) Proliferating chondrocytes form columns, proceeding towards the diaphysis. (3) Chondrocytes differentiate into hypertrophic chondrocytes which produce alkaline phosphatase, osteopontin, BSP, Osx, Bglap (osteocalcin), and Runx2 (Park et al. 2015), which induce calcification. (4) Hypertophic cells undergo apoptosis and calcify. (5) Osteoprogenitor cells differentiate into osteoblasts, causing the initiation of osteosis on the basis of calcified cartilage (Mescher 2013). The disruption of chondrocytes proliferation or differentiation (presented on the right side) makes the growth plate impenetrable for osteoblasts, which in turn begin to create a mineralized layer along the horizontal layer of chondrocytes at the end of the epiphyseal plate; they form a primary stratum perpendicular to the long axis of the medullary cavity. Prolonged periods of growth arrest result in the thickening of the primary stratum, which leads to the deposition of a Harris line (Scott and Hoppa 2015)

commonly mentioned are nutritional disorders (malnutrition, protein, vitamin, and mineral deficiencies), a history of smallpox, pneumonia or other diseases, food poisoning, or alcohol abuse (Nowak 1996). Among newer concepts, HLs can be linked to child abuse (Ross and Juarez 2016), systemic-onset juvenile idiopathic arthritis (Sifuentes Giraldo et al. 2016), tortures (Traczek 2017), psychosocial short stature (Kaspar Hauser syndrome; Khadilkar et al., 1998) osteopetrosis, hyper/hypoparathyroidism, sclerosing, spondylosis, radiation exposure, Cushing's Syndrome, rickets, avascular necrosis, osteoporosis, congenital syphilis, Paget's Disease, leukemia, scurvy, bone fracture (Sajko et al. 2011), and probably many more diseases and detrimental conditions. The wide spectrum of possible etiologies causes HLs to be considered as an indicator of an unspecific physiological stress or difficult living conditions rather than a specific diagnostic marker (Papageorgopoulou et al. 2011).

However, using HLs even in such a wide context is often questioned. In an in vivo experiment on rabbits, the authors noted that more HLs were formed during periods of rapid growth than in the period of nutritional stress (Alfonso-Durruty 2011). There was no statistically significant correlation between bone length and morphology and the occurrence of HL (Mays 1985; Nowak and Piontek 2002b). Moreover, numerous researchers have failed to find correlations between the age of enamel hypoplasia (EH) and HL formation, suggesting that HLs are a physiological rather than a pathological phenomenon (Piontek et al. 2001; Beom et al. 2014; Geber 2014; Zapala et al. 2016; Krenz-Niedbała 2017). Due to the similarities between the somatotropin (growth hormone) secretion curves, the long bone growth curves, and the distribution of HLs, it was suggested that HLs are associated with physiological periods of faster and slower growth (Papageorgopoulou et al. 2011).

Nevertheless, the lack of correlation between HL and EH may result from the disappearance of early-formed HLs as a result of bone remodeling at a later age (Mays 1995). In turn, the formation of HLs in a period of rapid growth corresponds to the theory of HLs as growth recovery lines. Moreover, if one consider the formation of HLs as a trace of physiological processes only, it is necessary to explain the differences in the frequency of HL occurrence between individuals and

populations found in numerous studies (Piontek et al. 2001; Beom et al. 2014; Geber 2014; Zapala et al. 2016; Krenz-Niedbała 2017). In addition, even if it will be concluded that HLs are poorly suited for determining the health of individuals (as it may be a result of non-pathological processes), they can still be useful for determining the overall health at the population level (Nowak and Piontek 2002b): assuming that the occurrence of HL unassociated with any pathologies is (more or less) constant, statistically different frequency of HL between the compared populations would result from different occurrence of HL associated with pathologies or physiological stress.

Regardless of the chosen HL formation model, it can be assumed that a HL is formed more or less in the time following the appearance of a stressor hindering growth to length. It is easy to deduce that the HL will be located where the growth plate was located when the growth was stopped/restored. The position of the HL is therefore related to the period of incidence of physiological stress inhibiting bone growth, which makes it possible to estimate the age at which the subject was exposed to it (Papageorgopoulou et al. 2011). Such information can be valuable in the study of archeological populations. The mere counting of HL allows to compare the level of physiological stress between specified groups. Calculation of the age of HL formation enables more comprehensive statistical approach. It can be concluded, which period of childhood or puberty in the study population was most abundant in adverse effects (Zítková et al. 2004; Krenz-Niedbała 2014; Boucherie et al. 2017)—and compared between specific groups (Jerszyńska and Nowak 1996). It is additional easily obtainable data that could improve the description of life of archeological populations. Therefore, various methods have been developed to determine the age of HL deposition (Allison et al. 1974; Hunt and Hatch 1981; Clarke 1982; Maat 1984; Hummert and Van Gerven 1985; Byers 1991).

In this review, six methods for calculating the age of HL origin will be presented: the Allison et al. (1974); McHenry and Schulz (1976), Hunt and Hatch (1981), Clarke (1982), Hummert and van Gerven (1985), Maat (1984) and Byers (1991) methods. To the best of the authors' knowledge, these are all known methods. In addition, a modification which enables calculations on non-adult bones will be proposed to the last of them. All tables required for calculations were included in Supplementary File 1, and all necessary measurements for each method—in Fig. 2. Summarized comparison of key features of all methods is presented in Table 1. Method output and detailed comparison are presented in the "Comparison of all methods" section.

However, before the presentation of methods, one important issue must be raised: what should be considered a Harris line?

What line should be considered a Harris line?

After death, HLs remain unchanged; they can be observed on the remains of more than 45,000 years (Nowakowski 2018). However, during a lifetime, the bone undergoes constant remodeling processes which results in a possible disappearance of the HL (Papageorgopoulou et al. 2011). This hinders the interpretation and use of HLs in archeological studies of the population, especially for the remains of older individuals.

Usually, when examining the bones of adult individuals, clear lines running along the entire length of the bones will not be found, but thin remains of distinct HLs will be visible instead. There are different approaches to what should be considered a HL. Some authors recommend taking into account lines of at least 25% of bone width (Goodman and Clark 1981; Piontek et al. 2001), others: at least one third (Alfonso et al. 2005; Chauveau et al. 2016) or half (Hummert and Van Gerven 1985; Scott and Hoppa 2015) of the bone. To the best of the authors' knowledge, there are no unambiguous guidelines suggesting the optimal solution in this matter.

Another approach is the arbitrary categorization of HLs; Maat (1984) categorized HLs into three types: weak (visible only upon careful inspection), medium, and strong, recognizing the third type as the most reliable determinant of physiological stress. However, to the best of the authors' knowledge, this division has not been applied in other studies.

What is more, the classification and counting of the Harris line is also hindered by possible discrepancies between observers (MacChiarelli et al. 1994; Grolleau-Raoux et al. 1997). A possible solution to this problem is the proposed semi-automatic Harris line detection system: HL-tool (Suter et al. 2008; Papageorgopoulou et al. 2011). However, although undoubtedly useful, reliable, and giving repeatable results, this program works quite slowly, especially on older computers. The program, tested by the authors of this review on a computer with the Windows Vista™ operating system, an Intel®Core™ 2 Quad CPU 2.5 GHz processor, and 4 GB RAM, needed 4 to 8 min for one bone, excluding the preparation of X-ray images for analysis.

Hence, children's bones are definitely worth the attention in studying HLs. Because the subjects are young, the HL is more likely not to be resorbed. Clear, pronounced HLs are also less probable to give different results between different observers. Numerous authors reported increased number or visibility of HL on juvenile bones (Piontek et al. 2001). More surprising is the small number of methods which enable the determination of the chronology of HLs on juvenile bones. Moreover, current methods allow to estimate the age of HL formation in the distal part of the juvenile tibia only. Therefore, it was necessary to develop a new method which would have wider application—and which is presented in the "Byers' modified formulas for juvenile bones" section.

The Scott and Hoppa study (Scott and Hoppa 2015) is also worth mentioning in the context of HL detection. The authors

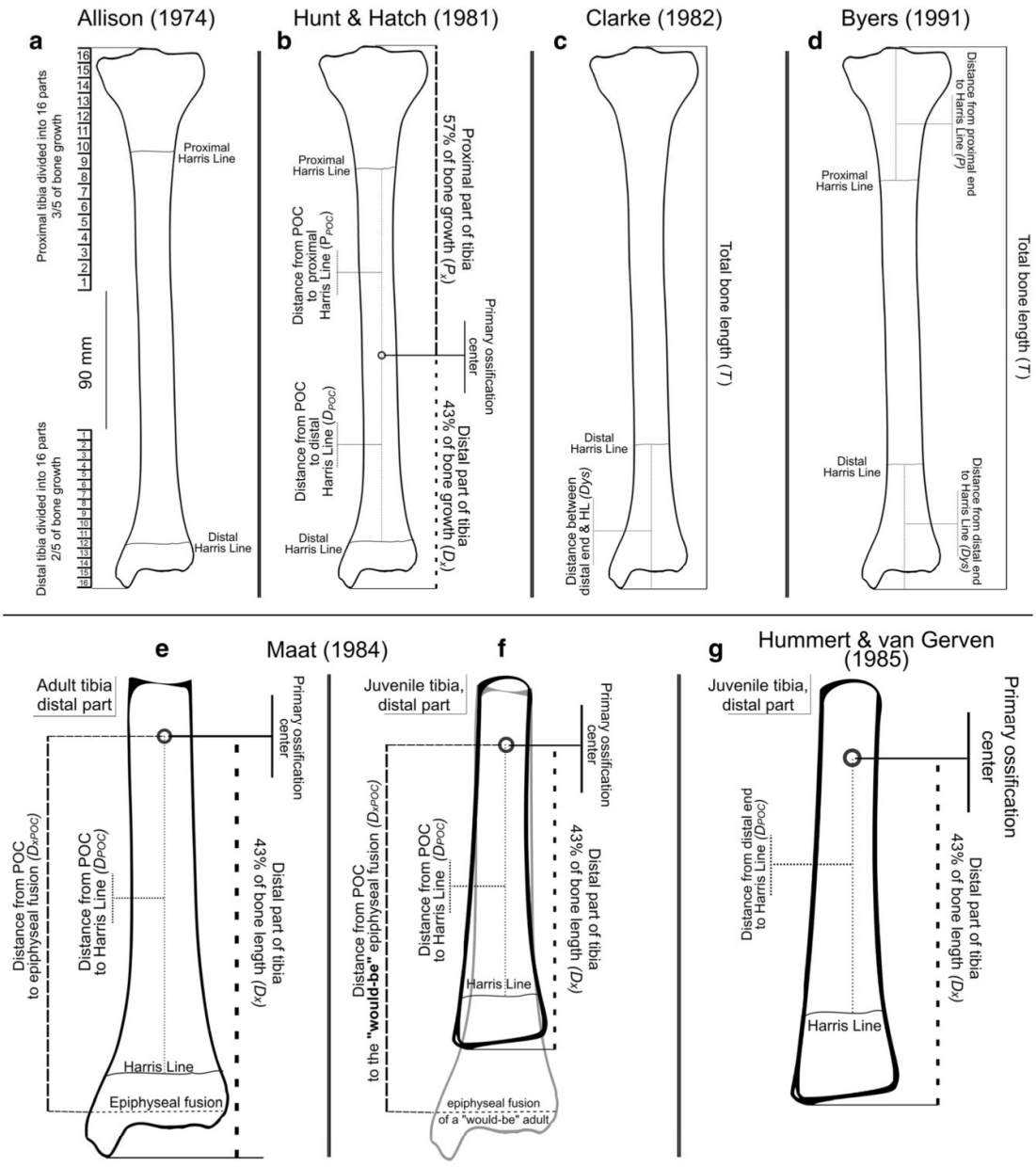

Fig. 2 All measurements needed for individual methods, on the example of the tibia. For more details on each method, please refer to the main text. **a** Allison's method. **b** Hunt and Hatch's method. The D_{POC} measurement needs to be referred to the appropriate table **c** Clarke's as it is made for other methods. The Dys/T ratio needs to be referred to the appropriate table. **d** Byers' method. Both T and Dys or P (depending on the distal or proximal position of the HL) need to be used in the formulas presented in Table 2. **e**, **f** Maat's method. The D_{POC}/D_{EPI} ratio needs to be referred to the appropriate table. **g** Hummert and van Gerven's method. D_{POC}/Dx needs to be referred to the appropriate table. All necessary tables can be found in Supplementary File 1

compared the visibility of HLs on bone X-ray images taken in the anterior-posterior view (A-P) and medial-lateral (M-L) view. Although A-P images are usually used for observation, the authors achieved better visibility with the M-L plane.

Table 1 Summarized characteristics of the methods reviewed. For more details, refer to the appropriate sections of this paper

Aspect	Allison and McHenry	Hunt and Hatch	Clarke	Maat	Hummert and van Gerven	Byers
Targeted bone(s)	Tibia and femur	Tibia and femur	Tibia (distal part only)	Tibia (distal part only)	Tibia (distal part only)	Tibia, femur, radius, humerus
Adequate for juvenile bones?	No	No	No	Yes	Yes	Yes (after modification presented in this article)
Possible inaccuracy reasons	1) Assumed equal bone growth during the whole lifetime 2) Measurements include epiphysis, region on which no HL would appear	1) Evaluation based on absolute measurements, not on the ratios; discrepancies on especially long or short bones	1) HL formation assumed at the end of the bone, not in the growth plate; results tend to be underestimated	None observed	Comparison Table 1) contains inaccurate age ranges 2) Does not include different bone growth in males and females	None observed
Source of comparison tables	N/A	Population of Denver, Colorado, (McCammon 1970).	Population of Yellow Spring, Ohio. (Gindhart 1973)	Population of Denver, Colorado, (Maresh 1955)	Medieval population of Kulubnarti (Sudan), (Hummer and van Gerven 1985)	Population of Denver, Colorado, (Maresh 1955), Boston and Yellow Spring (Anderson and Green 1948; Maresh 1955; Anderson et al. 1963; Gindhart 1973)
Necessary actions	1) Measure bone length and subtract 90 mm 2) Multiply the remaining length by an adequate multiplier 3) Divide the result to 16 equal sections and compare the HL position	1) Create bone growth curves (using mean bone length of the study population) 2) Find the POC 3) Measure the distance from the POC to the HL and compare with tables	1) Measure bone length 2) Measure the distance from the bone end to the HL 3) Divide measurement no. 1 by no. 2 and compare with the table	1) Find the POC 2) Measure distance from POC to the epiphyseal fusion 3) Measure distance from POC to the HL 4) Divide measurement no. 2 by no. 3 and compare with the table	1) Find the POC 2) Measure the distance from the POC to the distal end 3) Measure the distance from the POC to the HL 4) Divide measurement no. 2 by no. 3 and compare with the table	1) Measure bone length 2) Measure the distance from the bone end to the HL 3) Use the appropriate formula and compare the result with the table

The Allison et al. (1974) and McHenry and Schulz (1976) methods

These are the two oldest of the methods discussed; the former was used to determine the chronology of formation of HLs on the tibia, the latter—on the femur. Due to their high similarity and identical assumptions, they can be treated as one method.

Basic assumptions

The Allison method assumes that (a) the average bone length at birth is 90 mm, (b) the bone grows by the same length every year, and (c) 40% of growth occurs on the distal part of the bone, and 60%—on the proximal part.

Necessary measurements

To calculate the age of HL deposition using the Allison method, one needs to: (a) subtract 90 mm from the total bone length (T), (b) multiply the result by 60% to calculate the increase in the proximal part (or by 40% for a HL found on the distal part), and (c) divide the obtained length into 16 equal pieces, each correspondent to 1 year. Next, the position of the Harris Line should be compared to the obtained "ruler."

The McHenry method introduces one modification; it focuses on HLs on the femur, in which a 71% increase in length occurs on the distal part and a 29% one on the proximal part. Consequently, the percentages by which the bone length is multiplied change accordingly. However, McHenry does not specify in his paper if the bone length is also shortened by 90 mm or any other value.

Summary of the method

The method is depicted in Fig. 2a. The authors themselves note that the assumptions are not very precise; the length of the bones after birth can be different than 90 mm (Scheuer and Black 2000), and bone growth varies with age (Hoppa 1992; Ruff 2003). In addition, the total bone length is measured, ignoring the fact that HLs form at the epiphyseal plate, not at the end of the epiphyses (Ameen et al. 2005). Nevertheless, despite the obvious lack of precision, the method enables a rough categorization of HLs into those that were created in the early or late period of growth. In addition, it is relatively simple and fast to use and does not require a comparison of the results with tables or growth curves.

Hunt and Hatch's (1981) method

This method is based on a mathematical model of bone growth. Although the calculations themselves may seem difficult to understand, they are actually quite simple to use, especially when using the spreadsheets in Supplementary File 1. In short, the method requires the following steps: (1) creating growth curves for the study population, (2) creating curves showing the dependence of distance between the HL and the primary ossification center (POC) and the age of HL deposition, (3) determining the POC of the examined bone, and (4) measuring the distance from the HL to the POC and comparing the result with the curve defined in point 2.

Creating growth curves for the study population

The formulas were derived from long-term studies on the growth of long bones in the population of Denver, Colorado, collected by McCammon (1970). Hunt and Hatch derived the growth curves described by the formula:

$$\overline{g}(t) = \frac{a_1}{1 + e^{-b_1(t-c_1)}} + \frac{a_2}{1 + e^{-b_2(t-c_2)}}$$

The $\overline{g}(t)$ function describes mean diaphyseal bone length in time t. The first part of the equation (variables with 1 in the subscript) describes the growth in the prepubertal term, the second part (variables with 2 in the subscript)—in the adolescent term. Variables a are the upper limit of bone growth, b—the maximum slope at the point of inflection of the sigmoid left logistic function, c—age in the period of the fastest growth, and t—age in years (from 1 to 18).

Understanding how to derive this formula may be quite challenging, but it is not required for its proper use, so it will be omitted from this review; for more details, please refer to the original publication by Hunt and Hatch.

This method allows to create bone growth curves for the humerus, radius, ulna, fibula, femur, and tibia, and allows to estimate the age of HL formation in the last two types of bones. An exemplary growth curve for the tibia is shown in Fig. 3a. The remaining curves (with all necessary calculations) are included in Supplementary File 1.

Next, the bone growth curves should be fitted to the study population. To do so, it is necessary to determine the mean diaphyseal length of distinct bones of adults in this population. Then: (a) measure the total length of the bones, (b) subtract the average epiphysis thickness (determined by the authors—see the table in Supplementary File 1) from it to receive the variable $\bar{y}$. The next step is to modify the $\overline{g}(t)$ function using the average diaphyseal length obtained from the population under study. The equation looks as follows:

$$\bar{z}(t) = \frac{\bar{y}}{a_1 + a_2} \times \overline{g}(t)$$

Now, simply substitute numbers from 1 to 18 for t, and use the results to create a specific bone growth curve. This curve can be used to estimate the age of a particular individual.

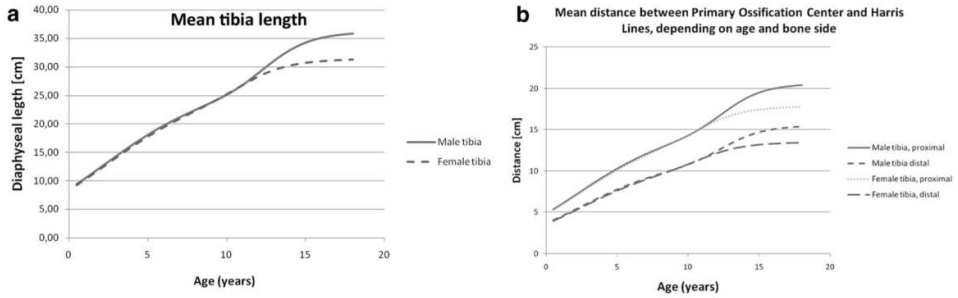

Fig. 3 Example growth curves derived from Hunt and Hatch's study. **a** Mean tibia growth. **b** Curve for the estimation of the age of HL deposition

Curves representing the interdependence of the distance between the HL and the primary ossification center (POC) and the age of HL deposition

Based on the research of Anderson et al. (1963), the authors of this method assumed that 29% of femoral growth occurs at the proximal end and 71% at the distal end. For the tibia, the proportion of proximal and distal growth is 57 and 43%, respectively. In order to create curves that will determine the position of the HL with respect to the POC depending on the age of birth, the following formulas should be used:

$0.29^{*}\,\bar{z}(t)$–for the proximal part of the femur
$0.71^{*}\,\bar{z}(t)$–for the distal part of the femur
$0.57^{*}\,\bar{z}(t)$–for the proximal part of the tibia
$0.43^{*}\,\bar{z}(t)$–for the distal part of the tibia

Numbers from 1 to 18 should be substituted for *t*. The results can be used to create appropriate curves (Fig. 3b).

Determining the primary ossification center (POC)

As described above, 29% of femur growth occurs in the proximal end and 71%—in the distal end. Accordingly, the POC is located at 71% of the length of the bone if measured from the distal end or at 29% of the length if measured from the proximal end. For the tibia, the proportion of proximal and distal growth is 57 and 43%, respectively, so the POC will be at 43% of the length of the bone, measured from the distal end.

The last stage of the procedure is to measure the distance from the HL to the POC and match the obtained measurement to the growth curve for a given bone and its proximal or distal part.

Summary of the method

The Hunt and Hatch method allows to estimate the age of HL formation in the bones of adult individuals, both for the distal and proximal parts of the tibia and femur. It is based on a fairly accurate model that can be adapted to different populations. The accuracy of this method and the wide range of applications are undoubtedly its greatest advantages.

Nevertheless, the method is quite sensitive to individual deviations; for particularly high or low individuals, the method will provide an underestimated or overestimated age of HL formation, respectively. A significant disadvantage of this method is its laboriousness; both understanding and using the Hunt and Hatch method takes a long time, and calculations can discourage less mathematically skilled anthropologists. However, supplementary materials attached to this publication should significantly facilitate the use and understanding of this method.

Clarke's method (1982)

Basic assumptions

Clarke's method was an attempt to improve the methods of Allison and McHenry. It does not assume even bone growth throughout the period of puberty and adolescence. Instead, the author created a table based on the Gindhardt study (1973), which reflects the variable bone growth; it reflects the ratio of bone length in an immature individual of a specific sex and age to the length of an adult bone (Supplementary File 1).

The reference table was adapted to calculations for HLs on the distal part of the tibia; according to Anderson et al. (1963) study, it is assumed that 43% of the tibia's growth at the distal end and 57% at the proximal end. Therefore, each of the results in the table was multiplied by 43%.

Necessary measurements

Application of the method requires the following steps:

a) Measuring the bone length (*T*), determining the sex of the subject
b) Measuring the distance from the distal end of the bone to the HL (Dys)

c) Calculation of Dys/$T \times 100\%$ equation and comparison of the result with the appropriate table

Necessary measurements are presented in Fig. 2c.

Summary of the method

The method is quite fast as it requires only two simple measurements. However, it has some serious imperfections: it takes into account the total length of the bone, omitting the fact that the line is formed within the growth plate, not at the end of the epiphysis, which generates a constant error. In addition, the method can only be used for the distal part of the tibia.

Maat's method (1984)

This method makes it possible to determine the age of HL formation at the distal end of the tibia. The author created a table (based on the research of Maresh (1955)) describing the length of the tibia diaphysis and its distal part depending on the age and sex, as well as the ratio of the distal length of the diaphysis at a given age to its average length in adults (Supplementary File 1).

Necessary measurements

Maat's method requires the determination of: (1) the primary ossification center (again, 43% of tibia length measured from the distal articular surface), (2) the POC's distance to the epiphyseal plate, (3) the distance between the primary ossification center and the HL. Then, divide measurement 3 by measurement 2 and refer the result to the table prepared by the author.

Summary of the method

This method is relatively easy to use, it requires few measurements and simple calculations, and it cannot be accused of inaccuracies; it includes the thickness of epiphyses; the comparable tables are based on reliable growth curves and it uses ratios instead of absolute measurements. However, this method is limited only to the distal part of the tibia. It can also be used to examine children's bones—if the age of the child was determined, the table can estimate the length of the bone diaphysis of a "would-be" adult and use this hypothetical length in the calculations.

The Hummert and van Gerven method (1985)

This method is designed mainly to assess the age of HLs in the bones of children and adolescents. It was dedicated to the assessment of HLs in the medieval population of Kulubnarti (Sudan). Data from this population was used to create a growth chart employed further in this method, assuming that the bone growth in this population may differ from the European or American populations, on which the growth curves of the previous methods were based.

Basic assumptions

Calculations on non-adult bones require the determination of the approximate age of the examined individual. Based on the previously collected data (Hummert 1983), the authors created a table that defines the ratio of the mean distal part of the tibia (again, 43%) in the subsequent developmental years to the length of the distal part of the tibia in the evaluated individual of known age (Supplementary File 1).

Necessary measurements

The Hummert and van Gerven method is another one that requires determining the POC according to the same assumptions as in the Hunt and Hatch (1981) and Maat (1984) methods, 43% length of the bone, measured from the distal end. The second measure is the distance between the HL and the distal end of the bone. Then, the second measurement should be divided by the first one and referred to the table created by the authors.

Summary of the method

The authors recommend not to rely on age estimation based solely on the bone length but also on other age determinants. They estimated the developmental age basing on sequences of dental formation and eruption (Uberlaker 1978). Among newer methods, age can be estimated based on the degree of epiphyseal union (Scheuer and Black 2000), the frontal sinus development (Moore and Ross 2017), and measurements of the ilium (Corron et al. 2017) or girdle bones (Cardoso et al. 2017). One quite obvious disadvantage of the Hummert and van Gerven method is the restriction to the distal part of the tibia. Moreover, the table obtained by the authors refers to the medieval population of Kulubnarti, so it is necessary to create a new table for a population with different dynamics of bone growth.

Byers' method (1991)

The last method is both easy to use and accurate. It is inventive, based on logical assumptions, and it allows to determine the chronology of the HL on four types of bones (tibia, femur, radius, and humerus). Since the authors of this review propose a modification to these formulas, it is necessary to introduce the concept of this method and show its derivation. However, as with the

Hummert and van Gerven models, understanding the derivation of the formulas is not required to use this method effectively.

Basic assumptions

Byers based his considerations and calculations on observations already included in the presentation of the previous methods: (a) Harris lines form in the place of the epiphyseal plate, (b) bone growth dynamics vary with age, but, based on literature data, tables/growth curves describing the growth of individual bones over time can be designed, and (c) bone growth differs at the distal and proximal parts of the bone.

Based on the works of Maresh (1955) (in which bone measurements of children aged 10–12 included the measurements with the epiphyses and without them), Byers calculated that the epiphyses constitute 8% (± 0.68%) of the total length of the humerus and the radius, 11% (± 0.29%) of the femur, and 13% (± 0.33%) of the tibia for both sexes. The growth tables were based on studies on children from Boston and Yellow Spring (Anderson and Green 1948; Maresh 1955; Anderson et al. 1963; Gindhart 1973). In addition to the aforementioned proportions of growth for the distal and proximal parts of the femur (29%/71%) and the tibia (43%/57%), he took into account the proportions for the humerus (81% on the proximal end) and the radius (75% on the distal end).

Formulas derivation

All Byers' formulas boil down to determining the ratio of bone length at the time of HL formation (T_d) to the total length of the subject's bone (T), which will then be referred to the growth table for individual bones. It can be defined with the $T_d/T \times 100\%$ formula.

While T is a trivial measurement, T_d is harder to determine; the location of the HL tells only where the epiphyseal plate was located at the time of deposition. Therefore, it was necessary to develop a formula allowing to estimate T_d based on the distance of the distal (Dys) or proximal (P) HL to the bone end. In this example, it is assumed that there is a HL on the proximal part of the tibia (Fig. 4):

a) The distance from the HL to the proximal end (P) is known. Because of a 43% tibia growth on the distal part, Dys will be $43/57 \times P$ or $0.75P$. The length of the diaphysis (bone shaft) at the time of deposition (S_d) will be $T - (\mathrm{Dys} + P)$ or $T - 1.75P$.
b) Since S_d was calculated, T_d (total length of bone during HL deposition) needs to be calculated. Since the length of the epiphyses is 13% of the whole tibia, it can be assumed that: $T_d = S_d + 0.13T_d$. Then, $S_d = 0.87T_d$ and further: $T_d = 1.15S_d$. Therefore, T_d can be represented as $T_d = 1.15(T - 1.75P)$.

The formulas shown in Table 2 can be derived analogously.

Necessary measurements

Only two measurements are required: (1) the total length of the bone (T) and (2) the distance from the HL to the nearest end of the bone (Dys or P). Both values can be used in appropriate formulas and the result can be compared with the values in the tables (Supplementary File 1).

Byers' modified formulas for juvenile bones

Byers' formulas seem to have only one disadvantage: they cannot be used to calculate the age of HL deposition in juvenile bones. However, the authors propose here a simple modification to Byers' method which will allow to make such calculations.

In children and adolescents, it is impossible to obtain the total length of the bones (due to lack of epiphyses), but only the length of diaphysis. The modification to the formulas is based on the assumption that $\frac{T_d}{T} = \frac{S_d}{S}$, where S_d is the length of the diaphysis at the time of formation of the HL, S—length of the diaphysis of the evaluated bone; de facto the total available bone length. Therefore, the main aim of the formulas is changed to $S_d/S \times 100\%$. Again, S is a trivial measurement, and S_d needs to be calculated.

Because of the lack of epiphyses, it is not possible to measure P or Dys (namely distance between the HL and the end of bone). It is possible, however, to measure P' or Dys', which will be the distance between the HL and the end of the diaphysis. Therefore, $S_d = S - (P' + \mathrm{Dys}')$. It is assumed that the P'/Dys' proportions are the same as P/Dys for all bones; therefore, all P and Dys in the original Byers' formulas can be replaced with P' and Dys'.

There is also a need to modify the following elements of Byers' formula: replace T with S and then remove the part of the formula "adding" the assumed length of the epiphyses to the calculated length of the bone shaft at the time of HL formation. The modified formulas are presented in Table 2.

Finally, it is required to compare the result with the modified Byers' table (Supplementary File 1) and read from it the approximate age of HL formation. Similarly to the Hummert and van Gerven methods, in order to be able to use it, the approximate age of the subjects should be determined beforehand.

Comparison of all methods

Models

To compare the outcomes of different methods, two models were created. The first consists of one enormously HLs-rich male tibia, which was scaled to the following lengths, 44, 39.2, and 34.5 cm (Fig. 5). Then, the age of formation of every single HL was calculated with all applicable methods. For the

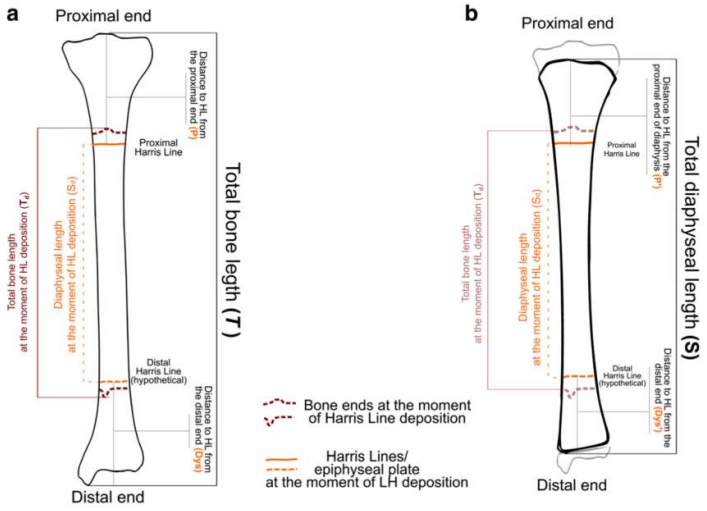

Fig. 4 **a** Explanation of Byers' method on the example of the tibia with one HL on the proximal part. The aim of this method is to determine the T_d/T ratio. T can simply be measured, while T_d needs some calculations. Subtract $T - (\text{Dys} + P)$ to get S_d, which in turn needs to be multiplied by 1.15 to receive T_d. Since Dys is unknown, it is necessary to estimate this length by multiplying P by 0.75. **b** Explanation of the modification of Byers' method for calculations on non-adult bones. The lack of epiphyses prevents obtaining T and P measurements; therefore, this method focuses on the diaphyses, not the entire bone length. The aim of this method is to determine the S_d/S ratio and it uses similar measurements as the original Byers' method

purpose of the Hunt and Hatch method, 39.2 cm is assumed as mean male tibia length.

The second model includes the distal part of juvenile tibia, 26.5 cm long bone of an 11-year-old, 20.5 cm bone of a 7-year-old, and 16.5 cm long bone of a 5-year-old (Fig. 6). Calculations for the proximal part of the tibia are not possible with the Maat or Hummert and van Gerven method; therefore, this part was not included in this model.

Bland-Altman plot

The outcomes of different methods were compared with the Bland-Altman test (Bland and Altman 1986). It is intended to clearly indicate the differences between the outcomes of two distinct methods. The *x*-axis presents the mean value of each pair of measurements, the *y*-axis—the difference between the results of the methods for particular measurements. The more consistent the methods, the more densely distributed the dots and the lower mean difference obtained. The plots were created in the R program (R Core Team 2018) with the BlandAltmanLeh package (Lehnert 2015).

The results are presented in Table 3. Selected Bland-Altman plots are presented in Figs. 7 and 8. Bland-Altman plots for all possible pairs of methods are presented in Supplementary File 2.

Results and discussion for the adult bone model

The Clarke, Byers, and Maat methods give results independent from the bone length because these three methods are based on ratios rather than absolute measurements. On the

Table 2 Original Byers equations and theirs modification

Bone and location of HL	Original Byers' equations	Modified Byers' equations
Tibia, distal	$\frac{1.15(T-2.33\text{Dys})}{T} \times 100\%$	$\frac{S-2.33\text{Dys}'}{S} \times 100\%$
Tibia, proximal	$\frac{1.15(T-1.75P)}{T} \times 100\%$	$\frac{S-1.75P'}{S} \times 100\%$
Femur, distal	$\frac{1.12(T-1.43\text{Dys})}{T} \times 100\%$	$\frac{S-1.43\text{Dys}'}{S} \times 100\%$
Femur, proximal	$\frac{1.12(T-3.33P)}{T} \times 100\%$	$\frac{S-3.33P'}{S} \times 100\%$
Radius, distal	$\frac{1.09(T-1.33\text{Dys})}{T} \times 100\%$	$\frac{S-1.33\text{Dys}'}{S} \times 100\%$
Radius, proximal	$\frac{1.09(T-4P)}{T} \times 100\%$	$\frac{S-4P'}{S} \times 100\%$
Humerus, distal	$\frac{1.09(T-5.26\text{Dys})}{T} \times 100\%$	$\frac{S-5.26\text{Dys}'}{S} \times 100\%$
Humerus, proximal	$\frac{1.09(T-1.23P)}{T} \times 100\%$	$\frac{S-1.23P'}{S} \times 100\%$

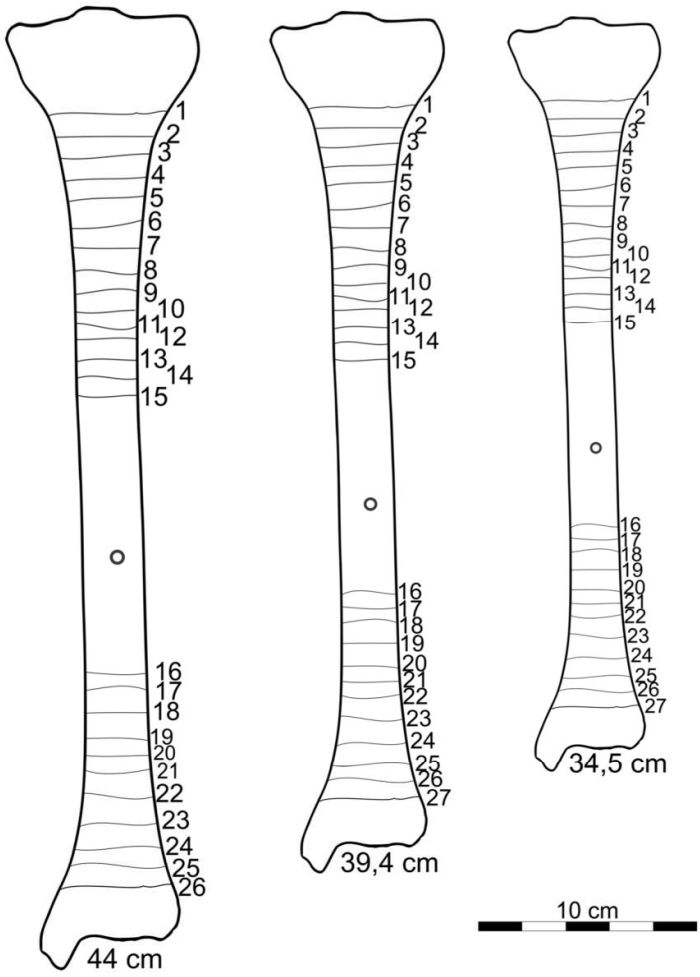

Fig. 5 Bone models for the comparison of methods. For the purpose of comparison of methods, one tibia with 27 HLs was created and then scaled to 44, 39.2, and 34.5 cm. For the purpose of the Hunt and Hatch method, it is assumed that the mean tibia length for males is 39.2 cm. The outcomes of a different method are presented in Table 3

contrary, the Allison and Hunt and Hatch methods are very sensitive to different bone lengths. The Allison is based on ratios; however, the assumed 90 mm of initial bone length (regardless of its total length) strongly influences the following calculations in bones of different lengths and, subsequently, the outcomes. The mean difference between the estimated age of HL formation for 44 and 34.5-cm bones is about 0.75 years and ranges from 0 to 2.5 years (Fig. 7a).

Even worse difference between long and short tibiae is obtained with the Hunt and Hatch method (mean difference 3.1 years, range 1–7 year., Fig. 7b). When compared with other methods, age for long tibiae is overestimated and for short—underestimated. It is noteworthy that the outcomes of the Hunt and Hatch method for 39.2-cm tibia give results comparable with the accurate Byers or Maat method (Fig. 7c). It can therefore be assumed that the Hunt and Hatch method may easily be improved by plotting distinct growth curve for each examined bone, based on its length. In such proceedings, the Hunt and Hatch method would become de facto ratio-based. However, without such modification, this method is inaccurate in the estimation of HLs formation in particularly long or short bones.

The Clarke method tends to underestimate the age of HLs formation (besides the earliest ones) when compared with the Byers or Maat method (Fig. 7d), as the thickness of epiphyses was not taken into consideration by Clarke in his calculations.

Byers and Maat methods should be considered the most accurate—they are based on correct premises and give almost identical results (Fig. 7e). However, as the Byers method is faster and allows to perform calculations on a broader range of bones, the authors of the current review strongly recommend choosing this method.

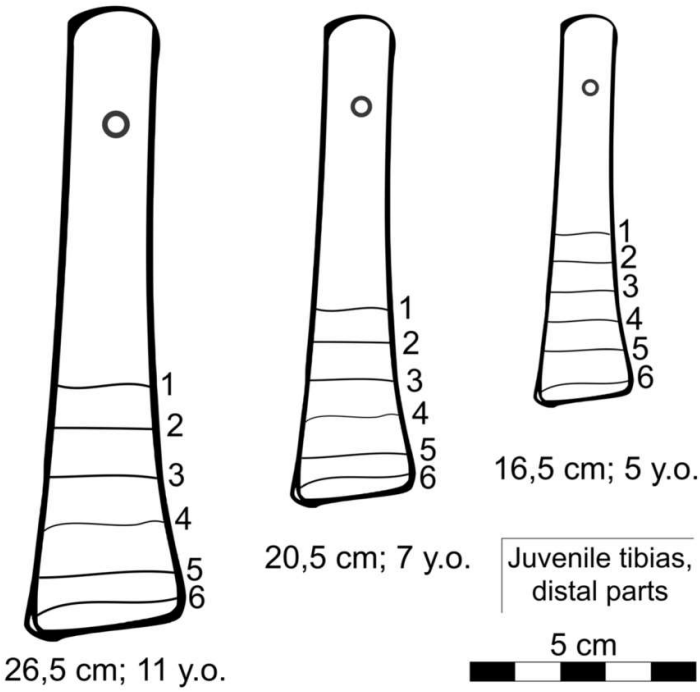

Fig. 6 Juvenile bones models for the comparison of methods. For the purpose of comparison of methods, three juvenile tibiae with six HLs were created. The Maat and Hummert and van Gerven methods can be used to evaluate the distal part of the tibia only; therefore, the presented model is based solely on this part of the bone. The outcomes of a different method are presented in Table 4

Results and discussion for the juvenile bone model

In this model, the results of the Maat, Hummert and van Gerven, and modified Byers methods were compared (Table 4). While the Maat and modified Byers methods give very similar results (differences ranging from − 0.5 to 0.5 years, Fig. 8b), the Hummer and van Gerven method gives quite different results (range 0–1 years, mean difference 0.4 years, Fig. 8a, c). It does not mean that the Hummert and van Gerven method is unreliable—the cause is rooted in the comparison tables.

The comparison tables for Maat and Byers are based on the same dataset and therefore the results produce very similar outcomes, Hummert and van Gerven—on the medieval Nubian population. The growth curves for medieval Nubian and twentieth century American population differs—which is reflected on the Bland-Altman plots.

This comparison shows that the assumption of the modified Byers method is correct. Therefore, it can be applied to the proximal part of the tibia, femur, radius, and humerus—which was not possible with the previous methods.

General remarks

In this review, the Byers method is recommended for calculations on adult bones and the modified Byers method—on non-adult bones. However, there are some issues which need to be raised, regardless of the method used.

Every reviewed method is linked with one false although indispensable assumption: "course of bone growth is identical for everyone; it differs only between the sexes." It is obviously untrue; the beginning of the adolescent growth spurt and its duration varies between individuals (Anderson et al. 1963). The estimation of HLs formed in this period is always biased, regardless of the method used. To the best of the authors' knowledge, there is no possible way to eliminate this error; however, a study on a large population should overcome the severity of this problem in statistical inference.

The majority of methods are based on some bone growth databases. However, these databases should not be considered universal. Besides the obvious difference in the mean adult bone length between different populations, the course and dynamics of bone growth may also vary significantly; these differences are well depicted by Bland-Altman plots comparing the modified Byers and Hummert and van Gerven methods—which are based on datasets originating from quite different populations.

If this issue is not taken into consideration, it may disturb the results and their interpretation. For example, Piontek et al. (2001) used the Byers method for adult and the Hunt and Hatch method for non-adult bones. They calculated that the mean age at formation of HLs in juvenile bones is 9–11 years of age, and in adult male bones, 11–12 years of age. However, the Hummert and van

Table 3 Results of different methods

		44 cm tibia		39.4 cm tibia		34.5 cm tibia		All tibias (ratio-based methods)		
	Line no.	Allison	Hunt and Hatch	Allison	Hunt and Hatch	Allison	Hunt and Hatch	Clarke	Maat	Byers
Proximal part	1	12.5	17–18	12.5	13.5	12.5	11.5	NA	NA	14
	2	12	14–15	12	12.5	11.5	11	NA	NA	13
	3	11	13.5	11	12	11	10	NA	NA	12
	4	10	13	10	11	10	9.5	NA	NA	11
	5	9.5	12	9.5	10.5	9	8.5	NA	NA	10
	6	8.5	11	8.5	9.5	8	7	NA	NA	9
	7	7.5	9.5	8	8	7.5	6	NA	NA	7.5
	8	7	8	7	7	6.5	4.5	NA	NA	6.5
	9	6	7.5	6	6	6	4.5	NA	NA	6
	10	5	6.5	5.5	5	5	3.5	NA	NA	5
	11	5.5	5.5	5	4.5	4.5	3	NA	NA	4
	12	4	5	4	4	4	3	NA	NA	4
	13	3	4	3.5	3	3	2	NA	NA	3
	14	3	3	3	2.5	2.5	1.5	NA	NA	2
	15	2	2.5	2.5	1.5	2	1	NA	NA	1.5
Distal part	16	1	2	Newborn	1.5	Newborn	0.5	2	1,5	1.5
	17	2	3	Newborn	2	Newborn	1	2	2	2
	18	3	4	1	3.5	1	2	3	3	3
	19	4	5.5	2.5	5	2	4.5	4	4.5	4.5
	20	5	7	4	5.5	3.5	4	6	5.5	5.5
	21	6	8.5	5	7	4.5	5	6	6.5	6.5
	22	7	10	5.5	8.5	5	6	7	8	8
	23	9	11.5	7	10	6.5	7.5	8.5	10	10
	24	10	13	8.5	11.5	8.5	9	10	11.5	11.5
	25	11	14	10	12.5	10	10	11	12.5	12.5
	26	12	16	11	13.5	10.5	11.5	12	13.5	14

Only Allison and Hunt and Hatch methods give different results for bones of different lengths. Methods based on the ratios rather than absolute measurements give the same results regardless of the bone length. The distribution of Harris lines is shown in Fig. 5. All Bland-Altman plots can be found in the Supplementary file 2 and selected Bland-Altman plots—in Fig. 7

Gerven method underestimates the age at formation of HLs when compared with the Byers method (as it is presented in the Bland-Altman plot). If they would use the same datasets, most probably they would find similarities rather than differences in this aspect of their study.

Moreover, the creation of new growth curves or comparison tables dedicated to the study population should always be considered, as it was done by Alfonso et al. (2005). However, such approach is rarely used and a vast number of studies are based on the comparison tables provided by authors of distinct methods.

As shown in the "Comparison of all methods" section, most probably every study based on the Allison, McHenry, Clarke, or Hunt and Hatch method is biased and could be reevaluated. The Bland-Altman plots provided in Supplementary File 2 should facilitate the reinterpretation of results in the publications in which the aforementioned methods were used.

Summary, perspectives, and challenges

The interest in Harris lines seems to have slightly increased over the last 18 years, basing on Google Scholar database records (Fig. 9). However, in the last few years, authors have been focusing on the presence and number of HLs rather than the age at their formation. According to publications indexed in the Google Scholar database, there was only one study using the Byers method published in the last 5 years (Krenz-Niedbała 2014) and, similarly, there was only one using the Hummert and van Gerven method (Boucherie et al. 2017).

The age at formation of HLs seems to be avoided recently. It is understandable, due to the controversies mentioned in the introduction, such as lack of correlation with other physiological stress indicators (Alfonso et al. 2005), disappearance of HLs resulting from ongoing bone remodeling (Mays 1995), or appearance of HLs unassociated with any physiological stress

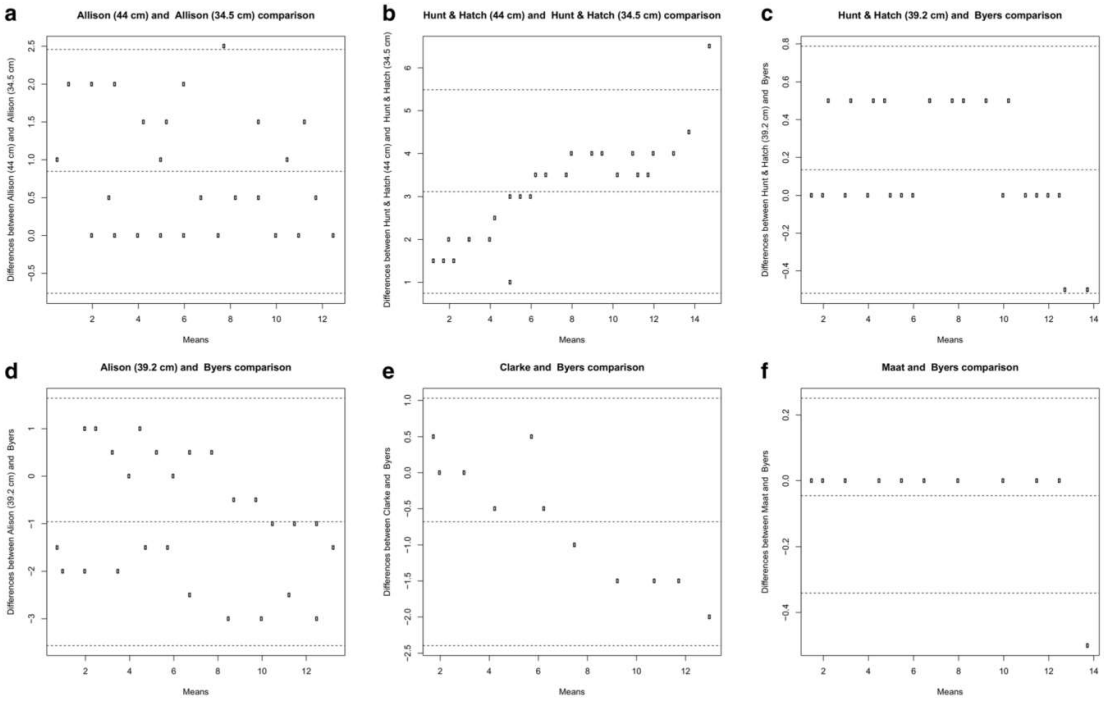

Fig. 7 Selected Bland-Altman plots comparing the methods used for adult bones. Bland-Altman plots clearly show concordance between the two compared methods. The middle dashed line shows the mean difference between the results of those two methods. The lower and higher dashed lines show ± 1.96 standard deviations. The *x*-axis presents the mean results calculated for each HL and *y*-axis—the difference between the first and second of the compared methods for each measurement. All results are given in years. **a** Results of the Allison method for two bones of different lengths. Varying length significantly affects the outcomes of this method. **b** The results of the Hummert and van Gerven method for long and short tibiae. The difference is even greater than in the Allison method. **c** The Hummert and van Gerven method for mean bone compared with the Byers method. Both methods show great concordance, which implies that the Hummer and van Gerven method is accurate for mean bones. The Byers method is also compared with the Allison (**d**), Clarke (**e**), and Maat (**f**) methods

(Alfonso-Durruty 2011). Moreover, the seemingly difficult and time-consuming calculations may also discourage from estimating the age at formation of HLs.

The present review is aimed at reversing this trend. The authors hope that this study, together with the attached figures and supplementation materials, will greatly simplify the

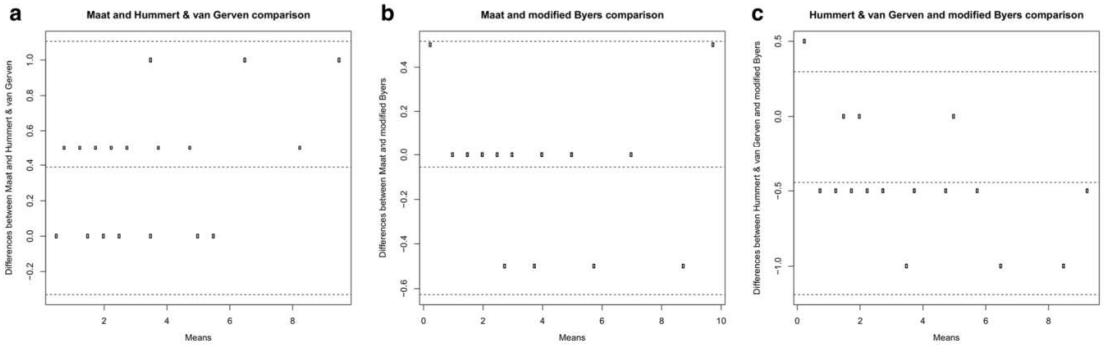

Fig. 8 Bland-Altman plots comparing the methods used for juvenile bones. While the Maat and Byers methods give very similar results, the Hummert and van Gerven method produces different outcomes. The cause is rooted in the different source of the comparison table used in the last method

Table 4 Results of different methods for juvenile bones

	Line no.	Distance from the HL to the POC (mm)	Distance from the HL to the distal end (mm)	Maat	Hummer and van Gerven	Modified Byers
26.5 cm; 11 years old	1	59	55	2.5	2	2.5
	2	68	46	4	3	4
	3	79	35	5	4.5	5
	4	90	24	7	6	7
	5	100	14	8.5	8	9
	6	107	7	10	9	9.5
20.5 cm; 7 years old	1	43	43	1.5	1	1.5
	2	50	36	2	1.5	2
	3	58	28	2.5	2.5	3
	4	67	19	3.5	3.5	4
	5	75	11	5	5	5
	6	80	6	5.5	5.5	6
16.5 cm; 5 years old	1	30.51	39	0.5	0.5	newborn
	2	37.12	33	1	0.5	1
	3	43.39	27	1.5	1.5	1.5
	4	49.81	20	2	2	2
	5	56.35	14	3	2.5	3
	6	63.79	6	4	3.5	4

The distribution of Harris lines is shown in Fig. 6. All Bland-Altman plots can be found in Supplementary file 2 and selected Bland-Altman plots—in Fig. 8

understanding and calculation of the chronology of Harris lines. The authors also encourage to perform the study primarily on juvenile bones; the HLs on them are less likely to be resorbed. Moreover, these HLs are more pronounced and clear, which could increase the intra- and interobserver agreement. New methods enable the estimation of the age at formation of HLs on juvenile femurs and the proximal part of tibiae—and thus increase the number of obtainable results, which will improve the statistical proceedings on archeological study populations.

The controversies connected with HL etiology should be considered as a challenge rather than an obstacle. Many authors who failed to find statistically significant correlation between the HL and other indicators admit that bone remodeling and the following HL disappearance may be responsible for the lack of such correlation (McHenry and Schulz 1976; Mays 1985, 1995, Nowak and Piontek 2002a, b). A similar study conducted on juvenile bones (which are less likely to resorb HL) could give statistically significant results. Moreover, the studies which used the Allison, McHenry, Clarke, or Hunt and Hatch method could also be reevaluated and repeated, as most probably they are biased.

Also, the histological model of formation of HLs could be improved—there is no unanimity whether the HLs are rather "growth arrest" (Scott and Hoppa 2015) or "growth recovery lines"(Sajko et al. 2011). Current biochemical models assume the involvement of GH and IGF-1 (Alfonso-Durruty 2011); however, bone growth and mineralization may be connected also with other proteins and pathways, such as TAZ/Runx2 and PI3K/Akt (Alkagiet and Tziomalos 2017; Zhang et al. 2017), or could involve miRNA (Han et al. 2017) and long non-coding RNA (Xi et al. 2018). Better understanding of the biochemical base of HL formation could improve the interpretation of results involving these lines.

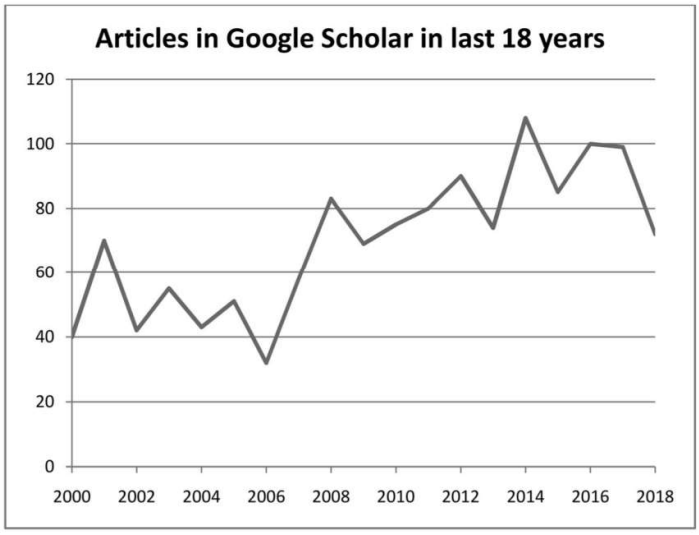

Fig. 9 Articles on HLs indexed by Google Scholar. The graph shows the number of papers published in the years 2000–2018 (by 21.11.2018) containing the phrase "Harris line"

In conclusion, there is much to discover in the field of Harris lines.

Acknowledgements The authors of this review would like to thank the creators of the presented age estimation methods for Harris lines formation: Marvin J. Allison, Daniel Mendoza, Alejandro Pezzia, Henry M. McHenry, Peter D. Schulz, Edward E. Hunt Jr., James W. Hatch, Steven K. Clarke, George J.R. Maat, James R. Hummert, Dennis P. Van Gerven, and Steve Byers. In the words of Sir Isaac Newton: "If I have seen further it is by standing on the shoulders of Giants".

References

Alfonso MP, Thompson JL, Standen VG (2005) Reevaluating Harris lines—a comparison between Harris lines and enamel hypoplasia. Coll Antropol 29:393–408

Alfonso-Durruty MP (2011) Experimental assessment of nutrition and bone growth's velocity effects on Harris lines formation. Am J Phys Anthropol 145:169–180. https://doi.org/10.1002/ajpa.21480

Alkagiet S, Tziomalos K (2017) Vascular calcification: the role of microRNAs. Biomol Concepts 8:119–123. https://doi.org/10.1515/bmc-2017-0001

Allison MJ, Mendoza D, Pezzia A (1974) A radiographic approach to childhood illness in precolumbian inhabitants of southern Peru. Am J Phys Anthropol 40:409–415. https://doi.org/10.1002/ajpa.1330400313

Ameen S, Staub L, Ulrich S, Vock P, Ballmer F, Anderson SE (2005) Harris lines of the tibia across centuries: a comparison of two populations, medieval and contemporary in Central Europe. Skelet Radiol 34:279–284. https://doi.org/10.1007/s00256-004-0841-3

Anderson M, Green WT (1948) Lengths of the femur and the tibia; norms derived from orthoroentgenograms of children from 5 years of age until epiphysial closure. Am J Dis Child 75:279–290

Anderson M, Green WT, Messner MB (1963) Growth and predictions of growth in the lower extremities. J Bone Joint Surg Am 45–A:1–14

Beom J, Woo EJ, Lee IS, Kim MJ, Kim YS, Oh CS, Lee SS, Lim SB, Shin DH (2014) Harris lines observed in human skeletons of Joseon Dynasty, Korea. Anat Cell Biol 47:66–72. https://doi.org/10.5115/acb.2014.47.1.66

Bland JM, Altman DG (1986) Statistical methods for assessing agreement between two methods of clinical measurement. Lancet 327:307–310. https://doi.org/10.1016/S0140-6736(86)90837-8

Boucherie A, Castex D, Polet C, Kacki S (2017) Normal growth, altered growth? Study of the relationship between Harris lines and bone form within a post-medieval plague cemetery (Dendermonde, Belgium, 16th century). Am J Hum Biol 29. https://doi.org/10.1002/ajhb.22885

Byers S (1991) Calculation of age at formation of radiopaque transverse lines. Am J Phys Anthropol 85:339–343. https://doi.org/10.1002/ajpa.1330850314

Cardoso HFV, Spake L, Humphrey LT (2017) Age estimation of immature human skeletal remains from the dimensions of the girdle bones in the postnatal period. Am J Phys Anthropol 163:772–783. https://doi.org/10.1002/ajpa.23248

Chauveau A, Augias A, Froment A, Beuret F, Charlier P (2016) Radioscannographic correlation of Harris lines in adults: forensic and anthropological perspectives. Eur J Forensic Sci 3:21–28. https://doi.org/10.5455/ejfs.200731

Clarke SK (1982) The association of early childhood enamel hypoplasias an radiopaque transverse lines in a culturally diverse prehistoric skeletal sample. Hum Biol 54:77–84

Corron L, Marchal F, Condemi S, Chaumoître K, Adalian P (2017) A new approach of juvenile age estimation using measurements of the ilium and multivariate adaptive regression splines (MARS) models for better age prediction. J Forensic Sci 62:18–29. https://doi.org/10.1111/1556-4029.13224

Geber J (2014) Skeletal manifestations of stress in child victims of the Great Irish Famine (1845-1852): prevalence of enamel hypoplasia, Harris lines, and growth retardation. Am J Phys Anthropol 155:149–161. https://doi.org/10.1002/ajpa.22567

Gindhart PS (1973) Growth standards for the tibia and radius in children aged one month through eighteen years. Am J Phys Anthropol 39:41–48. https://doi.org/10.1002/ajpa.1330390107

Goodman A, Clark G (1981) Harris lines as indicators of stress in prehistoric Illinois populations. In: Research report 20: biocultural adaptation. Comprehensive approaches to skeletal analysis. pp 35–47

Grolleau-Raoux JL, Crubézy E, Rougé D et al (1997) Harris lines: a study of age-associated bias in counting and interpretation. Am J Phys Anthropol 103:209–217. https://doi.org/10.1002/ccd.25884

Han J, Su L, Zhang C, Jiang R (2017) miR-539 mediates osteoblast mineralization by regulating Distal-less genes 2 in MC3T3-E1 cell line. pp 294–299

Hoppa RD (1992) Evaluating human skeletal growth: an Anglo-Saxon example. Int J Osteoarchaeol 2:275–288. https://doi.org/10.1002/oa.1390020403

Hummert JR (1983) Childhood growth and morbidity in a medieval population from Kulubnarti in the Batn el Hajar of Sudanese Nubia. University of Colorado

Hummert JR, Van Gerven DP (1985) Observations on the formation and persistence of radiopaque transverse lines. Am J Phys Anthropol 66:297–306. https://doi.org/10.1002/ajpa.1330660307

Hunt EE, Hatch JW (1981) The estimation of age at death and ages of formation of transverse lines from measurements of human long bones. Am J Phys Anthropol 54:461–469. https://doi.org/10.1002/ajpa.1330540404

Jerszyńska B, Nowak O (1996) Application of Byers method for reconstruction of age at formation of Harris lines in adults from a cementery of Cedynia (Poland). Var Evol 5:75–82

Khadilkar VV, Frazer FL, Skuse DH, Stanhope R (1998) Metaphyseal growth arrest lines in psychosocial short stature. Arch Dis Child 79:260–262. https://doi.org/10.1136/adc.79.3.260

Krenz-Niedbała M (2014) A biocultural perspective on the transition to agriculture in Central Europe. Anthropologie 52:115–132

Krenz-Niedbała M (2017) Growth and health status of children and adolescents in medieval Central Europe. Anthropol Rev 80:1–36. https://doi.org/10.1515/anre-2017-0001

Laor T, Jaramillo D (2009) MR imaging insights into skeletal maturation: what is normal? Radiology 250:28–38. https://doi.org/10.1148/radiol.2501071322

Lehnert B (2015) BlandAltmanLeh: plots (slightly extended)

Maat GJR (1984) Dating and rating of Harris's lines. Am J Phys Anthropol 63:291–299. https://doi.org/10.1002/ajpa.1330630305

MacChiarelli R, Bondioli L, Censi L, Hernaez MK, Salvadei L, Sperduti A (1994) Intra- and interobserver concordance in scoring Harris lines: a test on bone sections and radiographs. Am J Phys Anthropol 95:77–83. https://doi.org/10.1002/ajpa.1330950107

Maresh MM (1955) Linear growth of extremities from infancy through adolescence. Am J Dis Child 89:725–742

Mays SA (1985) The relationship between Harris line formation and bone growth and development. J Archaeol Sci 12:207–220. https://doi.org/10.1016/0305-4403(85)90021-4

Mays S (1995) The relationship between Harris lines and other aspects of skeletal development in adults and juveniles. J Archaeol Sci 22:511–520. https://doi.org/10.1006/jasc.1995.0049

McCammon R (1970) Human growth and development. Charles C. Thomas, Springfield, Ill

McHenry HM, Schulz PD (1976) The association between Harris lines and enamel hypoplasia in prehistoric California Indians. Am J Phys Anthropol 44:507–511. https://doi.org/10.1002/ajpa.1330440313

Mescher A (2013) Junqueira's basic histology: text and atlas, 13th ed. McGraw-Hill Medical

Miszkiewicz JJ (2015) Histology of a Harris line in a human distal tibia. J Bone Miner Metab 33:462–466. https://doi.org/10.1007/s00774-014-0644-0

Moore K, Ross A (2017) Frontal sinus development and juvenile age estimation. Anat Rec 300:1609–1617. https://doi.org/10.1002/ar.23614

Nowak O (1996) Linie Harrisa jako miernik reakcji morfologicznej na warunki życia: interpretacje, kontrowersje, propozycje badawcze. Przegląd Antropol 59:77–86

Nowak O, Piontek J (2002a) The frequency of appearance of transverse (Harris) lines in the tibia in relationship to age at death. Ann Hum Biol 29:314–325. https://doi.org/10.1080/03014460110086105

Nowak O, Piontek J (2002b) Does the occurrence of Harris lines affect the morphology of human long bones? HOMO 52:254–276. https://doi.org/10.1078/0018-442X-00033

Nowakowski D (2018) Frequency of appearance of transverse (Harris) lines reflects living conditions of the Pleistocene bear-Ursus ingressus-(Sudety Mts., Poland). PLoS One 13:e0196342. https://doi.org/10.1371/journal.pone.0196342

Papageorgopoulou C, Suter SK, Rühli FJ, Siegmund F (2011) Harris lines revisited: prevalence, comorbidities, and possible etiologies. Am J Hum Biol 23:381–391. https://doi.org/10.1002/ajhb.21155

Park J, Gebhardt M, Golovchenko S, Perez-Branguli F, Hattori T, Hartmann C, Zhou X, deCrombrugghe B, Stock M, Schneider H, von der Mark K (2015) Dual pathways to endochondral osteoblasts: a novel chondrocyte-derived osteoprogenitor cell identified in hypertrophic cartilage. Biol Open 4:608–621. https://doi.org/10.1242/bio.201411031

Piontek J, Jerszyńska B, Nowak O (2001) Harris lines in subadult and adult skeletons from the medieval cemetery in Cedynia, Poland. Var Evol 9:33–43

Primeau C, Jakobsen LS, Lynnerup N (2016) CT imaging vs. traditional radiographic imaging for evaluating Harris lines in tibiae. Anthropol Anz 73:99–108. https://doi.org/10.1127/anthranz/2016/0587

R Core Team (2018) R: a language and environment for statistical computing. R Foundation for Statistical Computing, Vienna

Ross AH, Juarez CA (2016) Skeletal and radiological manifestations of child abuse: implications for study in past populations. Clin Anat 29:844–853. https://doi.org/10.1002/ca.22683

Ruff C (2003) Growth in bone strength, body size, and muscle size in a juvenile longitudinal sample. Bone 33:317–329. https://doi.org/10.1016/S8756-3282(03)00161-3

Sajko S, Stuber K, Wessely M (2011) Growth restart/recovery lines involving the vertebral body: a rare, incidental finding and diagnostic challenge in two patients. J Can Chiropr Assoc 55:313–317

Scheuer L, Black S (2000) Developmental juvenile osteology. Elsevier Ltd, Bath

Scott AB, Hoppa RD (2015) Brief communication: a re-evaluation of the impact of radiographic orientation on the identification and interpretation of Harris lines. Am J Phys Anthropol 156:141–147. https://doi.org/10.1002/ajpa.22635

Sifuentes Giraldo W, Boteanu A, Gamir Gamir M (2016) Park-Harris growth arrest lines associated with systemic-onset juvenile idiopathic arthritis. Austin J Musculoskelet Disord 3:1030

Suter S, Harders M, Papageorgopoulou C, Kuhn G, Székely G, Rühli FJ (2008) Technical note: standardized and semiautomated Harris lines detection. Am J Phys Anthropol 137:362–366. https://doi.org/10.1002/ajpa.20901

Traczek DN (2017) A historical and osteological examination of torture. University of Wyoming

Uberlaker D (1978) Human skeletal remains. Aldine Publishing Co, Chicago

Xi L, Li H, Yin D (2018) Long non-coding RNA-2271 promotes osteogenic differentiation in human bone marrow stem cells. 404–412

Zapala MA, Tsai A, Kleinman PK (2016) Growth recovery lines are more common in infants at high vs. low risk for abuse. Pediatr Radiol 46:1275–1281. https://doi.org/10.1007/s00247-016-3621-z

Zhang G, Cheng X, Zhou G, Xue H, Shao S, Wang Z (2017) New pathway of icariin-induced MSC osteogenesis: transcriptional activation of TAZ/Runx2 by PI3K/Akt. Open. Life Sci 12:228–236. https://doi.org/10.1515/biol-2017-0027

Zítková P, Velemínský P, Dobisíková M, Likovský J (2004) The incidence of Harris lines in the non-adult Great Moravian population of Mikulčice (Czech Republic) with reference to social position. J Natl Museum, Nat Hist Ser 173:145–156

life

MDPI

Article

New Equations for the Estimation of the Age of the Formation of the Harris Lines

Michał J. Kulus [1,*], Kamil Cebulski [2], Piotr Kmiecik [3], Patrycja Sputa-Grzegrzółka [4], Joanna Grzelak [4] and Paweł Dąbrowski [4]

[1] Division of Ultrastructural Research, Wroclaw Medical University, 50-367 Wrocław, Poland
[2] Division of Histology and Embryology, Department of Human Morphology and Embryology, Wroclaw Medical University, 50-367 Wrocław, Poland; kamilcebulski112@gmail.com
[3] Institute of Natural and Technical Studies, The Angelus Silesius University of Applied Sciences, 58-300 Wałbrzych, Poland; pkmiecik@ans.edu.pl
[4] Division of Anatomy, Department of Human Morphology and Embryology, Wroclaw Medical University, 50-367 Wrocław, Poland; patrycja.sputa-grzegrzolka@umw.edu.pl (P.S.-G.); joanna.grzelak@umw.edu.pl (J.G.); pawel.dabrowski@umw.edu.pl (P.D.)
* Correspondence: michal.kulus@umw.edu.pl; Tel.: +48-71-748-1681

Abstract: Harris Lines (HLs) are transverse, sclerotic lines that can be visualized by X-ray imaging and that occur in long bones, most commonly in the tibia and femur. HLs are associated with disrupted bone mineralization during endochondral ossification, affecting the normal growth process. The etiology of HLs is debated, with some claims linking their presence to detrimental factors such as inflammation, malnutrition, alcohol abuse, and diseases. The age at which HLs form can be estimated based on their location, which allows for a retrospective assessment of the individual's health status during childhood or youth. The current study is concerned with providing new equations to estimate the age of Harris Line occurrences using a simple calculating tool. Bone growth curves were derived based on a dataset provided by Byers in 1991 using non-linear estimation. The best model was chosen with the Akaike Information Criterion. New and old methods were compared through Bland–Altman plots. As a result, we managed to produce reliable, well-fitted growth curves, concordant with previous methods.

Keywords: growth model; skeletal indicators; growth recovery lines; anthropometrics

Citation: Kulus, M.J.; Cebulski, K.; Kmiecik, P.; Sputa-Grzegrzółka, P.; Grzelak, J.; Dąbrowski, P. New Equations for the Estimation of the Age of the Formation of the Harris Lines. *Life* **2024**, *14*, 501. https://doi.org/10.3390/life14040501

Academic Editor: Clinton T. Rubin

Received: 8 March 2024
Revised: 5 April 2024
Accepted: 12 April 2024
Published: 13 April 2024

1. Introduction

Harris Lines (HLs, also Park–Harris Lines) are transverse, sclerotic lines that can be visualized by X-ray imaging, as shown in Figure 1 [1], although they are visible also in computed tomography [2] or on histological slides [3]. They may form in any bone growing through the process of endochondral ossification. However, they occur most often in the tibia and femur [4]. The first reports of them were in 1874 by Wegner. Later, independent studies conducted by Henry Harris and Edwards Park in the late 1920s described and popularized them [5]. During the last century, HLs were studied intensively in biological anthropology [4], as well as in current radiology [5].

HLs are also referred to as "growth arrest lines" or "growth recovery lines". According to the model related to the first term, HLs form as a result of disrupted bone mineralization during endochondral ossification. Normally, chondrocytes in the epiphyseal plate proliferate, become hypertrophied, and undergo apoptosis; their remains serve as scaffolds for a new bone matrix produced by osteoblasts. When the proliferation and delivery of chondrocytes to the calcification zone is disrupted, osteoblasts do not receive scaffolding for further bone growth, cannot penetrate the growth plate, and form a thickened layer of bioapatite on an already existing bone [6]. Other models suggest that a thickened layer of bone matrix forms during growth recovery rather than the growth arrest period [7].

Regardless of which model is correct, HL formation is directly linked to transitional bone growth inhibition.

Figure 1. Example of Harris Lines (orange arrows) on juvenile tibia. Source: own archive.

The etiology of HLs remains disputed; their presence has been linked to a broad range of detrimental factors, such as acute inflammation, malnutrition or undernourishment, alcohol abuse, diseases, and others [8–11]. A recent review by Georgiadis and Gannon [5]

provides a list of possible etiologies behind the formation of Harris Lines due to the nature of adverse factors. According to them, physiological, metabolic, endocrine, systemic, post-traumatic, pharmaceutical, and anthropological factors may contribute to their formation.

However, some studies question the reliability of HLs as non-specific detrimental event indicators, which was discussed in a recent review [4]. Furthermore, the assessment of HLs is susceptible to both intra- and inter-observer bias. Some HLs may be missed while, conversely, small cracks may be incorrectly identified as HLs. Differences between observers can be substantial, particularly for faint lines [12]. Intra-observer bias tends to be less significant and is contingent upon the observer's level of experience. Therefore, it is important to establish clear rules for classifying HLs before beginning measurements to minimize potential discrepancies. Additionally, the use of computed tomography instead of radiographs for assessing HLs results in a slight decrease in inter-observer error [13].

Despite the aforementioned studies questioning the reliability of HLs, they are still used in biological anthropology and paleopathology as non-specific indicators of malnutrition, disease, and other detrimental events [5,14–16]. Although bones are remodeled during life, HLs may persist and are detectable for decades, which enables a retrospective evaluation of the health condition of an individual during childhood and adolescence [17]. Thus, the observation of HLs remains a useful tool for paleopathologists, biological anthropologists, and others, but they tend to be considered supportive information rather than standalone proof and are used along with other indicators, such as cribra orbitalia, enamel hypoplasia [16], or traces of physical injury [15].

Among the advantages of evaluating HLs in bioarcheological studies, it should be emphasized that it is an affordable and widely available method, which may be important for low-income countries or for low-cost studies conducted by students or novice scientists.

Besides recording the presence and number of HLs, it is possible to estimate age at their formation [4], which may provide additional information on archeological populations [10,18–20]. For example, Hughes et al. [21] noted different distributions of age at HL formation in different age groups, and Jerszyńska and Nowak [18] observed different distributions of HLs in males and females. However, the chronology of the HL formation is rarely calculated despite many available methods. There were 357 articles including the phrase "Harris Lines" published between 2020 and 2023 and indexed by the Google Scholar search engine, yet (to the best of our knowledge) most of them solely recorded the presence of HLs, without their chronology estimation. We managed to find only three recent articles that actually estimated age at HL formation [22–24]. Yet there are many articles in which the calculation of HL chronology turned out to be a valuable tool [18–20]. Why, then, recently, has the age at HL deposition rarely been taken into consideration?

Besides the controversies mentioned above, the calculation of age at HL formation may still be considered time-consuming and hard to understand and calculate. Six methods exist for estimating age at HL formation: Allison and McHenry's [25,26]; Hunt and Hatch's [27]; Clarke's [28], Maat's [29]; Hummert and van Gerven's [30]; and Byers' [31], recently modified by Kulus and Dąbrowski [4]. Until recently, there were no reviews on how to calculate it and which method may be considered the best one [4]. Research related to determining the chronology of the formation of Harris Lines thus involves a lengthy search for appropriate methods, often described in great detail and requiring a lot of time to learn.

This applies not only to HLs but other indicators; for example, age at linear enamel hypoplasia (LEH) formation may be also calculated with many methods [32–34], yet there are a vast number of publications that solely record its presence or lack thereof [35,36]. This may be caused by controversies regarding the precision of LEH chronology estimation [37] or difficulties in calculations and seemingly complex methodologies.

Henriquez and Oxenham [38] recently simplified the calculations of LEH chronology, increasing, concurrently, the precision of age at LEH formation estimation. Their idea was simple yet effective—using existing growth tables, they derived equations describing age at LEH formation as a function of LEH positions on the tooth. Their work simplifies calculations greatly and may help in many further studies on LEH.

The current study is aimed at providing a new tool for fast and precise age at HL formation estimation based on growth curves rather than growth tables using a methodology similar to the one developed by Henriquez and Oxenham for the estimation of LEH chronology. This approach will result in the faster, easier, and more precise calculation of HLs, making them more accessible for scientific use.

2. Materials and Methods

2.1. Study Population

To evaluate the consistency of the new method, it was used to estimate the age of HL formation in bones from the archeological population of the St. Barbara Church parish cemetery, Wrocław, Poland (Figure 2). The cemetery was established in the 13th century and remained an active burial ground until the 19th century [39]. The remains used for this study were excavated from the area used between the 16th and 18th centuries, which was also confirmed by radiocarbon dating [40].

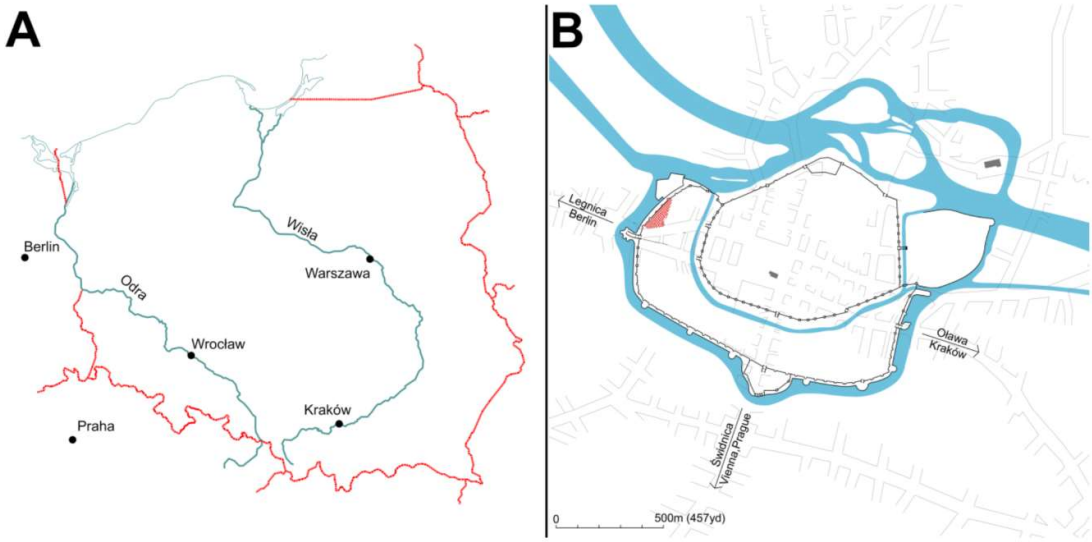

Figure 2. (**A**) Localization of Wrocław, Poland, and (**B**) cemetery of St. Barbara Church (red area).

The cemetery located within the parish of St. Barbara initially served as a burial ground primarily for indigent craftsmen [39]. Later, however, wealthier individuals also found their final resting places here. The necropolis underwent several expansions, continuing until the latter part of the 18th century [41]. The skeletal remains used for the current study were excavated in the latest part of the cemetery and consisted of an early modern population.

The sample consisted of 12 adult tibiae (from 6 males and 6 females) with 137 visible HLs, 6 non-adult tibiae (with 95 visible HLs), and 8 non-adult (age range: 1.5–8 years) femora (with 52 visible HLs). Only bones with abundant HLs were selected for this study.

Bones were imaged with the RTG Quantum Medical Imaging system (SWX RAY, Dallas, TX, USA), using standard parameters (45–50 kV; 17 mA; exposure time, 0.1 s). The total length of the bones and distance from HLs to the nearest bone end were measured using the MicroDicom Viewer (MicroDicom, Sofia, Bulgaria) to the nearest 0.1 cm. Transverse lines extending more than 1/4 the width of the bone were considered valid HLs.

2.2. Bone Growth Equation Development and Selection

The method presented in this article is based on Byers [31], which may be considered the best for the estimation of age at HL deposition; among the methods developed to date, this is the most precise. Previous models were discarded because they were

based on incorrect assumptions or had significant limitations. The methods of Allison and McHenry [25,26] assumed constant bone growth throughout life. Hunt and Hatch's method [27] included changes in the bone growth ratio during life; their method was based on precise equations but did not include differences in body (or bone) height between individuals. Clarke's method [28] did not include epiphyseal thickness, which introduced a constant error. The methods by Maat [29] and Hummert and van Gerven [30] are limited to the distal part of the tibia only.

Byers' method is free from these disadvantages. It is based on correct and logical assumptions and is not susceptible to errors associated with different bone lengths. It is also suitable for both the distal and proximal parts of the femur and tibia. Further details on the comparison of these methods are presented elsewhere [4]. The principles of Byers' method and its modification were presented in our latest review [4]; the required measurements are shown in Figure 3.

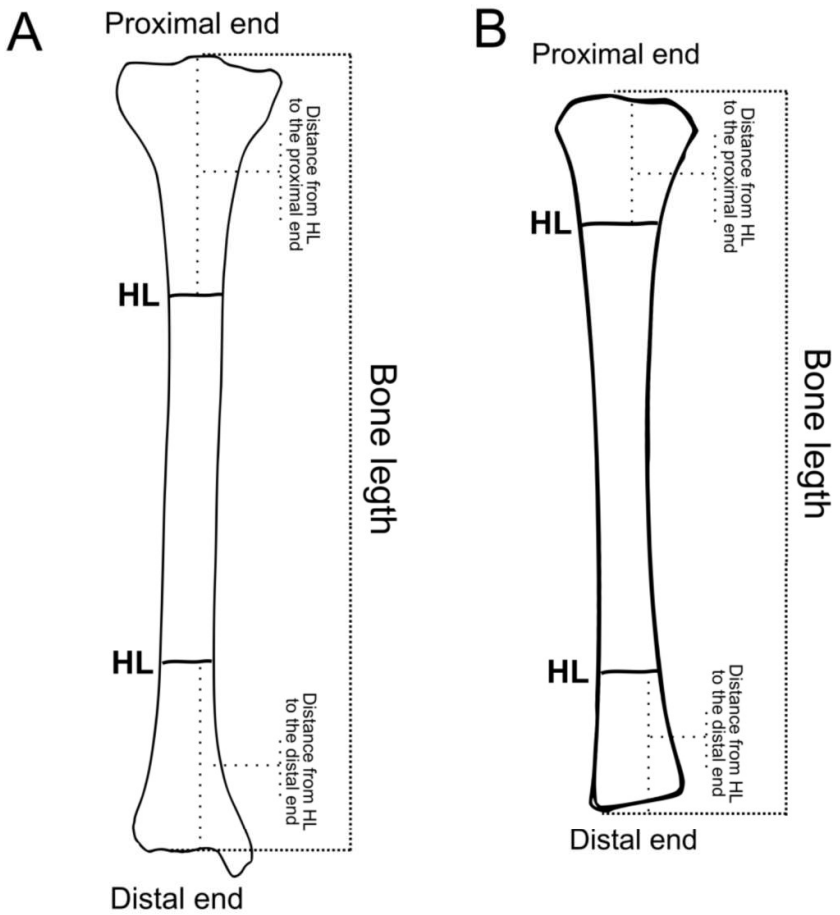

Figure 3. Measurements required for calculation of age at HL deposition with Byers' method. Calculations require two measurements: (a) total bone length and (b) distance from the HL to the nearest bone end. The method's principle is described in a recent open-access review [4]. (**A**) adult bone; (**B**) bone of non-adult.

Briefly, this method requires measurement of (a) the total bone length and (b) the distance from HLs to the closest bone end. Byers [31] developed equations that can determine the ratio of bone length at HL formation to the adult bone length using those

two measurements. The calculated ratio may be compared with values in the suitable table to determine age at HL formation. This method was further modified by [4], so it can be used for adult bones and non-adult bones.

Byers' equations and tables are based on datasets provided by Maresh [42], Gindhart [43], Anderson and Green [44], and Anderson et al. [45]. The data were collected in the mid-20th century (1943–1973) from various institutions in the United States, including the Children's Hospital in Boston [44,45], the Department of Maternal and Child Health of the Harvard School of Public Health [45], the Fels Research Institute for the Study of Human Development [43], the Child Research Council, and the University of Colorado School of Medicine [42]. It is important to note that the data were collected from white individuals of European descent [43].

The current study required the development of a simple, mathematical model describing the age at LEH formation as a function of the "bone length at HL formation/adult bone length" ratio. Growth curves were developed for tibiae and femora, as these two bone types are used most commonly in the study of HLs [46]. This approach allows for the creation of equations that describe the approximate age at which HL formation occurs. These equations are faster and easier to use than tables that require the calculation of HL chronology to the nearest 0.5 years, as was required in the previous method.

It should be emphasized that using this method does not require an understanding of its basic assumptions. It is enough to look at the diagrams showing the necessary measurements and to follow them.

Growth curves were developed based on the dataset adapted by Byers [31] from the aforementioned studies [42–45]. Three types of curves were fitted to the mentioned dataset using the non-linear estimation Levenberg–Marquardt algorithm provided by Statistica 13.1 (TIBCO Software Inc., Palo Alto, CA, USA): linear ($y = a \times x + b$), quadratic ($y = a \times x^2 + b \times x + c$), and exponential ($y = a \times e^{(b \times x)} + c$). In this equation, y represents the age at HL formation (in years), while x represents the ratio of bone length at HL formation to adult bone length. The parameters a, b, and c are curve-fitting parameters that have been established experimentally.

The optimal model was chosen with the Akaike Information Criterion (AIC), with correction for small samples (AICc) [47,48]. AIC/AICc enables the estimation of the best-fitted and least complicated equations from a set of different models. It helps to find the optimal tradeoff between model complexity and goodness of fit, preventing curve overfitting [49]. Models with the fewest parameters and lowest residuals are scored with the lowest AIC and are considered the best ones.

AIC/AICc were calculated with the AICcmodavg package [50] in the R environment [51]. For the purpose of further calculations, models with the lowest AICc were chosen.

2.3. Age at HL Calculation Tool Development

All equations derived in this study are sufficient for standalone calculations of age at HL formation. However, for the convenience of users, they are also provided as ready-to-use formulas, referred to as the 'age at HL calculation tool'. The age at HL calculation tool was designed as a Microsoft Excel spreadsheet (Supplementary File S1) that uses the equations chosen in Table 1. The spreadsheet automatically calculates the "bone length at HL formation/adult bone length" ratio and approximate age at HL formation. Instructions for the tool are available in the first sheet (entitled "About").

Table 1. Choosing the optimal equation. The *y* stands for age (given in years); *x* stands for the "bone length at HL formation/adult bone length" ratio (given in percentages); The lowest AIC indicates the optimal curve; AICc represents the AIC with correction for small groups. Residuals represent the sum of squared differences between the model and source values. Equations with the lowest AICc are bold.

Bone	Equation Type	Equation	AIC	AICc	Residuals
Femur (males)	Linear	$y = 0.217859 \times x - 6.43422$	25.82	27.82	3.234
	Quadratic	$\mathbf{y = 0.00106893 \times x^2 + 0.077086 \times x - 2.28129}$	**−18.35**	**−14.71**	**0.1804**
	Exponential	$y = 11.5213 \times e^{0.00979342 \times x} - 14.5196$	−15.94	−12.30	0.2098
Femur (females)	Linear	$y = 0.191588 \times x - 5.93988$	24.19	26.59	3.007
	Quadratic	$y = 0.00114036 \times x^2 + 0.0387797 \times x - 1.33028$	−12.01	−7.56	0.1963
	Exponential	$\mathbf{y = 6.84604 \times e^{0.0121551 \times x} - 9.07047}$	**−14.22**	**−9.77**	**0.1676**
Tibia (males)	Linear	$y = 0.216145 \times x - 6.14786$	20.56	22.56	2.328
	Quadratic	$\mathbf{y = 0.000860092 \times x^2 + 0.103426 \times x - 2.84765}$	**−13.35**	**−9.71**	**0.2467**
	Exponential	$y = 16.227 \times e^{0.00787971 \times x} - 19.5643$	−11.19	−7.55	0.2823
Tibia (females)	Linear	$y = 0.19219 \times x - 5.90254$	22.61	25.01	2.685
	Quadratic	$y = 0.00105703 \times x^2 + 0.0508895 \times x - 1.64875$	−4.59	−0.15	0.3333
	Exponential	$\mathbf{y = 7.78153 \times e^{0.011363 \times x} - 10.1631}$	**6.38**	**−1.94**	**0.2933**
Tibia (unisex)	Liner	$y = (0.211442) \times x + (-6.50326)$	33.78	35.78	5.318
	Quadratic	$y = 0.00128889 \times x^2 + (0.0374516) \times x + (-1.24991)$	4.29	7.93	0.7431
	Exponential	$\mathbf{y = (6.79694) \times exp^{0.0128072 \times x} + (-9.00042)}$	**1.11**	**4.75**	**0.6093**
Femur (unisex)	Linear	$y = (0.211759) \times x + (-6.65994)$	36.57	38.57	6.331
	Quadratic	$y = (0.00142038) \times x^2 + (0.0191624) \times x + (-0.812149)$	6.1	9.74	0.8323
	Exponential	$\mathbf{y = (5.61797) \times exp^{0.0140969 \times x} + (-7.60929)}$	**2.58**	**6.21**	**0.6677**

2.4. Bland–Altman Comparison of Method Outputs

To compare the performance of Byers' method and the method developed in the current study, Bland–Altman plots were used [52]. Each Bland–Altman plot compares the performance of two methods. The X-axis represents the mean value of each pair of results, and the Y-axis represents the difference between the output of the two methods for each pair of measurements. Concordant methods tend to have densely distributed dots and low mean differences. Discrepant methods have more dispersed points and a large mean difference.

3. Results

3.1. Bone Growth Curve Selection

Table 1 contains bone growth curves based on a dataset provided by Byers [31] for the tibia and femur. Distinct curves were designed for males and females. Moreover, for the calculations of the bones of non-adults, equations based on an averaged dataset were derived since the sex of non-adults (especially infants) cannot be reliably determined [53]. Figure 4 shows curves derived for the tibia.

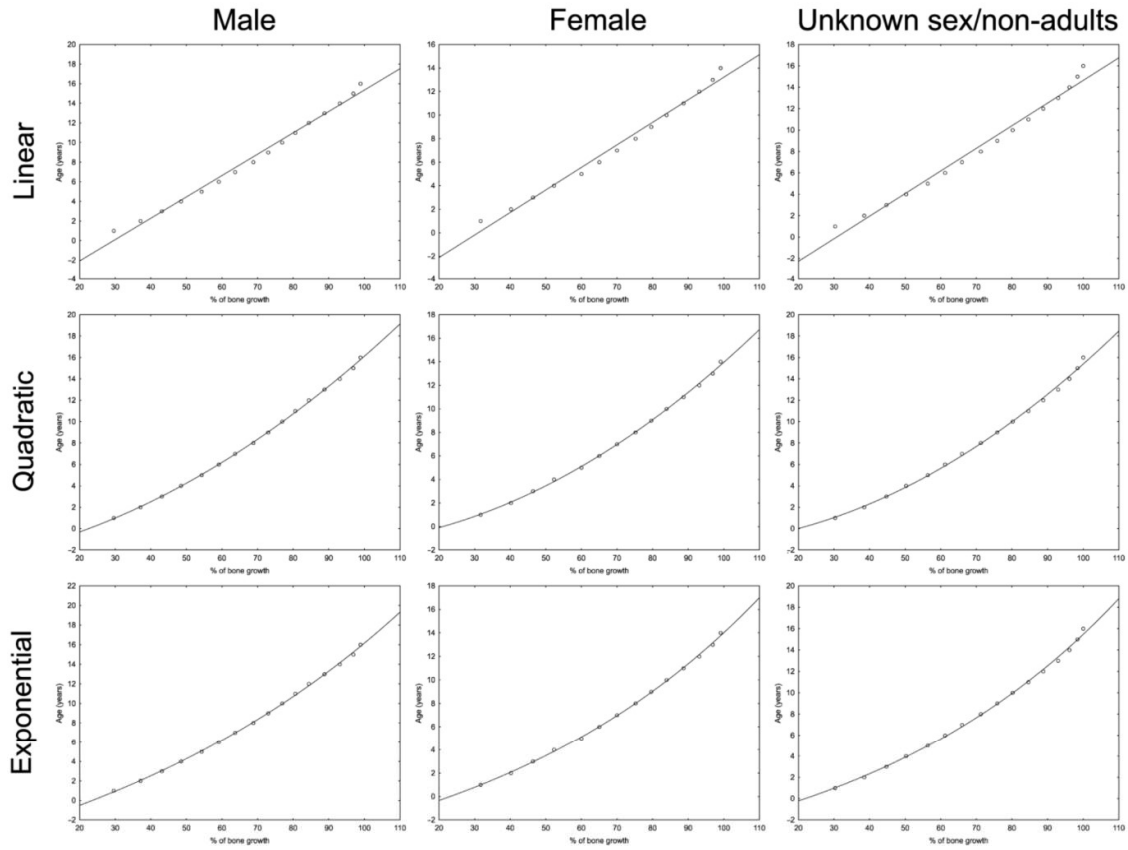

Figure 4. Bone growth curves. Dots indicate the values from bone growth tables provided by Byers [31]. Equations for each curve are shown in Table 1.

Each model was scored with AIC and AICc. The model with the lowest AICc was chosen for the age at HL formation calculation tool, although all the models can be used as standalone equations, available for use in any calculation software.

3.2. Age at HL Calculation Tool Development

Optimal curves were used to create an age at HL calculation tool, which is available for download as Supplementary File S1. Calculations require bone length [cm], the distance from HL to the closest bone end [cm], the localization of HL (distal or proximal bone part), and sex. The spreadsheet automatically calculates the "bone length at HL formation/adult bone length" ratio (with formulas derived by Byers [4,31]) and approximate age at HL formation (with formulas derived in the current study).

For the bones of children and juveniles, an estimated age of an individual is required. The spreadsheet additionally calculates the ratio of the current bone and "would-be-adult" bone length, which is used for the calculation of approximate age at HL formation.

Detailed instructions are present in the first sheet of Supplementary File S1.

3.3. New Method and Byers' Method Comparison

A comparison of the methods is shown in Figure 5. Bland–Altman plots show great concordance between Byers' method and the equations derived from the current study—the mean of the difference does not exceed 0.1 years, and the maximum difference does not

exceed 0.7 years. The differences between the methods are the result of the imprecision of Byers' method; his growth tables provide results for full years only, so the estimated result must be rounded to full-year or half-year intervals. Our new method is based on curve equations and does not have such limitations.

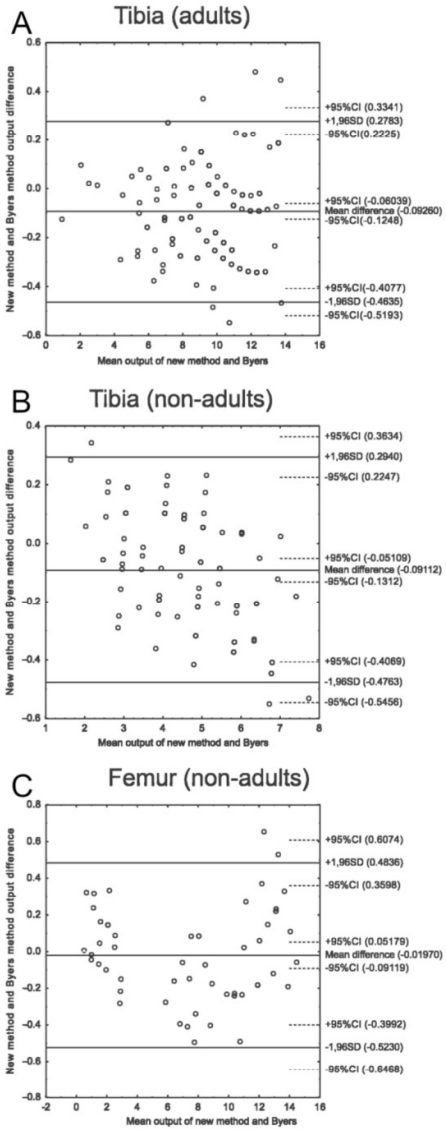

Figure 5. Bland–Altman plot comparing Byers' method and the new equations. The X-axis represents the mean output of two methods for one HL; the Y-axis represents the difference between the method outputs for each HL. The mean difference for tibias (**A**,**B**) is low and does not exceed 0.5 years; slightly worse results were obtained for femurs (**C**).

4. Discussion

In biological anthropology (and related fields), vast amounts of data may be ignored just because of the difficulties in calculations. Providing new, fast, and accurate tools may increase the quality of future studies. Although the method developed by Byers is still

applicable, it has one major disadvantage—the tables provided for age at HL deposition present values for full years only; therefore, the final results must be given in one-year or half-year intervals. Rounding the age at which HLs form can lead to decreased accuracy, particularly for HLs that are so close together that they must be classified as forming at the same time, which is an obvious error.

Moreover, without the latest modification [4], Byers' method could only be used for adult bones. Methods based on equations rather than tables are more accurate and less subjective [38]. Moreover, they enable faster calculations and may be easily used after basic training. These derived and selected equations fit the bone growth datasets accurately and enable calculations for adult and non-adult bones.

The previous, modified Byers' method [4] was tested for consistency using an artificial model of bones with abundant HLs. For a change, the method developed in this study was evaluated using actual bones. Although the population was rather limited, the equations derived in the current study show great concordance with the previous method, with differences not exceeding 0.7 years. It may be assumed that both methods are highly concordant and valid, but the newer method allows for increased estimation accuracy.

The method developed in this study is intended for use in biological anthropology and related fields, although it is not limited to them. Observing Harris Lines has clinical significance [5] and may be used to estimate age at HL formation in contemporary populations—the dataset used for the development of the current method was obtained in the 20th century [31] and shows similar growth patterns to modern populations.

Importantly, the application of this method does not require a prior understanding of its underlying assumptions. Users can achieve successful implementation by following the provided diagrams, which clearly illustrate the required measurements, and then using appropriate equations or Supplementary Material File S1. However, there is room for the optimization of this method. The modification that yields the best results, albeit the most challenging, is the source dataset for bone growth. It is important to note that different populations may exhibit variations in bone growth patterns, particularly during the adolescent growth spurt [54–56]. Creating our own growth curves based on the study population would result in the most accurate estimation of age at the formation of HLs. This is particularly important for populations that differ significantly from the mid-20th century white North American population.

A future tool for calculating age at HL formation may allow the equations to be customized based on the growth patterns of the population being studied. Assuming the same tibia (or femur)/body height ratio, based on decile charts for distinct populations, it may be quite possible to create customized equations for them. Although this would require more sophisticated tools than those used for the current study, it may be considered a future direction in the calculation of age at HL formation.

HLs cannot be correlated with bone length and morphology [1,57] or age at linear enamel hypoplasia (LEH) formation [58,59]. The lack of correlation with LEH may be considered a contradiction since both HLs and LEH possibly share similar etiologies [33,58]. However, this may be logically explained: LEH usually forms on anterior teeth, which are formed during early childhood [60]. HLs may form during the whole bone growth period; however, early HLs tend to disappear during the bone-remodeling process [58]. The evaluation of LEH and HLs in juvenile or infant individuals, who tend to have more pronounced and visible HLs [30], could lead to finding some correlation between both indicators. However, to the best of our knowledge, no such study has been conducted. Moreover, the reason may also be linked to the calculation methods of age at LEH/HL formation.

Until recently, the most accurate method of LEH formation estimation was the decile growth chart-based method developed by Reid and Dean [32,61]. The equation-based method by Goodman and Rose was deemed too simplistic to properly describe enamel growth [38,62]. Cumulative inaccuracies may impede the correlation of both indicators. A study on the remains of juvenile individuals, utilizing the Henriquez and Oxenham method for age at LEH formation estimation and the currently developed method for age

at HL formation estimation could bring more insights into the correlation (or lack thereof) between the two indicators.

It is important to note that the growth curves derived in this study are not universal. Byers' bone growth tables were developed based on a study of the North American white population in the mid-20th century [42–45], so they may be unsuitable for populations with different growth patterns. To achieve the most accurate estimation of HL chronology, new bone growth tables and models should be developed for the population under study following the methods presented in this study.

Also, this method shares inevitable disadvantages with the previous methods, as described in our previous review [4]. This method cannot take into consideration individual variations in bone growth, such as delayed or premature adolescent spurts, developmental defects, stunted growth, and others. Moreover, when evaluating age at HL formation in non-adult individuals, the possible inaccuracy of age estimation further decreases the precision of age at HL estimation. Therefore, it is important to evaluate age at HL formation in fairly large populations of study, to blur the influence of individual variability, and to include the abovementioned sources of inaccuracies in the limitations of studies.

5. Conclusions

This study introduces a novel equation-based method of estimating the age at which Harris Lines (HLs) form in bones, presenting significant improvements over previous approaches. An evaluation of its consistency using actual bones demonstrates high concordance with the existing methodologies but also higher accuracy. The new method paves the way for fast, accurate, and reliable age at HL formation estimation in biological anthropology and related fields.

Supplementary Materials: The following supporting information can be downloaded at https://www.mdpi.com/article/10.3390/life14040501/s1: File S1: Age at HL formation calculation tool. A Microsoft Excel spreadsheet facilitating the calculation of HL chronology. All instructions are included in the first sheet (entitled, "About").

Author Contributions: Conceptualization, M.J.K. and P.D., methodology, M.J.K., P.D. and J.G.; software, M.J.K.; validation, K.C., P.K. and J.G.; formal analysis, M.J.K. and K.C.; investigation, M.J.K.; resources, M.J.K.; data curation, M.J.K.; writing—original draft preparation, M.J.K., P.D., K.C., P.K. and P.S.-G.; writing—review and editing, M.J.K., P.D., K.C., P.K. and P.S.-G.; visualization, M.J.K.; supervision, P.D.; project administration, P.D.; funding acquisition, P.D. All authors have read and agreed to the published version of the manuscript.

Funding: This research was financed by the National Science Center, Poland, under the "OPUS 13" project, decision number: DEC-2017/25/B/HS3/02006; grant acquired by PD, Wroclaw Medical University.

Institutional Review Board Statement: Not applicable.

Informed Consent Statement: Not applicable.

Data Availability Statement: The data are contained within the article and Supplementary Material File S1.

Acknowledgments: The authors express their gratitude to Marzenna Podhorska-Okołów for her valuable consultations and John Patrick Perrin for proofreading.

Conflicts of Interest: The authors declare no conflicts of interest.

References

1. Nowak, O.; Piontek, J. Does the occurrence of Harris lines affect the morphology of human long bones? *HOMO—J. Comp. Hum. Biol.* **2002**, *52*, 254–276. [CrossRef]
2. Chauveau, A.; Augias, A.; Froment, A.; Beuret, F.; Charlier, P. Radio-Scannographic Correlation of Harris Lines in Adults: Forensic and Anthropological Perspectives. *Eur. J. Forensic Sci.* **2016**, *3*, 21–28. [CrossRef]
3. Miszkiewicz, J.J. Histology of a Harris line in a human distal tibia. *J. Bone Miner. Metab.* **2015**, *33*, 462–466. [CrossRef] [PubMed]
4. Kulus, M.J.M.J.; Dąbrowski, P. How to calculate the age at formation of Harris lines? A step-by-step review of current methods and a proposal for modifications to Byers' formulas. *Archaeol. Anthropol. Sci.* **2019**, *11*, 1169–1185. [CrossRef]

5. Georgiadis, A.G.; Gannon, N.P. Park-Harris Lines. *J. Am. Acad. Orthop. Surg.* **2022**, *30*, e1483–e1494. [CrossRef] [PubMed]
6. Scott, A.B.; Hoppa, R.D. Brief communication: A re-evaluation of the impact of radiographic orientation on the identification and interpretation of Harris lines. *Am. J. Phys. Anthropol.* **2015**, *156*, 141–147. [CrossRef] [PubMed]
7. Simpson, R. New and Emerging Prospects for the Paleopathological Study of Starvation. *Pathways* **2020**, *1*, 66–83. [CrossRef]
8. Nowak, O. Linie Harrisa jako miernik reakcji morfologicznej na warunki życia: Interpretacje, kontrowersje, propozycje badawcze. *Przegląd Antropol.* **1996**, *59*, 77–86. [CrossRef]
9. González-Reimers, E.; Pérez-Ramírez, A.; Santolaria-Fernández, F.; Rodríguez-Rodríguez, E.; Martínez-Riera, A.; Durán-Castellón, M.d.C.; Alemán-Valls, M.R.; Gaspar, M.R. Association of Harris lines and shorter stature with ethanol consumption during growth. *Alcohol* **2007**, *41*, 511–515. [CrossRef] [PubMed]
10. Piontek, J.; Jerszyńska, B.; Nowak, O. Harris Lines in subadult and adult skeletons from the medieval cemetery in Cedynia, Poland. *Var. Evol.* **2001**, *9*, 33–43.
11. Nowakowski, D. Frequency of appearance of transverse (Harris) lines reflects living conditions of the Pleistocene bear-Ursus ingressus-(Sudety Mts., Poland). *PLoS ONE* **2018**, *13*, e0196342. [CrossRef] [PubMed]
12. MacChiarelli, R.; Bondioli, L.; Censi, L.; Hernaez, M.K.; Salvadei, L.; Sperduti, A. Intra- and interobserver concordance in scoring Harris lines: A test on bone sections and radiographs. *Am. J. Phys. Anthropol.* **1994**, *95*, 77–83. [CrossRef] [PubMed]
13. Primeau, C.; Jakobsen, L.S.; Lynnerup, N. CT imaging vs. traditional radiographic imaging for evaluating Harris Lines in tibiae. *Anthropol. Anz.* **2016**, *73*, 99–108. [CrossRef] [PubMed]
14. Tomaszewska, A.; Psonak, D. The affinity of the Harris lines to bone massiveness. *Anthropol. Anz.* **2020**, *78*, 207. [CrossRef] [PubMed]
15. González-Ramírez, A.; Pacheco Miranda, A.; Sáez, A.; Arregui Wunderlich, I. Infants from the Tarapacá 40 cemetery (Northern Chile, Formative Period, 1000 BC–AD 600). *Int. J. Osteoarchaeol.* **2019**, *29*, 874–880. [CrossRef]
16. Geber, J. Skeletal manifestations of stress in child victims of the Great Irish Famine (1845–1852): Prevalence of enamel hypoplasia, Harris lines, and growth retardation. *Am. J. Phys. Anthropol.* **2014**, *155*, 149–161. [CrossRef] [PubMed]
17. Primeau, C.; Homøe, P.; Lynnerup, N. Childhood health as reflected in an adult urban and a rural samples from medieval Denmark. *Homo* **2018**, *69*, 6–16. [CrossRef] [PubMed]
18. Jerszyńska, B.; Nowak, O. Application of Byers method for reconstruction of age at formation of Harris lines in adults from a cemetery of Cedynia (Poland). *Var. Evol.* **1996**, *5*, 75–82.
19. Ameen, S.; Staub, L.; Ulrich, S.; Vock, P.; Ballmer, F.; Anderson, S.E. Harris lines of the tibia across centuries: A comparison of two populations, medieval and contemporary in Central Europe. *Skeletal Radiol.* **2005**, *34*, 279–284. [CrossRef] [PubMed]
20. Nowak, O.; Piontek, J. The frequency of appearance of transverse (Harris) lines in the tibia in relationship to age at death. *Ann. Hum. Biol.* **2002**, *29*, 314–325. [CrossRef] [PubMed]
21. Hughes, C.; Heylings, D.J.A.; Power, C. Transverse (Harris) lines in Irish archaeological remains. *Am. J. Phys. Anthropol.* **1996**, *101*, 115–131. [CrossRef]
22. Wojenka, M.; Jaskulska, E.; Popović, D.; Baca, M.; Frog; Fetner, R.; Wertz, K.; Rataj, K.; Gryczewska, N.; Kosiński, T.; et al. The girl with finches: A unique post-medieval burial in Tunel Wielki Cave, southern Poland. *Praehist. Zeitschrift* **2021**, *96*, 286–309. [CrossRef]
23. Welsh, H. Investigating Patterns of Growth and Development in Subadults from the 10th–13th Century Cemetery of St. Étienne de Toulouse, France, McMaster University. 2021. Available online: https://macsphere.mcmaster.ca/bitstream/11375/26917/2/Welsh_Hayley_finalsubmission2021September_MA.pdf (accessed on 11 April 2024).
24. Debard, J. *Les Conditions Socio-Économiques Pendant L'âge du Fer en Suisse Occidentale: Intégration des Paramètres Archéologiques, Bioanthropologiques, Paléopathologiques et Paléoalimentaires*; l'Université de Genève: Geneva, Switzerland, 2020.
25. Allison, M.J.; Mendoza, D.; Pezzia, A. A radiographic approach to Childhood illness in precolumbian inhabitants of Southern Peru. *Am. J. Phys. Anthropol.* **1974**, *40*, 409–415. [CrossRef] [PubMed]
26. McHenry, H.M.; Schulz, P.D. The association between Harris lines and enamel hypoplasia in prehistoric California Indians. *Am. J. Phys. Anthropol.* **1976**, *44*, 507–511. [CrossRef] [PubMed]
27. Hunt, E.E.; Hatch, J.W. The estimation of age at death and ages of formation of transverse lines from measurements of human long bones. *Am. J. Phys. Anthropol.* **1981**, *54*, 461–469. [CrossRef]
28. Clarke, S.K. The association of early childhood enamel hypoplasias an radiopaque transverse lines in a culturally diverse prehistoric skeletal sample. *Hum. Biol.* **1982**, *54*, 77–84. [PubMed]
29. Maat, G.J.R. Dating and rating of Harris's lines. *Am. J. Phys. Anthropol.* **1984**, *63*, 291–299. [CrossRef] [PubMed]
30. Hummert, J.R.; Van Gerven, D.P. Observations on the formation and persistence of radiopaque transverse lines. *Am. J. Phys. Anthropol.* **1985**, *66*, 297–306. [CrossRef] [PubMed]
31. Byers, S. Calculation of age at formation of radiopaque transverse lines. *Am. J. Phys. Anthropol.* **1991**, *85*, 339–343. [CrossRef] [PubMed]
32. Reid, D.J.; Dean, M.C. Variation in modern human enamel formation times. *J. Hum. Evol.* **2006**, *50*, 329–346. [CrossRef] [PubMed]
33. Goodman, A.H.; Song, R.J. Sources of Variation in Estimated Ages at Formation of Linear Enamel Hypoplasias. In *Human Growth in the Past: Studies from Bones and Teeth*; Hoppa, R., FitzGerald, C., Eds.; Cambridge University Press: Cambridge, UK, 1999; pp. 210–239.

34. Swärdstedt, T. *Odontological Aspects of a Medieval Population in the Province of Jamtland, Mid-Sweden*; University of Lund: Lund, Sweden, 1966.
35. Belcastro, G.; Rastelli, E.; Mariotti, V.; Consiglio, C.; Facchini, F.; Bonfiglioli, B. Continuity or discontinuity of the life-style in central Italy during the Roman Imperial Age-Early Middle Ages transition: Diet, health, and behavior. *Am. J. Phys. Anthropol.* **2007**, *132*, 381–394. [CrossRef] [PubMed]
36. Ham, A.C.; Temple, D.H.; Klaus, H.D.; Hunt, D.R. Evaluating life history trade-offs through the presence of linear enamel hypoplasia at Pueblo Bonito and Hawikku: A biocultural study of early life stress and survival in the Ancestral Pueblo Southwest. *Am. J. Hum. Biol.* **2020**, *33*, e23506. [CrossRef] [PubMed]
37. Ritzman, T.B.; Baker, B.J.; Schwartz, G.T. A fine line: A comparison of methods for estimating ages of linear enamel hypoplasia formation. *Am. J. Phys. Anthropol.* **2008**, *135*, 348–361. [CrossRef] [PubMed]
38. Henriquez, A.C.; Oxenham, M.F. New distance-based exponential regression method and equations for estimating the chronology of linear enamel hypoplasia (LEH) defects on the anterior dentition. *Am. J. Phys. Anthropol.* **2019**, *168*, 510–520. [CrossRef]
39. Burak, M.; Okólska, H. *Cmentarze Dawnego Wrocławia*; Wydawnictwo Muzeum Architektury: Wroclaw, Poland, 2007.
40. Dąbrowski, P.; Kulus, M.J.; Grzelak, J.; Olchowy, C.; Staniowski, T.; Paulsen, F. Nutritional reconstruction in an early modern population: Searching for a relationship between dental microwear and bone element composition. *Ann. Anat.-Anat. Anzeiger* **2022**, *240*, 151884. [CrossRef] [PubMed]
41. Labuda, A.S. *Wrocławski Ołtarz św. Barbary i Jego Twórcy: Studium o Malarstwie Śląskim Połowy XV Wieku*; Wydawnictwo Uniwersytetu Adama Mickiewicza: Poznań, Poland, 1984.
42. Maresh, M.M. Linear Growth of Extremities from Infancy Through Adolescence. *Am. J. Dis. Child.* **1955**, *89*, 725–742.
43. Gindhart, P.S. Growth standards for the tibia and radius in children aged one month through eighteen years. *Am. J. Phys. Anthropol.* **1973**, *39*, 41–48. [CrossRef] [PubMed]
44. Anderson, M.; Green, W.T. Lengths of the femur and the tibia; norms derived from orthoroentgenograms of children from 5 years of age until epiphysial closure. *Am. J. Dis. Child.* **1948**, *75*, 279–290. [CrossRef] [PubMed]
45. Anderson, M.; Green, W.T.; Messner, M.B. Growth and predictions of growth in the lower extremities. *J. Bone Jt. Surg. Am.* **1963**, *45-A*, 1–14. [CrossRef]
46. Papageorgopoulou, C.; Suter, S.K.; Rühli, F.J.; Siegmund, F. Harris lines revisited: Prevalence, comorbidities, and possible etiologies. *Am. J. Hum. Biol.* **2011**, *23*, 381–391. [CrossRef] [PubMed]
47. Akaike, H. A new look at the statistical model identification. *IEEE Trans. Automat. Contr.* **1974**, *19*, 716–723. [CrossRef]
48. Pan, W. Akaike's Information Criterion in Generalized Estimating Equations. *Biometrics* **2001**, *57*, 120–125. [CrossRef]
49. Lever, J.; Krzywinski, M.; Altman, N. Points of Significance: Model selection and overfitting. *Nat. Methods* **2016**, *13*, 703–704. [CrossRef]
50. Mazerolle, M.J. AICcmodavg: Model Selection and Multimodel Inference Based on (Q)AIC(c). 2020. Available online: https://cran.r-project.org/web/packages/AICcmodavg/AICcmodavg.pdf (accessed on 11 April 2024).
51. *R Core Team R: A Language And Environment for Statistical Computing*; R Foundation for Statistical Computing: Vienna, Austria, 2021.
52. Bland, J.M.; Altman, D.G. Statistical Methods for Assessing Agreement between Two Methods of Clinical Measurement. *Lancet* **1986**, *327*, 307–310. [CrossRef]
53. Buikstra, J.E.J.; Ubelaker, D.H.D. *Standards for Data Collection from Human Skeletal Remains*; Arkansas Archeological Survey: Fayetteville, AR, USA, 1994; Volume 44, ISBN 9781563490750.
54. Miles, A.E.W.; Bulman, J.S. Growth curves of immature bones from a Scottish island population of sixteenth to mid-nineteenth century: Limb-bone diaphyses and some bones of the hand and foot. *Int. J. Osteoarchaeol.* **1994**, *4*, 121–136. [CrossRef]
55. Aldegheri, R.; Agostini, S. A chart of anthropometric values. *J. Bone Jt. Surg. Br.* **1993**, *75*, 86–88. [CrossRef]
56. Taranger, J.; Hägg, U. The timing and duration of adolescent growth. *Acta Odontol. Scand.* **1980**, *38*, 57–67. [CrossRef] [PubMed]
57. Mays, S.A. The relationship between harris line formation and bone growth and development. *J. Archaeol. Sci.* **1985**, *12*, 207–220. [CrossRef]
58. Mays, S. The relationship between harris lines and other aspects of skeletal development in adults and juveniles. *J. Archaeol. Sci.* **1995**, *22*, 511–520. [CrossRef]
59. Alfonso, M.P.; Thompson, J.L.; Standen, V.G. Reevaluating Harris lines—A comparison between Harris lines and enamel hypoplasia. *Coll. Antropol.* **2005**, *29*, 393–408. [PubMed]
60. Nelson, S.J. *Wheeler's Dental Anatomy, Physiology, and Occlusion*, 3rd ed.; Elsevier: St. Louis, MI, USA, 2015; ISBN 9780323263238.
61. Reid, D.J.; Dean, M.C. Brief communication: The timing of linear hypoplasia on human anterior teeth. *Am. J. Phys. Anthr.* **2000**, *113*, 135–139. [CrossRef]
62. Krenz-Niedbała, M.; Kozłowski, T. Comparing the chronological distribution of enamel hypoplasia in Rogowo, Poland (2nd century AD) using two methods of defect timing estimation. *Int. J. Osteoarchaeol.* **2013**, *23*, 410–420. [CrossRef]

Podsumowanie i wnioski

1. Analiza urazów na badanej czaszce wskazuje na zaawansowane stadium syfilisu kostnego.

2. Stężenie rtęci w badanych kościach nie pozwala na stwierdzenie zastosowania terapii z użyciem soli rtęci.

3. Czaszka syfilityka z cmentarza Salwatora odznaczała się szczególnie dużą zawartością arsenu, co może być powiązane z próbami leczenia tej choroby. Nie można wykluczyć również innych źródeł pochodzenia arsenu, takich jak długoletnia praca w kopalni arsenu lub kopalni złota bądź spożywanie wody zanieczyszczonej związkami arsenu.

4. Porównanie dotychczasowych metod obliczania czasu powstania linii Harrisa pozwoliło wskazać metodę opracowaną przez Byersa jako najlepszą. Dzięki wprowadzonym modyfikacjom może zostać ona zastosowana również na kościach niedojrzałych osobników.

5. Opracowanie serii wzorów do obliczania wieku powstania linii Harrisa na podstawie ich odległości od końca kości oraz całkowitej długości kości stanowi znaczący postęp. Podejście to oferuje dokładniejszą i szybszą metodę szacowania wieku powstania linii Harrisa niż wcześniej ustalone techniki.

Załączniki

Oświadczenia współautorów publikacji stanowiących podstawę Pracy Doktorskiej

Oświadczenia do pracy „A case of syphilis with high bone arsenic concentration from early modern cemetry (Wrocław, Poland)”.

Imię i nazwisko
Paweł Dąbrowski

Zakład Anatomii Prawidłowej UMW

Miejscowość i data
Wrocław, 23.09.2024

OŚWIADCZENIE

Oświadczam, że w pracy

Dabrowski, Pawel, Kulus, Michal Jerzy, Cieslik, Agata, Domagala, Zygmunt, Wiglusz, Rafał J., Kuropka, Piotr, Kuryszko, Jan, Thannhauser, Agata, Szleszkowski, Lukasz, Wojtulek, Piotr Marian, Solinski, Daniel and Dziegiel, Piotr. **"A case of syphilis with high bone arsenic concentration from early modern cemetery (Wroclaw, Poland)"** *Open Life Sciences*, vol. 14, no. 1, 2019, pp. 427-439. https://doi.org/10.1515/biol-2019-0048

mój udział polegał na: opracowanie antropologiczne i paleopatologiczne materiału, zebranie literatury, opracowanie koncepcji artykułu.

Podpis

Wrocław, 24.09.2024

dr Agata Cieślik
Instytut Immunologii i Terapii Doświadczalnej PAN im. Ludwika Hirszfelda
We Wrocławiu
ul. Weigla 12
53-114 Wrocław

OŚWIADCZENIE

Oświadczam, że w pracy

Dabrowski, Pawel, Kulus, Michal Jerzy, Cieslik, Agata, Domagala, Zygmunt, Wiglusz, Rafał J., Kuropka, Piotr, Kuryszko, Jan, Thannhauser, Agata, Szleszkowski, Lukasz, Wojtulek, Piotr Marian, Solinski, Daniel and Dziegiel, Piotr. **"A case of syphilis with high bone arsenic concentration from early modern cemetery (Wroclaw, Poland)"** *Open Life Sciences*, vol. 14, no. 1, 2019, pp. 427-439. https://doi.org/10.1515/biol-2019-0048

mój udział polegał na: współtworzeniu pierwotnej wersji manuskryptu (opis materiału kostnego, interpretacja zmian patologicznych), współtworzeniu wersji finalnej draftu (recenzja, edytowanie)

Podpis

Zygmunt Domagała
Imię i nazwisko
Afiliacja
Zakład Anat Patrol

Miejscowość i data

OŚWIADCZENIE

Oświadczam, że w pracy

Dabrowski, Pawel, Kulus, Michal Jerzy, Cieslik, Agata, Domagala, Zygmunt, Wiglusz, Rafał J., Kuropka, Piotr, Kuryszko, Jan, Thannhauser, Agata, Szleszkowski, Lukasz, Wojtulek, Piotr Marian, Solinski, Daniel and Dziegiel, Piotr. **"A case of syphilis with high bone arsenic concentration from early modern cemetery (Wroclaw, Poland)"** *Open Life Sciences*, vol. 14, no. 1, 2019, pp. 427-439. https://doi.org/10.1515/biol-2019-0048

mój udział polegał na:

— finansach
— ocena kultur mikrobiologicznych

Podpis
Koordynator Programu Erasmus +
Wydział Lekarski
Erasmus + Coordinator
dr Zygmunt Domagała

Ithaca, USA, 30.09.2024 r.

Prof. dr hab. Rafał J. Wiglusz,
Instytut Niskich Temperatur i Badań Strukturalnych
Polska Akademia Nauk
Oddziału Fizykochemii Biomedycznej
ul. Okólna2, 50-422 Wrocław
tel.: (+48) (071) 3954159
e-mail: R.Wiglusz@intibs.pl
web-page: http://www.intibs.pl

OŚWIADCZENIE

Oświadczam, że w pracy

Dabrowski, Pawel, Kulus, Michal Jerzy, Cieslik, Agata, Domagala, Zygmunt, Wiglusz, Rafał J., Kuropka, Piotr, Kuryszko, Jan, Thannhauser, Agata, Szleszkowski, Lukasz, Wojtulek, Piotr Marian, Solinski, Daniel and Dziegiel, Piotr. "**A case of syphilis with high bone arsenic concentration from early modern cemetery (Wroclaw, Poland)**" *Open Life Sciences*, vol. 14, no. 1, 2019, pp. 427-439. https://doi.org/10.1515/biol-2019-0048

mój udział polegał na badaniu i analizie składu pierwiastkowego w materiałach pobranych z czaszki pozyskanej podczas wykopalisk prowadzonych w latach 2006-2007 na pl. Czystym (*niem*. Salvator Platz) Wrocławiu (Polska), na dawnym cmentarzu parafialnym ewangelickiego Kościoła Chrystusa Zbawiciela (*niem.* Salvatorkirche).

Podpis

Podpisany elektronicznie przez
Rafał Jakub Wiglusz
30.09.2024
15:18:59 -04'00'

dr hab. Piotr Kuropka, prof. UPWr
Zakład Histologii i Embriologii
Katedra Biostruktury i Fizjologii Zwierząt
Wydział Medycyny Weterynaryjnej
Uniwersytet Przyrodniczy we Wrocławiu

Wrocław, 06.06.2024

OŚWIADCZENIE

Oświadczam, że w pracy

Dabrowski, Pawel, Kulus, Michal Jerzy, Cieslik, Agata, Domagala, Zygmunt, Wiglusz, Rafał J., Kuropka, Piotr, Kuryszko, Jan, Thannhauser, Agata, Szleszkowski, Lukasz, Wojtulek, Piotr Marian, Solinski, Daniel and Dziegiel, Piotr. **"A case of syphilis with high bone arsenic concentration from early modern cemetery (Wroclaw, Poland)"** *Open Life Sciences*, vol. 14, no. 1, 2019, pp. 427-439. https://doi.org/10.1515/biol-2019-0048

mój udział polegał na: analizie mikroskopowej kości w świetle fluorescencyjnym

Podpis

KIEROWNIK ZAKŁADU HISTOLOGII I EMBRIOLOGII
dr hab. Piotr Kuropka prof. nadzw.

Profesor Jan Kuryszko zmarł 29 października 2021.

Dr n.med i n. o zdr. Agata Thannhäuser
Katedra Medycyny Sądowej
Zakład Prawa Medycznego
Uniwersytetu Medycznego im. Piastów Śląskich we Wrocławiu

Wrocław, 11.06.2024

OŚWIADCZENIE

Oświadczam, że w pracy

Dąbrowski Paweł, Kulus Michał Jerzy, Cieślik Agata, Domagała Zygmunt, Wigliusz Rafał J., Kuropka Piotr, Kuryszko Jan, Thannhäuser Agata, Szleszkowski Łukasz, Wojtulek Piotr Marian, Soliński Daniel and Dzięgiel Piotr **„ A case of syphilis with high bone arsenic concentration from early modern cementery (Wroclaw, Poland)"** *Open Life Sciences*, vol, 14, no 1, 2019, pp.427-439

https://doi.org/10.1515/biol-2019-0048

mój udział polegał na: opisie antropologiczno-medyczno-sądowym czaszki, wykonaniu dokumentacji fotograficznej.

Łukasz Szleszkowski
Katedra Medycyny Sądowej UMW we Wrocławiu

Wrocław, 30/09/24

OŚWIADCZENIE

Oświadczam, że w pracy

Dabrowski, Pawel, Kulus, Michal Jerzy, Cieslik, Agata, Domagala, Zygmunt, Wiglusz, Rafał J., Kuropka, Piotr, Kuryszko, Jan, Thannhauser, Agata, Szleszkowski, Lukasz, Wojtulek, Piotr Marian, Solinski, Daniel and Dziegiel, Piotr. **"A case of syphilis with high bone arsenic concentration from early modern cemetery (Wroclaw, Poland)"** *Open Life Sciences*, vol. 14, no. 1, 2019, pp. 427-439. https://doi.org/10.1515/biol-2019-0048

mój udział polegał na: przeprowadzeniu analizy sądowo-medycznej materiału

Uniwersytet Medyczny we Wrocławiu
Katedra i Zakład Medycyny Sądowej
PRACOWNIA TANATOLOGII SĄDOWEJ
Kierownik
dr n. med. Łukasz Szleszkowski

dr n.med.Łukasz Szleszkowski

Podpis

Piotr Wojtulek
Instytut Nauk Geologicznych, Uniwersytet Wrocławski

Wrocław, 25.09.2024

OŚWIADCZENIE

Oświadczam, że w pracy

Dabrowski, Pawel, Kulus, Michal Jerzy, Cieslik, Agata, Domagala, Zygmunt, Wiglusz, Rafał J., Kuropka, Piotr, Kuryszko, Jan, Thannhauser, Agata, Szleszkowski, Lukasz, Wojtulek, Piotr Marian, Solinski, Daniel and Dziegiel, Piotr. **"A case of syphilis with high bone arsenic concentration from early modern cemetery (Wroclaw, Poland)"** *Open Life Sciences*, vol. 14, no. 1, 2019, pp. 427-439. https://doi.org/10.1515/biol-2019-0048

mój udział polegał na wykonaniu preparatów mikroskopowych przedmiotu badań wraz z analizą mineralogiczną materiału oraz dostarczeniem częściowej interpretacji związanej z charakterem biomineralizacji. Pragnę jednak podkreślić, że analiza ta miała charakter jedynie cząstkowy, dostarczając wyłącznie dodatkowych argumentów na poparcie głównego modelu, który został zaprezentowany w przedmiotowym artykule.

Piotr Wojtulek

Podpis

Wrocław, 30.09.2024

Daniel Soliński

OŚWIADCZENIE

Oświadczam, że w pracy

Dabrowski, Pawel, Kulus, Michal Jerzy, Cieslik, Agata, Domagala, Zygmunt, Wiglusz, Rafał J., Kuropka, Piotr, Kuryszko, Jan, Thannhauser, Agata, Szleszkowski, Lukasz, Wojtulek, Piotr Marian, Solinski, Daniel and Dziegiel, Piotr. **"A case of syphilis with high bone arsenic concentration from early modern cemetery (Wroclaw, Poland)"** *Open Life Sciences*, vol. 14, no. 1, 2019, pp. 427-439. https://doi.org/10.1515/biol-2019-0048

mój udział polegał na: analizie radiologicznej dostarczonego materiału kostnego.

Podpis

Soliński

Prof. dr hab. Piotr Dzięgiel
Zakład Histologii i Embriologii
Katedry Morfologii i Embriologii Człowieka

Wrocław, 10.06.2024

OŚWIADCZENIE

Oświadczam, że w pracy

Dabrowski, Pawel, Kulus, Michal Jerzy, Cieslik, Agata, Domagala, Zygmunt, Wiglusz, Rafał J., Kuropka, Piotr, Kuryszko, Jan, Thannhauser, Agata, Szleszkowski, Lukasz, Wojtulek, Piotr Marian, Solinski, Daniel and Dziegiel, Piotr. **"A case of syphilis with high bone arsenic concentration from early modern cemetery (Wroclaw, Poland)"** *Open Life Sciences*, vol. 14, no. 1, 2019, pp. 427-439. https://doi.org/10.1515/biol-2019-0048

mój udział polegał na:

Nadzorze nad prowadzonymi badaniami, krytycznej ocenie i korekcie manuskryptu

Uniwersytet Medyczny we Wrocławiu
ZAKŁAD HISTOLOGII I EMBRIOLOGII
kierownik
prof. dr hab. Piotr Dzięgiel

Podpis

Oświadczenie do pracy „How to calculate the age atf ormation of Harris lines? A step-by-step review od current methods and a proposal for modifications to Byers' formulas

Imię i nazwisko
Paweł Dąbrowski
Zakład Anatomii Prawidłowej UMW

Miejscowość i data
Wrocław, 23.09.2024

OŚWIADCZENIE

Oświadczam, że w pracy

Kulus, Michał Jerzy, Paweł Dąbrowski. "How to calculate the age at formation of Harris lines? A step-by-step review of current methods and a proposal for modifications to Byers' formulas." *Archaeological and Anthropological Sciences* 11.4 (2019): 1169-1185.

mój udział polegał na: kwerendzie bilbiotecznej, współtworzeniu koncepcji, krytycznym przeglądzie artykułu

Podpis

Oświadczenia do pracy „New equations for the estimation of the age of the formation of the Harris lines"

Kamil Cebulski
Zakład Histologii i Embriologii
Katedra Morfologii i Embriologii Człowieka
Uniwersytet Medyczny we Wrocławiu

Wrocław 24.09.2024

OŚWIADCZENIE

Oświadczam, że w pracy Kulus, Michał J., Kamil Cebulski, Piotr Kmiecik, Patrycja Sputa-Grzegrzółka, Joanna Grzelak, and Paweł Dąbrowski. 2024. "New Equations for the Estimation of the Age of the Formation of the Harris Lines" *Life* 14, no. 4: 501. https://doi.org/10.3390/life14040501\ mój udział polegał na: weryfikacji wzorów matematycznych i programu do obliczania wieku linii Harrisa, współtworzeniu koncepcji pracy, krytycznej rewizji manuskryptu.

Kamil Cebulski

dr inż. arch. Piotr Kmiecik
Akademia Nauk Stosowanych Angelusa Silesiusa

Wrocław, 25.9.2024

OŚWIADCZENIE

Oświadczam, że w pracy

Kulus, Michał J., Kamil Cebulski, Piotr Kmiecik, Patrycja Sputa-Grzegrzółka, Joanna Grzelak, and Paweł Dąbrowski. 2024. "New Equations for the Estimation of the Age of the Formation of the Harris Lines" *Life* 14, no. 4: 501. https://doi.org/10.3390/life14040501

mój udział polegał na:

Określenie datowania i warunków środowiskowych na podstawie danych z zakresu archeologii i historii architektury. Opracowanie części materiałów graficznych do publikacji.

Podpis

Patrycja Sputa-Grzegrzółka
Zakład Anatomii Prawidłowej
Katedra Morfologii i Embriiologii Człowieka
Uniwersytet Medyczny we Wrocławiu

Wrocław, 23.09.2024

OŚWIADCZENIE

Oświadczam, że w pracy

Kulus, Michał J., Kamil Cebulski, Piotr Kmiecik, Patrycja Sputa-Grzegrzółka, Joanna Grzelak, and Paweł Dąbrowski. 2024. "New Equations for the Estimation of the Age of the Formation of the Harris Lines" *Life* 14, no. 4: 501. https://doi.org/10.3390/life14040501

mój udział polegał na: pisaniu pierwotnej wersji manuskryptu publikacji, redagowaniu oraz ostatecznej korekcie.

Podpis

Patrycja Sputa-Grzegrzółka

Joanna Grzelak
Uniwersytet Medyczny we Wrocławiu

Wrocław, 25.09.2024

OŚWIADCZENIE

Oświadczam, że w pracy

Kulus, Michał J., Kamil Cebulski, Piotr Kmiecik, Patrycja Sputa-Grzegrzółka, Joanna Grzelak, and Paweł Dąbrowski. 2024. "New Equations for the Estimation of the Age of the Formation of the Harris Lines" *Life* 14, no. 4: 501. https://doi.org/10.3390/life14040501\

mój udział polegał na: pozyskaniu materiału do badań (selekcji materiału kostnego do badań, koordynowaniu pracy jednostki zewnętrznej wykonującej skany RTG oraz asyście przy wykonywaniu zdjęć)

Podpis

Joanna Grzelak

Imię i nazwisko
Paweł Dąbrowski
Zakład Anatomii Prawidłowej UMW

Miejscowość i data
Wrocław, 23.09.2024

OŚWIADCZENIE

Oświadczam, że w pracy

Kulus, Michał J., Kamil Cebulski, Piotr Kmiecik, Patrycja Sputa-Grzegrzółka, Joanna Grzelak, and Paweł Dąbrowski. 2024. "New Equations for the Estimation of the Age of the Formation of the Harris Lines" *Life* 14, no. 4: 501. https://doi.org/10.3390/life14040501\

mój udział polegał na: opracowanie antropologiczne materiału, zebranie literatury, opracowanie koncepcji artykułu.

Podpis

Dorobek Naukowy

Wykaz publikacji

Michał Kulus

1. Publikacje w czasopismach naukowych

1.1 Publikacje w czasopiśmie z IF

Lp.	Opis bibliograficzny	IF	Punkty
1	Zadka Łukasz,Kram Paweł,Kościński Jeremi,Jankowski Roman,Kaczmarek Mariusz,Piątek Katarzyna,Kulus Michał,Gomułkiewicz Agnieszka,Piotrowska Aleksandra,Dzięgiel Piotr:Association between interleukin-10 receptors and the CD45-immunophenotype of central nervous system tumors: a preliminary study, Anticancer Research, 2017, vol. 37, nr 10, s. 5777-5783, DOI:10.21873/anticanres.12019	1,865	20
2	Zadka Łukasz,Dzięgiel Piotr,Kulus Michał,Olajossy Marcin:Clinical phenotype of depression affects interleukin-6 synthesis, Journal of Interferon and Cytokine Research, 2017, vol. 37, nr 6, s. 231-245, DOI:10.1089/jir.2016.0074	2,419	25
3	Zadka Łukasz,Kulus Michał,Kurnol Krzysztof,Piotrowska Aleksandra,Glatzel-Plucińska Natalia,Jurek Tomasz,Czuba Magdalena,Nowak Aleksandra,Chabowski Mariusz,Janczak Dariusz,Dzięgiel Piotr:The expression of IL10RA in colorectal cancer and its correlation with the proliferation index and the clinical stage of the disease, Cytokine, 2018, vol. 110, s. 116-125, DOI:10.1016/j.cyto.2018.04.030	3,078	25
4	Zadka Łukasz,Kulus MichałJ.,Piątek K.:ADAM protein family - its role in tumorigenesis, mechanisms of chemoresistance and potential as diagnostic and prognostic factors, Neoplasma, 2018, vol. 65, nr 6, s. 823-839, DOI:10.4149/neo_2018_171220N832	1,771	15
5	Dąbrowski Paweł,Grzelak Joanna,Kulus Michał,Staniowski Tomasz:Diagnodent and VistaCam may be unsuitable for the evaluation of dental caries in archeological teeth, American Journal of Physical Anthropology, 2019, vol. 168, nr 4, s. 797-808, DOI:10.1002/ajpa.23785	2,414	140
6	Kulus MichałJerzy,Dąbrowski Paweł:How to calculate the age at formation of Harris lines? A step-by-step review of current methods and a proposal for modifications to Byers' formulas, Archaeological and Anthropological Sciences, 2019, vol. 11, nr 4, s. 1169-1185, DOI:10.1007/s12520-018-00773-5	2,063	100
7	Dąbrowski Paweł,Kulus Michał,Cieślik A.,Staszak Katarzyna,Staniowski Tomasz:Inverted and horizontal impacted third molars in an Early Modern skull from Wroclaw, Poland: a case report, Folia Morphologica, 2019, vol. 78, nr 1, s. 214-220, DOI:10.5603/FM.a2018.0071	0,941	70
8	Dąbrowski Paweł,Kulus MichałJerzy,Cieślik Agata,Domagała Zygmunt,Wiglusz Rafał J.,Kuropka Piotr,Kuryszko Jan,Thannhauser Agata,Szleszkowski Łukasz,Wojtulek Piotr,Soliński Daniel,Dzięgiel Piotr:A case of syphilis with high bone arsenic concentration from early modern cemetery (Wroclaw, Poland), Open Life Sciences, 2019, vol. 14, s. 427-439, DOI:10.1515/biol-2019-0048	0,69	40

1

9	Dąbrowski Paweł,Kulus Michał,Grzelak Joanna,Radzikowska Magdalena,Oziembłowski Maciej,Domagała Zygmunt,Krajcarz Maciej T.:Assessing weaning stress - relations between enamel hypoplasia, δ18O and δ13C values in human teeth obtained from early modern cemeteries in Wroclaw, Poland, Annals of Anatomy-Anatomischer Anzeiger, 2020, vol. 232, art.151546 [13 s.], DOI:10.1016/j.aanat.2020.151546	2,698	100
10	Kmiecik Janusz,Kulus MichałJerzy,Popiel Jarosław,Cekiera Agnieszka,Cegielski Marek:Antlerogenic stem cells extract accelerate chronic wound healing: a preliminary study, BMC Complementary Medicine and Therapies, 2021, vol. 21, art.158 [8 s.], DOI:10.1186/s12906-021-03336-9	2,838	100
11	Dąbrowski Paweł,Kulus MichałJerzy,Furmanek Mirosław,Paulsen Friedrich,Grzelak Joanna,Domagała Zygmunt:Estimation of age at onset of linear enamel hypoplasia. New calculation tool, description and comparison of current methods, Journal of Anatomy, 2021, vol. 239, nr 4, s. 920-931, DOI:10.1111/joa.13462	2,921	140
12	Łuczak Anna,Małecki Rafał,Kulus Michał,Madej Marta,Szahidewicz-Krupska Ewa,Doroszko Adrian:Cardiovascular risk and endothelial dysfunction in primary Sjogren syndrome is related to the disease activity, Nutrients, 2021, vol. 13, nr 6, art.2072 [12 s.], DOI:10.3390/nu13062072	6,706	140
13	Dąbrowski Paweł,Kulus MichałJerzy,Grzelak Joanna,Olchowy Cyprian,Staniowski Tomasz,Paulsen Friedrich:Nutritional reconstruction in an early modern population: searching for a relationship between dental microwear and bone element composition, Annals of Anatomy-Anatomischer Anzeiger, 2022, vol. 240, art.151884 [10 s.], DOI:10.1016/j.aanat.2021.151884	2,2	100
14	Buzalewicz Igor,Mrozowska Monika,Kmiecik Alicja,Kulus Michał,Haczkiewicz-Leśniak Katarzyna,Dzięgiel Piotr,Podhorska-Okołów Marzenna,Zadka Łukasz:Quantitative phase imaging detecting the hypoxia-induced patterns in healthy and neoplastic human colonic epithelial cells, Cells, 2022, vol. 11, nr 22, art.3599 [20 s.], DOI:10.3390/cells11223599	6	140
15	Solarska-Ściuk Katarzyna,Adach Kinga,Fijałkowski Mateusz,Haczkiewicz-Leśniak Katarzyna,Kulus Michał,Olbromski Mateusz,Glatzel-Plucińska Natalia,Szelest Oskar,Bonarska-Kujawa Dorota:Identifying the molecular mechanisms and types of cell death induced by bio- and pyr-silica nanoparticles in endothelial cells, International Journal of Molecular Sciences, 2022, vol. 23, nr 9, art.5103 [18 s.], DOI:10.3390/ijms23095103	5,6	140
16	Mączka Grzegorz,Kulus Michał,Grzelak Joanna,Porwolik Michał,Dobrzyński Maciej,Dąbrowski Paweł:Morphology of the antegonial notch and its utility in the determination of sex on skeletal materials, Journal of Anatomy, 2022, vol. 241, nr 4, s. 919-927, DOI:10.1111/joa.13731	2,4	140
17	Mączka Grzegorz,Kulus Michał,Grzelak Joanna,Dobrzyński Maciej,Staniowski Tomasz,Skośkiewicz-Malinowska Katarzyna,Dąbrowski Paweł:Symmetry and asymmetry of the antegonial notch, Symmetry-Basel, 2022, vol. 14, nr 8, art.1558 [10 s.], DOI:10.3390/sym14081558	2,7	70
18	Zawadzka-Knefel Anna,Rusak Agnieszka,Mrozowska Monika,Machałowski Tomasz,Żak Andrzej,Haczkiewicz-Leśniak Katarzyna,Kulus Michał,Kuropka Piotr,Podhorska-Okołów Marzenna,Skośkiewicz-Malinowska Katarzyna:Chitin scaffolds derived from the marine demosponge Aplysina fistularis stimulate the differentiation of dental pulp stem cells, Frontiers in Bioengineering and Biotechnology, 2023, vol. 11, art.1254506 [20 s.], DOI:10.3389/fbioe.2023.1254506	4,3	100

19	Ochota Małgorzata,Kulus MichałJerzy,Młodawska Wiesława,Kardasz-Kamocka Marta,Haczkiewicz-Leśniak Katarzyna,Podhorska-Okołów Marzenna,Niżański Wojciech:Ultrastructural changes in feline oocytes during ovary storage for 24- and 48-hours, Theriogenology, 2023, vol. 197, s. 101-110, [W tekście błędnie Marzenna Podchorska-Okołów], DOI:10.1016/j.theriogenology.2022.11.025	2,4	140
20	Wąsik Adrian,Podhorska-Okołów Marzenna,Dzięgiel Piotr,Piotrowska Aleksandra,Kulus MichałJerzy,Kmiecik Alicja,Ratajczak-Wielgomas Katarzyna:Correlation between periostin expression and pro-angiogenic factors in non-small-cell lung carcinoma, Cells, 2024, vol. 13, nr 17, art.1406 [25 s.], DOI:10.3390/cells13171406	5,1*	140
21	Kulus MichałJerzy,Golema Wojciech,Jurek Tomasz,Jasiński Ryszard:Histological analysis of forearm superficial veins structure, Folia Morphologica, 2024, vol. 83, nr 2, s. 374-381, DOI:10.5603/fm.96131	1,2*	70
22	Kulus MichałJ.,Cebulski Kamil,Kmiecik Piotr,Sputa-Grzegrzółka Patrycja,Grzelak Joanna,Dąbrowski Paweł:New equations for the estimation of the age of the formation of the Harris lines, Life, 2024, vol. 14, nr 4, art.501 [13 s.], DOI:10.3390/life14040501	3,2*	70
23	Szlasa Wojciech,Sauer Natalia,Baczyńska Dagmara,Ziętek Marcin,Haczkiewicz-Leśniak Katarzyna,Karpiński Paweł,Fleszar Mariusz,Fortuna Paulina,Kulus MichałJ.,Piotrowska Aleksandra,Kmiecik Alicja,Barańska Agnieszka,Michel Olga,Novickij Vitalij,Tarek Mounir,Kasperkiewicz Paulina,Dzięgiel Piotr,Podhorska-Okołów Marzenna,Saczko Jolanta,Kulbacka Julita:Pulsed electric field induces exocytosis and overexpression of MAGE antigens in melanoma, Scientific Reports, 2024, vol. 14, art.12546 [22 s.], DOI:10.1038/s41598-024-63181-x	3,8*	140
24	Alkali Isa Mohammed,Colombo Martina,De Iorio Teresina,Piotrowska Aleksandra,Rodak Olga,Kulus MichałJerzy,Niżański Wojciech,Dzięgiel Piotr,Luvoni Gaia Cecilia:Vitrification of feline ovarian tissue: comparison of protocols based on equilibration time and temperature, Theriogenology, 2024, vol. 224, s. 163-173, DOI:10.1016/j.theriogenology.2024.05.023	2,4*	140
	Podsumowanie	71,704	2305

*IF 2023

2. Monografie naukowe

2.1 Książka autorska -

2.2 Książka redagowana -

2.3 Rozdziały

Lp.	Opis bibliograficzny	Punkty
1	Dąbrowski Paweł,Grzelak Joanna,Kotylak Aleksandra,Olchowy Cyprian,Kulus Michał,Kurc-Darak Bożena,Domagała Zygmunt,Jura Maksym,Woźniak Sławomir,Rohan-Fugiel Anna,Pinkowska Agnieszka:Wstępna ocena stanu zdrowia i kondycji biologicznej ludności pochowanej na cmentarzu miejskim w Raciborzu (XIX/XX w.), W: Zagrożenie życia i zdrowia człowieka, (red.) Józef Tatarczuk, Bożena Zboina, Paweł Dąbrowski, Lublin 2017, NeuroCentrum, s. 39-62, ISBN 978-83-61495-71-0, [Publikacja w wydawnictwie spoza listy MNiSW]	5

2	Jeleń Łukasz,Kulus Michał,Jurek Tomasz:Pattern recognition framework for histological slide segmentation, W: Computer information systems and industrial management : 17th International Conference, CISIM 2018. Olomouc, Czech Republic, September 27-29, 2018. Proceedings, (red.) Khalid Saeed, Władysław Homenda, Cham 2018, Springer Nature Switzerland AG, s. 37-45, (Lecture Notes in Computer Science; nr 11127), ISBN 978-3-319-99953-1, DOI:10.1007/978-3-319-99954-8_4	40
3	Miselis Bartosz,Kulus Michał,Jurek Tomasz,Rusiecki Andrzej,Jeleń Łukasz:Deep neural network for whole slide vein segmentation, W: Computer information systems and industrial management : 17th International Conference, CISIM 2018. Olomouc, Czech Republic, September 27-29, 2018. Proceedings, (red.) Khalid Saeed, Władysław Homenda, Cham 2018, Springer Nature Switzerland AG, s. 57-67, (Lecture Notes in Computer Science; nr 11127), ISBN 978-3-319-99953-1, DOI:10.1007/978-3-319-99954-8_6	40
4	Oziembłowski Maciej,Dąbrowski Paweł,Styczyńska Marzena,Kulus Michał,Grzelak Joanna:Próba rekonstrukcji diety mieszkańców dawnego Wrocławia na podstawie analizy wybranych mikro- i makroelementów materiału kostnego, W: Postęp w naukach o żywieniu człowieka, (red.) Grażyna Jaworska*[i in.]*, Rzeszów 2020, Wydawnictwo Uniwersytetu Rzeszowskiego, s. 63-78, ISBN 978-83-7996-837-4	20
5	Dąbrowski Paweł,Domagała Dominika,Kulus Michał,Piotrowska Aleksandra,Melnyk Oleg,Nowakowski Dariusz,Grzelak Joanna:Współczesna problematyka badań staroegipskich zmumifikowanych szczątków ludzkich - doniesienie wstępne, W: XIII Sympozjum "Współczesna Myśl Techniczna w Naukach Technicznych i Biologicznych". Wrocław, 27-28 września 2024 roku. Materiały konferencyjne, Wrocław 2024, Oddział Polskiej Akademii Nauk we Wrocławiu, s. 24-25	0
	Podsumowanie	105

3. Abstrakty

Lp.	Opis bibliograficzny
1	Kulus Michał:Interacting genes of GDF15 - comprehensive predictive protein, W: I Ogólnopolska Konferencja "Biomarkery w chorobach nowotworowych". Wrocław, 9-10 październik 2015 2015, [66-68]
2	Cegielski Marek,Kulus Michał,Haczkiewicz Katarzyna,Piotrowska Aleksandra,Zubkiewicz-Zarębska Anna,Kiełbowicz Zdzisław,Niżański Wojciech,Partyka Agnieszka,Chodaczek Grzegorz:Spermatogonialne komórki macierzyste jelenia szlachetnego (Cervus elaphus), W: 50 Sympozjum Polskiego Towarzystwa Histochemików i Cytochemików "Od przeszłości do teraźniejszości...". Wojanów, 5-8 września 2016. Program, streszczenia 2016, s. 33, ISBN 978-83-7055-575-7
3	Kulus Michał,Haczkiewicz Katarzyna,Cegielski Marek:Ultrastruktura linii komórkowej spermatogoniów jelenia szlachetnego (Cervus elaphus), W: 50 Sympozjum Polskiego Towarzystwa Histochemików i Cytochemików "Od przeszłości do teraźniejszości...". Wojanów, 5-8 września 2016. Program, streszczenia 2016, s. 50, ISBN 978-83-7055-575-7
4	Zadka Łukasz,Kram Paweł,Kościński Jeremi,Jankowski Roman,Kaczmarek Mariusz,Piątek Katarzyna,Kulus Michał,Gomułkiewicz Agnieszka,Piotrowska Aleksandra,Dzięgiel Piotr:Ekspresja receptorów interleukiny-10 w guzach mózgu oraz w ich nacieku leukocytarnym, W: 50 Sympozjum Polskiego Towarzystwa Histochemików i Cytochemików "Od przeszłości do teraźniejszości...". Wojanów, 5-8 września 2016. Program, streszczenia 2016, s. 53-54, ISBN 978-83-7055-575-7

5	Kulus Michał,Haczkiewicz Katarzyna,Piotrowska Aleksandra,Zubkiewicz-Zarębska Anna,Kiełbowicz Zdzisław,Partyka Agnieszka,Chodaczek Grzegorz,Cegielski Marek:Spermatogonialne komórki macierzyste jelenia szlachetnego (Cervus elaphus). Charakterystyka i perspektywy ich wykorzystania, W: VII Sympozjum "Współczesna myśl techniczna w naukach medycznych i biologicznych". Wrocław, 24-25 czerwca 2016 r. Materiały konferencyjne, Wrocław 2016, Oddział Polskiej Akademii Nauk we Wrocławiu, s. 55-56, ISBN 978-83-942714-3-5
6	Zadka Łukasz,Kulus Michał,Kurnol Krzysztof,Piotrowska Aleksandra,Glatzel-Plucińska Natalia,Nowak Aleksandra,Chabowski Mariusz,Dzięgiel Piotr:Ekspresja IL10RA koreluje ze stopniem zaawansowania nowotworów jelita grubego = Expression of IL10RA correlates with colorectal tumor stage, W: 51. Sympozjum Polskiego Towarzystwa Histochemików i Cytochemików "Tkanki, komórki, geny". Warszawa, 12-14 września 2017. Streszczenia prezentacji ustnych oraz plakatowych 2017, 17-18 poz.U22
7	Kulus Michał,Dąbrowski Paweł,Wiglusz Rafał,Kuryszko Jan,Kuropka Piotr,Dzięgiel Piotr:Interdyscyplinarne badania szczątków kostnych syfilityka z wczesnonowożytnej nekropolii wrocławskiej = Interdisciplinary study on skeletal remains of syphilitic from early modern necropoly in Wrocław, W: 51. Sympozjum Polskiego Towarzystwa Histochemików i Cytochemików "Tkanki, komórki, geny". Warszawa, 12-14 września 2017. Streszczenia prezentacji ustnych oraz plakatowych 2017, 7-8 poz.U9
8	Dąbrowski Paweł,Kulus Michał,Wiglusz Rafał,Kuryszko Jan,Kuropka Piotr,Wojtulek Piotr:Terapia arsenem? Przypadek czaszki syfilityka z wczesnonowożytnej nekropolii wrocławskiej – perspektywa bioarcheologiczna, W: VIII Sympozjum "Współczesna myśl techniczna w naukach medycznych i biologicznych". Wrocław, 23-24 czerwca 2017. Materiały konferencyjne, Wrocław 2017, Oddział Polskiej Akademii Nauk we Wrocławiu, s. 29-30, ISBN 978-83-942714-5-9
9	Haczkiewicz Katarzyna,Piotrowska Aleksandra,Partyńska Aleksandra,Mieszała Katarzyna,Kulus Michał,Dzięgiel Piotr,Podhorska-Okołów Marzenna:Autofagia w raku gruczołu piersiowego - badania wstępne, W: 52. Zjazd Naukowy Polskiego Towarzystwa Histochemików i Cytochemików "Immunohistochemia i biologia molekularna w morfologii". Białystok, 13-16 września 2018. Streszczenia prezentacji ustnych oraz plakatowych 2018, 18 poz.U16
10	Kulus Michał,Dąbrowski Paweł:Nowa metoda obliczania biologicznego wieku powstania linii Harrisa u dzieci i młodzieży - doniesienie wstępne, W: IX Sympozjum "Współczesna myśl techniczna w naukach medycznych i biologicznych". Wrocław, 22-23 czerwca 2018 r. Materiały konferencyjne, Wrocław 2018, Oddział Polskiej Akademii Nauk we Wrocławiu, s. 43-44, ISBN 978-83-942714-8-0
11	Słowik Grzegorz P.,Dąbrowski Paweł,Kulus Michał,Trusek Anna:The issues of selecting biomarkers of life in laboratory conditions for the needs of the Venus clouds biotope assessment, W: 17th Meeting of the Venus Exploration and Analysis Group (VEXAG). Boulder, Colorado, November 6-8, 2019. Program and abstracts [online] 2019, poz.8046
12	Dąbrowski Paweł,Kulus Michał,Grzelak Joanna,Staniowski Tomasz:Diagnodent and VistaCam may be unsuitable for the evaluation of dental caries in archeological teeth, W: 3rd Wroclaw Scientific Meetings. Wrocław, 1st-2nd March 2019, (red.) Julita Kulbacka, Nina Rembiałkowska, Joanna Weżgowiec, Wrocław 2019, Wydawnictwo Naukowe TYGIEL sp. z o.o., 64 poz.P10, ISBN 978-83-65932-64-8
13	Dąbrowski Paweł,Kulus Michał,Grzelak Joanna,Krajcarz Maciej,Radzikowska Magdalena:Changes of the diet in weaning time and the assessment of enamel developmental defects in SEM and the content of δ18O and δ13C in the permanent teeth of the historical population from Wrocław, Poland, W: 53rd Symposium of the Polish Society for Histochemistry and Cytochemistry "From ultrastructure to in vivo imaging: progress in microscopical techniques". Gdańsk, 15-18 September 2019. Program, abstracts, Gdańsk 2019, Polish Society for Histochemistry and Cytochemistry ; Department of Histology Medical University of Gdańsk, 87 poz.P10, ISBN 978-83-61216-07-0

14	Dąbrowski Paweł,Kulus Michał,Grzelak Joanna,Krajcarz Maciej,Radzikowska Magdalena:Assessing weaning stress - relations between enamel hypoplasia, δ18O and δ13C values in teeth from early modern cemeteries in Wroclaw, Poland, W: 53rd Symposium of the Polish Society for Histochemistry and Cytochemistry "From ultrastructure to in vivo imaging: progress in microscopical techniques". Gdańsk, 15-18 September 2019. Program, abstracts, Gdańsk 2019, Polish Society for Histochemistry and Cytochemistry ; Department of Histology Medical University of Gdańsk, 96 poz.P19, ISBN 978-83-61216-07-0
15	Słowik Grzegorz P.,Trusek Anna,Dąbrowski Paweł,Kulus MichałJ.,Ziółkowska Agnieszka,Limaye Sanjay S.:Measuring the properties of acidophilic bacteria under Venus cloud conditions, W: International Venus Conference 2019 : The 74th Fujihara Seminar "Akatsuki : Novel Development of Venus Science". Hokkaido, Japan, May 31 (Fri.) - June 3 (Mon.), 2019. Abstracts 2019, [69-70] poz.P47 IVC2019-0042, [[Dostęp 26.07.2019]. Dostępny w: https://www.cps-jp.org/~akatsuki/venus2019/program/IVC2019_Abstracts.pdf]
16	Dąbrowski Paweł,Grzelak Joanna,Krajcarz Maciej,Kulus Michał,Oziembłowski Maciej:The evaluation of the living conditions of the inhabitants of old Wrocław city based on developmental defects, micro-injuries of the dental crowns and the content of stable isotopes: carbon and oxygen in the enamel, W: Sympozjum Naukowe "Zielone Forum". Wrocław, 29-30.03.2019. Streszczenia 2019, s. 10-11, [4th International Conference "Man-food-health". Wrocław, Poland, 29.03.2019. Abstracts]
17	Dąbrowski Paweł,Kulus Michał,Grzelak Joanna,Krajcarz Maciej:Ocena wieku odstawienia od piersi - powiązania hipoplazji szkliwa i zawartości stabilnych izotopów^{18}O i^{13}C w zębach z wczesnonowożytnych cmentarzy Wrocławskich, W: X Sympozjum "Współczesna myśl techniczna w naukach medycznych i biologicznych". Wrocław, 14-15 czerwca 2019 r. Materiały konferencyjne, Wrocław 2019, Oddział Polskiej Akademii Nauk we Wrocławiu, s. 26-28, ISBN 978-83-942714-9-7
18	Dąbrowski Paweł,Grzelak Joanna,Krajcarz Maciej,Kulus Michał,Oziembłowski Maciej:Ocena jakości życia dzieci we wczesnonowożytnym Wrocławiu na podstawie defektów rozwojowych oraz zawartości izotopów stabilnych węgla i tlenu w szkliwie zębów stałych, W: XLVII Ogólnopolska Konferencja Naukowa Polskiego Towarzystwa Antropologicznego "Antropos - między naturą a kulturą". Kraków, 11-13 września 2019 r. Program oraz streszczenia referatów i prezentacji plakatowych 2019, s. 14
19	Dąbrowski Paweł,Kulus Michał,Grzelak Joanna:Mikrourazy szkliwa zębów stałych a pierwiastki ziem alkalicznych - poszukiwanie związku w ocenie diety dawnych mieszkańców Wrocławia, W: 34. Ogólnopolski Kongres Polskiego Towarzystwa Anatomicznego. Szczecin, 14 - 16 wrzesień 2022 r. Książka streszczeń 2022, Szczecin, s. 52-53
20	Kulus Michał,Ochota Małgorzata,Młodawska Wiesława,Kardasz-Kamocka Marta,Haczkiewicz-Leśniak Katarzyna,Podhorska-Okołów Marzenna,Niżański Wojciech:Zmiany ultrastrukturalne w kocich oocytach w zależności od czasu przechowywania jajnika, W: XI Sympozjum "Współczesna myśl techniczna w naukach medycznych i biologicznych". Wrocław, 18-19 listopada 2022. Materiały konferencyjne, Wrocław 2022, Oddział Polskiej Akademii Nauk we Wrocławiu, s. 108-109, ISBN 978-83-954493-3-8
21	Dąbrowski Paweł,Kulus Michał,Grzelak Joanna:Wybrane metody mikro, makroskopowe i fizyczno-chemiczne w rekonstrukcji diety oraz nawyków żywieniowych dawnych mieszkańców Wrocławia, W: XI Sympozjum "Współczesna myśl techniczna w naukach medycznych i biologicznych". Wrocław, 18-19 listopada 2022. Materiały konferencyjne, Wrocław 2022, Oddział Polskiej Akademii Nauk we Wrocławiu, s. 49-51, ISBN 978-83-954493-3-8
22	Budrewicz Sławomir,Koszewicz Magdalena,Podhorska-Okołów Marzenna,Kulus Michał,Słotwiński Krzysztof:Fulminant life-threatening myopathy of the genetic origin, Clinical Neurophysiology, 2023, vol. 150, e85 poz.N°39, [18th European Congress of Clinical Neurophysiology (ECCN). Marseille, France, May 9-12, 2023. Abstracts], DOI:10.1016/j.clinph.2023.03.051

23	Kulus Michał,Dąbrowski Paweł,Kapczyńska Katarzyna,Szymczak-Kulus Katarzyna,Styczyńska Marzena,Zawiślak Ireneusz,Domagała Dominika,Kmiecik Piotr:Kwasy tłuszczowe wyizolowane z archeologicznych ludzkich kości a diageneza, European Journal of Clinical and Experimental Medicine, 2023, nr suppl., s. 29, [55 Jubileuszowe Sympozjum Polskiego Towarzystwa Histochemików i Cytochemików. Rzeszów, 20-22 września 2023. Książka abstraktów]
24	Haczkiewicz-Leśniak Katarzyna,Dzięgiel Piotr,Piotrowska Aleksandra,Partyńska Aleksandra,Kulus Michał,Gomułkiewicz Agnieszka,Jabłońska Karolina,Kmiecik Alicja,Ratajczak-Wielgomas Katarzyna,Baran-Pelc Magdalena,Ratajczak Katarzyna,Rusak Agnieszka,Migocka-Patrzałek Marta,Iwaneczko Ewelina,Matkowski Rafał,Podhorska-Okołów Marzenna:Ekspresja białka LC3-B w różnych podtypach molekularnych raka gruczołu piersiowego – badania wstępne, European Journal of Clinical and Experimental Medicine, 2023, nr suppl., s. 32, [55 Jubileuszowe Sympozjum Polskiego Towarzystwa Histochemików i Cytochemików. Rzeszów, 20-22 września 2023. Książka abstraktów]
25	Dąbrowski Paweł,Kulus Michał,Domagała Dominika,Grzelak Joanna:Rekonstrukcja diety i wieku weaning stress u mieszkańców wczesnonowożytnego Wrocławia w oparciu o mikroskopowe i fizyczno-chemiczne metody badań, W: XII Sympozjum "Współczesna myśl techniczna w naukach medycznych i biologicznych". Wrocław, 29-30 wrzesień 2023. Materiały konferencyjne, Wrocław 2023, Oddział Polskiej Akademii Nauk we Wrocławiu, s. 28-30, ISBN 978-83-954493-4-5
26	Domagała Dominika,Grzelak Joanna,Kulus Michał,Dąbrowski Paweł:Charakterystyka diety dawnych mieszkańców Wrocławia w oparciu o analizę kamienia nazębnego, W: XII Sympozjum "Współczesna myśl techniczna w naukach medycznych i biologicznych". Wrocław, 29-30 wrzesień 2023. Materiały konferencyjne, Wrocław 2023, Oddział Polskiej Akademii Nauk we Wrocławiu, s. 41-42, ISBN 978-83-954493-4-5
27	Dąbrowski Paweł,Kulus Michał,Domagała Dominika,Grzelak Joanna:Rekonstrukcja diety oraz nawyków żywieniowych wczesnonowożytnych mieszkańców parafii św. Barbary we Wrocławiu (XVI-XVIII w.) w oparciu o mikroskopowe i chemiczne metody badań, W: XLIX Ogólnopolska Konferencja Naukowa Polskiego Towarzystwa Antropologicznego "Antropologia – nauka interdyscyplinarna". Gdańsk, 20-22 września 2023 2023, s. 15
28	Grzelak Joanna,Domagała Dominika,Kulus Michał,Dąbrowski Paweł:Występowanie zmian próchnicowych a ekspozycja na pierwiastki ziem alkalicznych w materiałach szkieletowych z cmentarza przy kościele św. Barbary we Wrocławiu (XVI-XVIII w), W: XLIX Ogólnopolska Konferencja Naukowa Polskiego Towarzystwa Antropologicznego "Antropologia – nauka interdyscyplinarna". Gdańsk, 20-22 września 2023 2023, s. 22
29	Powązka Marcelina,Kulus MichałJ.,Dąbrowski Paweł:Harris lines - an aid in assessing well-being deficits in childhood and adolescence - preliminary study, W: The International Scientific Conference Progressio Infantis 2024 "Children, parents and experts on the way to development". Wrocław, [24-25.05.2024]. Book of abstracts, (red.) Karolina Alasińska, Aleksandra Dawidziak, Ewa Gieysztor, Wrocław 2024, s. 31
30	Wąsik Adrian,Podhorska-Okołów Marzenna,Dzięgiel Piotr,Piotrowska Aleksandra,Kulus Michał,Kmiecik Alicja,Ratajczak-Wielgomas Katarzyna:Korelacja ekspresji periostiny (POSTN) z czynnikami proangiogennymi w niedrobnokomórkowych rakach płuc (NSCLC), W: XIII Sympozjum "Współczesna Myśl Techniczna w Naukach Technicznych i Biologicznych". Wrocław, 27-28 września 2024 roku. Materiały konferencyjne, Wrocław 2024, Oddział Polskiej Akademii Nauk we Wrocławiu, s. 113-114
31	Grzelak Joanna,Domagała Dominika,Kulus Michał,Piotrowska Aleksandra,Melnyk Oleg,Nowakowski Dariusz,Dąbrowski Paweł:Współczesne metody obrazowania w badaniach szczątków ludzkich jako sposób zachowania dziedzictwa kulturowego, W: XIII Sympozjum "Współczesna Myśl Techniczna w Naukach Technicznych i Biologicznych". Wrocław, 27-28 września 2024 roku. Materiały konferencyjne, Wrocław 2024, Oddział Polskiej Akademii Nauk we Wrocławiu, s. 43-44

32	Grzeszczuk Maciej,Ciesielska Urszula,Rusak Agnieszka,Kulus Michał,Haczkiewicz-Leśniak Katarzyna,Jabłońska Karolina,Kmiecik Alicja,Podhorska-Okołów Marzenna,Dzięgiel Piotr,Nowińska Katarzyna:Wpływ hipoksji na wydzielanie iryzyny przez ludzkie kardiomiocyty, W: XIII Sympozjum "Współczesna Myśl Techniczna w Naukach Technicznych i Biologicznych". Wrocław, 27-28 września 2024 roku. Materiały konferencyjne, Wrocław 2024, Oddział Polskiej Akademii Nauk we Wrocławiu, s. 45-46
33	Kulus Michał,Ochota M.,Brągiel N.,Perrin J.,Młodawska W.,Niżański W.:Ultrastrukturalne zmiany w kocich oocytach związane z wiekiem i dojrzewaniem, W: XIII Sympozjum "Współczesna Myśl Techniczna w Naukach Technicznych i Biologicznych". Wrocław, 27-28 września 2024 roku. Materiały konferencyjne, Wrocław 2024, Oddział Polskiej Akademii Nauk we Wrocławiu, s. 64-65

Impact factor: 71,704

Punkty ministerialne: 2410,0

Signed by /
Podpisano przez:

Dominika
Sidorska

Date / Data:
2024-10-10 11:28

OSOBA SPORZĄDZAJĄCA: BEATA MAJEWSKA
DZIAŁ BIBLIOGRAFII I BIBLIOMETRII BG UMW